SAR TOMOGRAPHY

Spectral Analysis (Specan) techniques

Laurent Ferro-Famil

ISAE-SUPAERO, Centre d'Etudes Spatiales de la Biosphère

- *From 3-D SAR Imaging to the Beamformer*
- *PolTomSAR imaging using 1D Specan techniques*
- *Advanced PolTomSAR imaging using Specan*
- *Polarimetric TomoSAR tomography*

  Full-Rank specan & and SKP decomposition
- *Spaceborne 3-D imaging using correlation SAR tomography*

From 3-D
Synthetic Aperture Imaging
To the Beamformer

2-D SAR impulse response

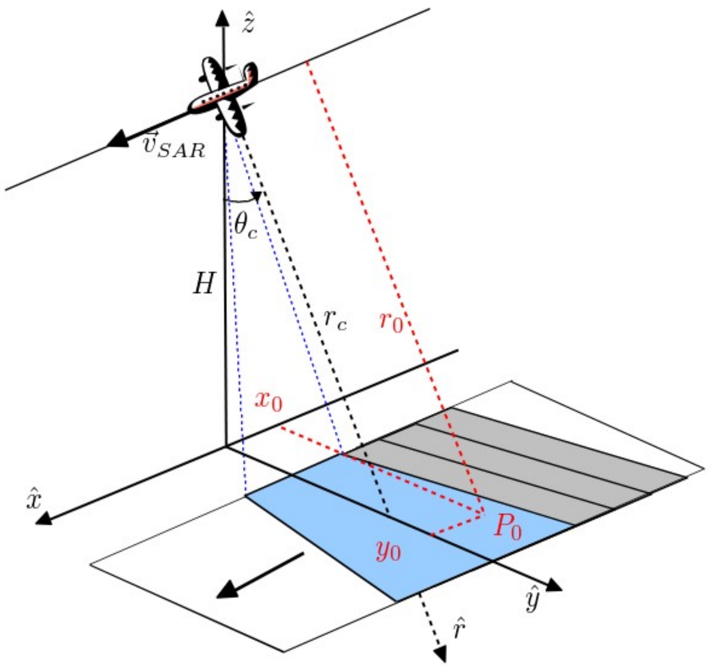

2-D focused signal (x-r domain)

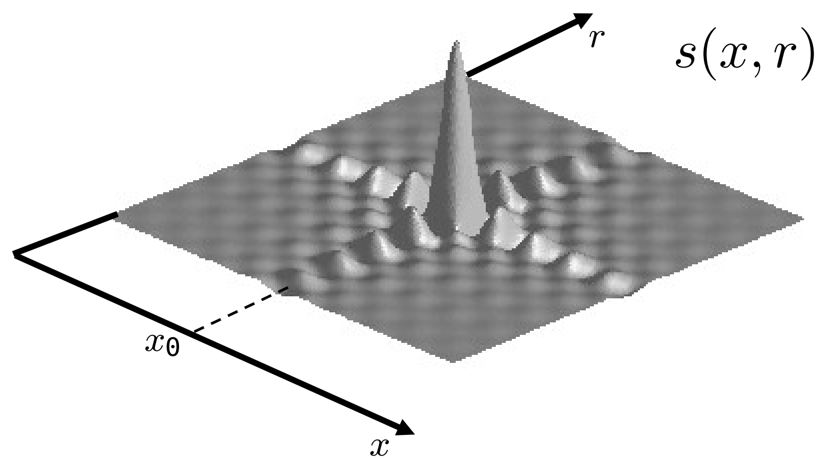

$$
\begin{aligned}
s(x, r) = \quad & a_c && \rightarrow \textbf{complex reflection coefficient} \\
& h_r(d - r_0) && \rightarrow \text{delayed range impulse response} \\
& h_a(x - x_0) && \rightarrow \text{delayed azimuth impulse response} \\
& \exp\left(-j\tfrac{4\pi}{\lambda_c} r_0\right) && \rightarrow \textbf{two-way propagation phase}
\end{aligned}
$$

2-D SAR imaging

SAR imaging: coherent integration of a reflectivity density

$$s(x,r) = \int a_c(x',r',\nu')h(x'-x,r'-r)\,\mathrm{e}^{-j\frac{4\pi}{\lambda_c}d(x'-x,r'-r)}\,\mathrm{d}x'\mathrm{d}r'\mathrm{d}\nu$$

$$s(x,r) \approx \int_{\mathcal{C}} a_c(x,r,\nu)\,\mathrm{e}^{-jk_c r(\nu)}\,\mathrm{d}\nu$$

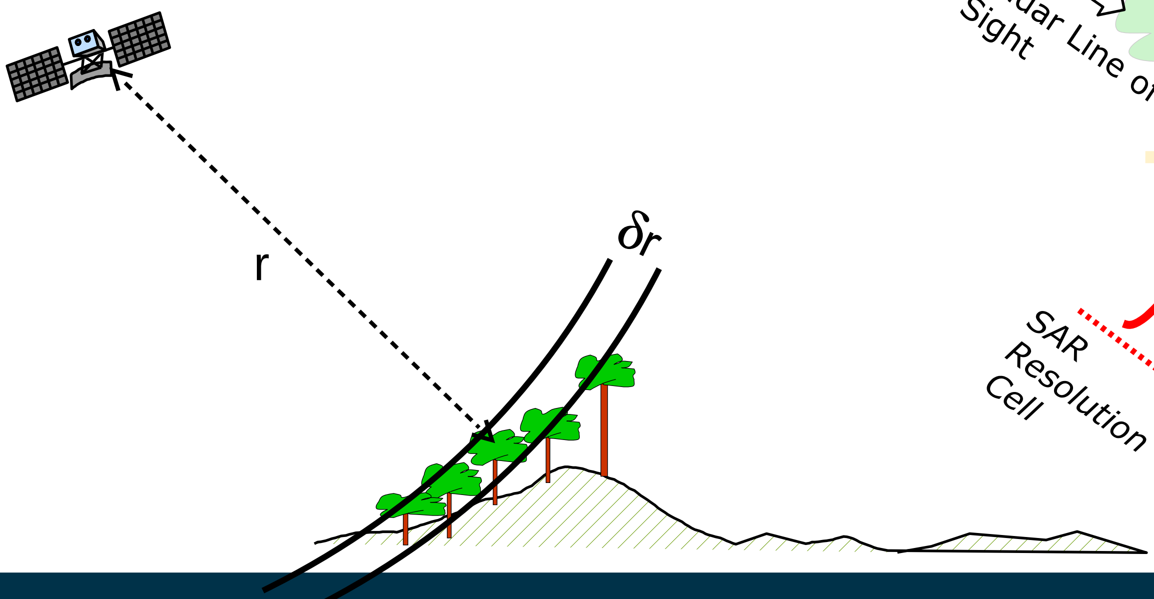

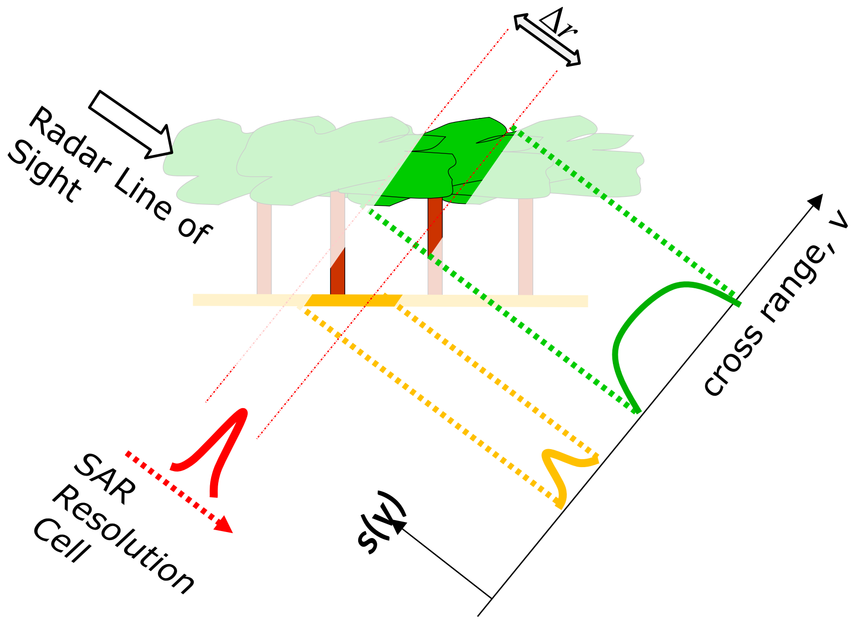

3-D SAR imaging

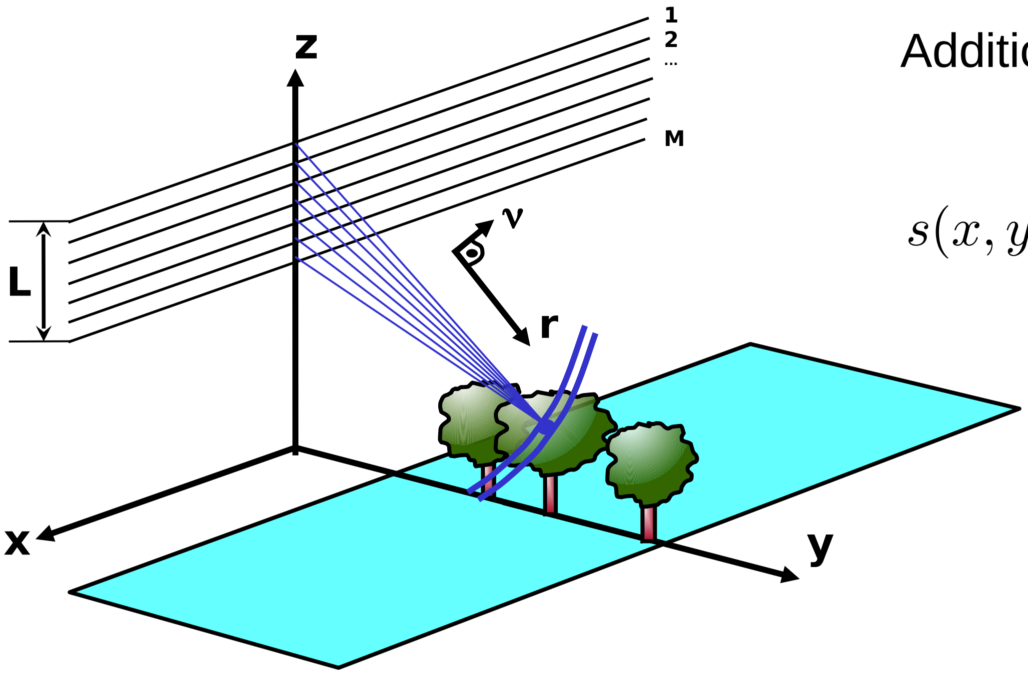

Additional aperture in elevation:
2-D → 3-D focusing

$$s(x,y,z) = \sum_{i=1}^{M} s_i(x, r(y,z))\, \mathrm{e}^{jk_c r(y,z)}$$

Vertical aperture : L_{tomo}

Resolution : $\delta_z = \delta_n \sin\theta$ with $\delta_n = \frac{\lambda R_0}{2L_{tomo}}$

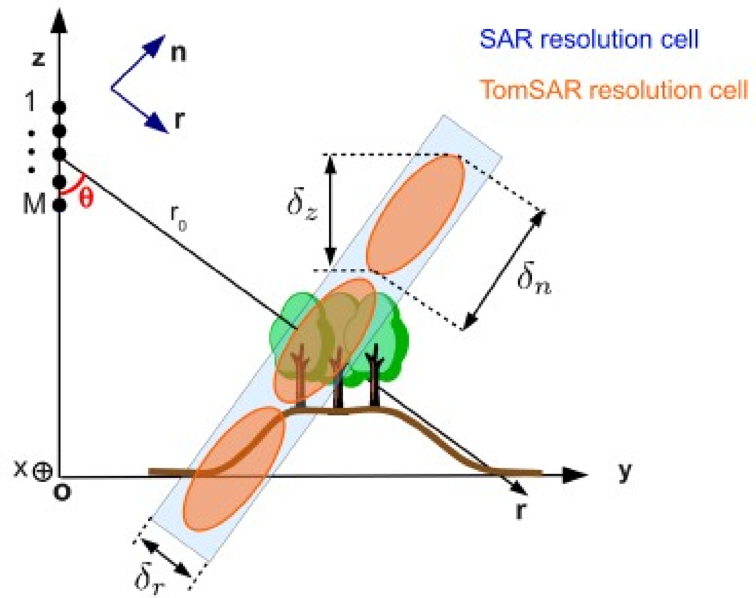

3-D SAR imaging

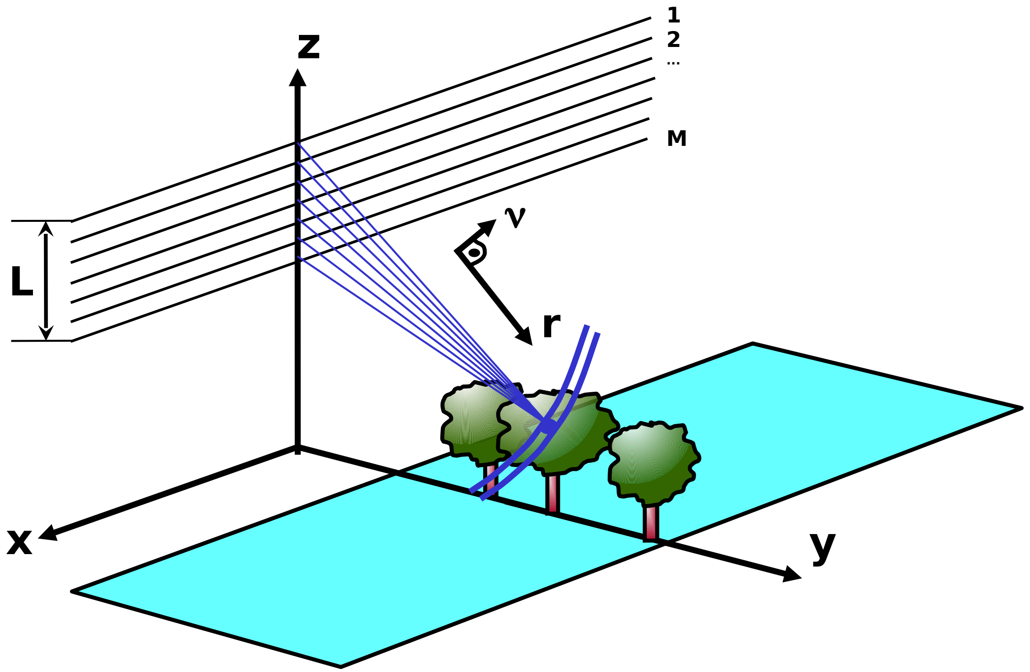

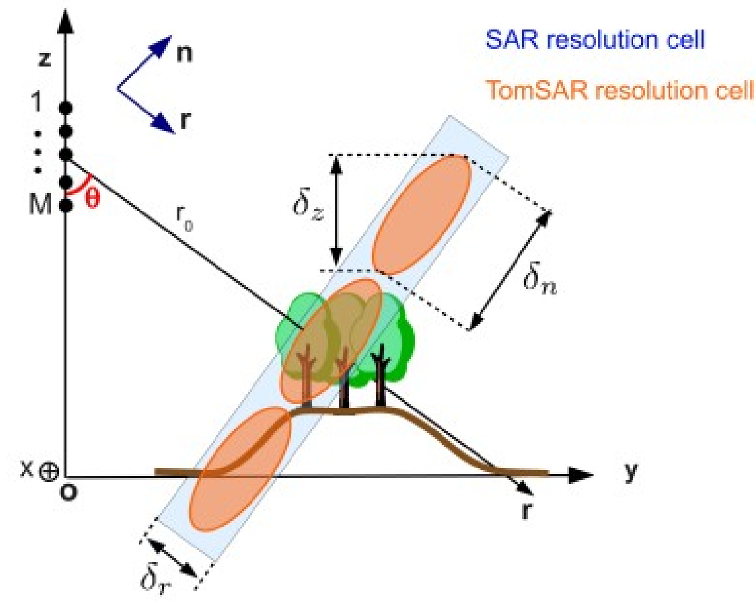

$$s(x, y, z) = \sum_{i=1}^{M} s_i(x, r(y, z))\, \mathrm{e}^{jk_c r(y,z)}$$

Interpolation

HF term

3-D SAR imaging

Co-registration on a reference plane

Valid for $z \in z_{ref} \pm \Delta z_{val}/2$

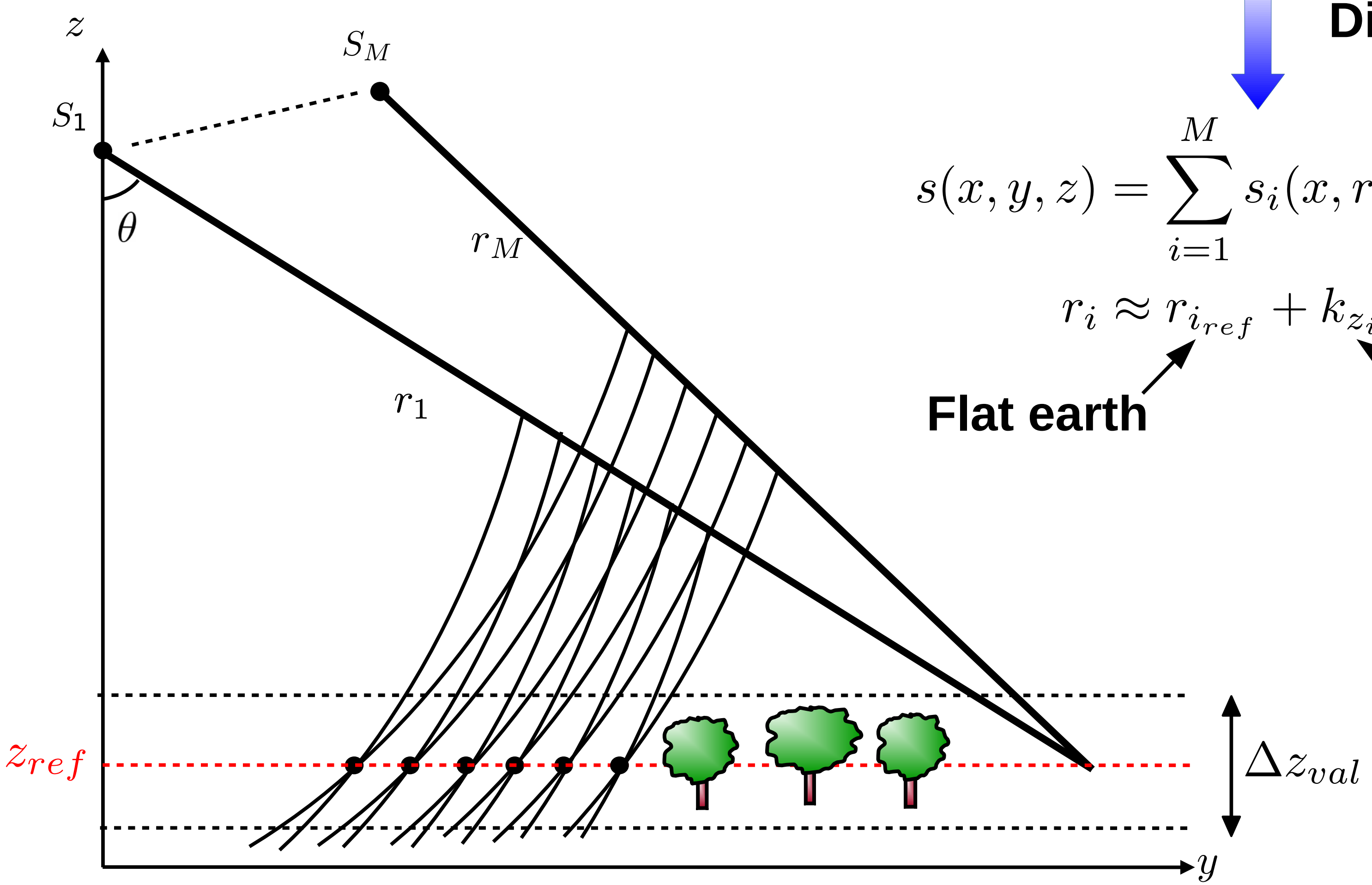

$$s(x,y,z) = \sum_{i=1}^{M} s_i(x, r(y,z))\, e^{jk_c r(y,z)}$$

Discretization NN-interp.

$$s(x,y,z) = \sum_{i=1}^{M} s_i(x, r_{i_{ref}})\, e^{jk_c r_i}$$

$$r_i \approx r_{i_{ref}} + k_{z_i} z$$

Flat earth **Elevation**

3-D SAR imaging

Co-registration on a reference plane

Valid for $z \in z_{ref} \pm \Delta z_{val}/2$

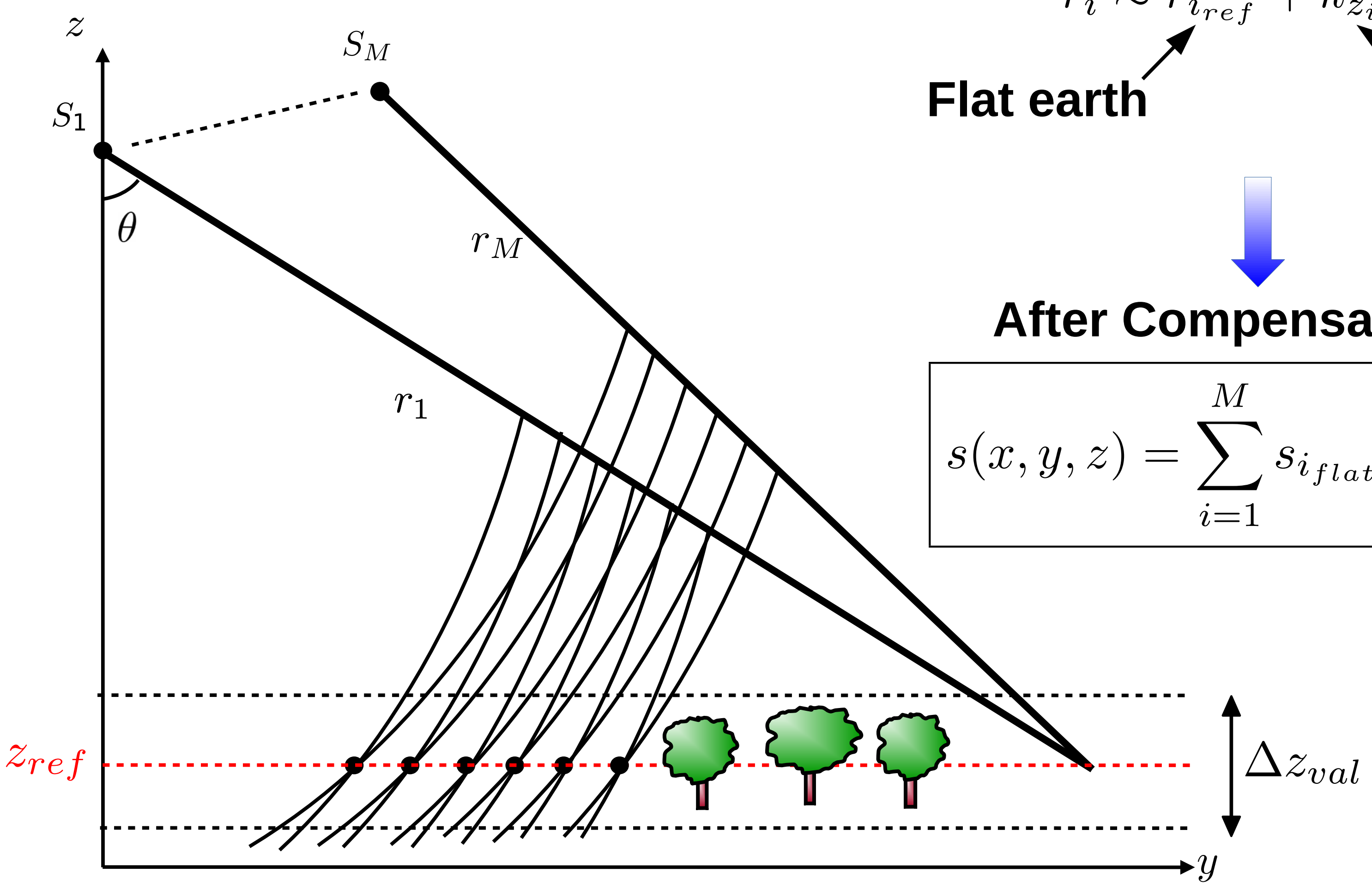

$$s(x,y,z) = \sum_{i=1}^{M} s_i(x, r_{i_{ref}})\, \mathrm{e}^{jk_c r_i}$$

$$r_i \approx r_{i_{ref}} + k_{z_i} z$$

Flat earth **Elevation**

After Compensation

$$\boxed{s(x,y,z) = \sum_{i=1}^{M} s_{i_{flat}}(x, r_{i_{ref}})\, \mathrm{e}^{jk_{z_i} z}}$$

3-D SAR imaging: 2D + 1D processing

3-D Synthetic Aperture imaging

$$s(x,y,z) = \sum_{i=1}^{M} s_i(x, r_{i_{ref}})\, \mathrm{e}^{jk_{z_i}z}$$

Filter-like formulation for a given 2-D resolution cell

Coregistered
Resampled
Flattened
Single Look Complex
(SLC) data

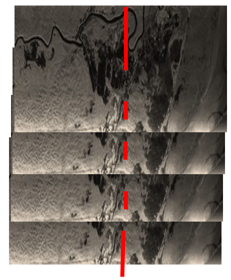

$$\Rightarrow \mathbf{y} = \begin{bmatrix} y_1 \\ \vdots \\ y_M \end{bmatrix} = \begin{bmatrix} s_1(x, r_{1_{ref}}) \\ \vdots \\ s_M(x, r_{M_{ref}}) \end{bmatrix}$$

1D Linear filter

$$\boxed{s(z) = \sum_{i=1}^{M} y_i\, \mathrm{e}^{-jk_{z_i}z} = \mathbf{a}^H(z)\mathbf{y}}$$

Steering vector

$$\mathbf{a} = [1, \mathrm{e}^{jk_{z_2}z}, \ldots, \mathrm{e}^{jk_{z_M}z}]^T$$

TomoSAR imaging
using
Monodimensional
Spectral Analysis Techniques

Interferometric phase variations with height

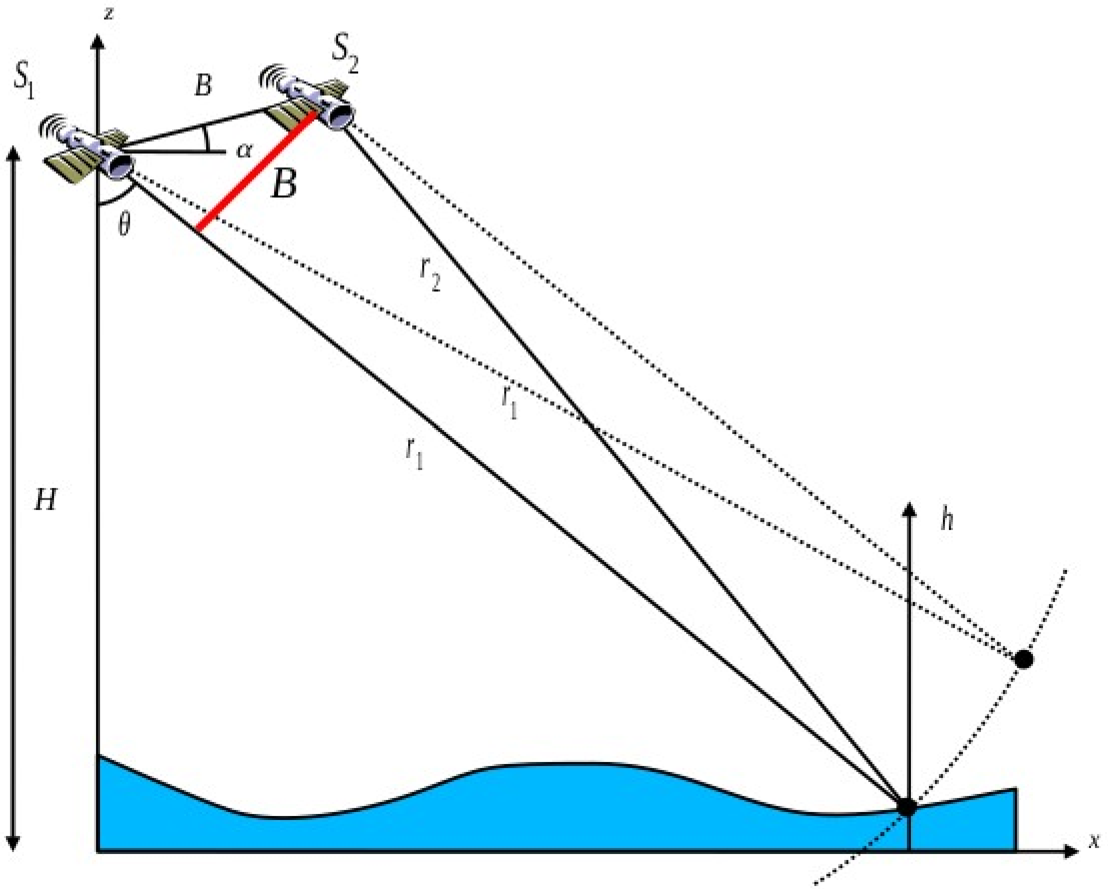

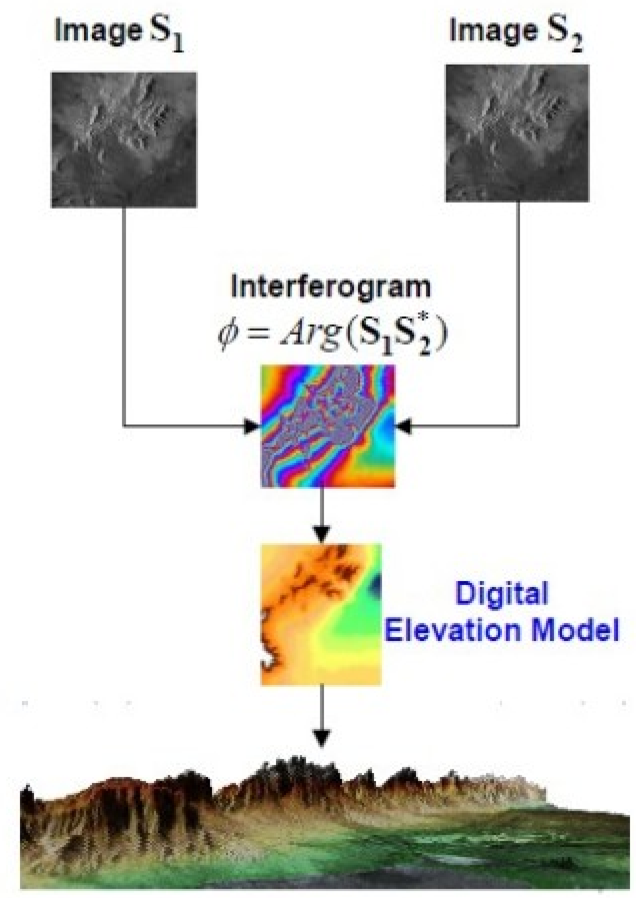

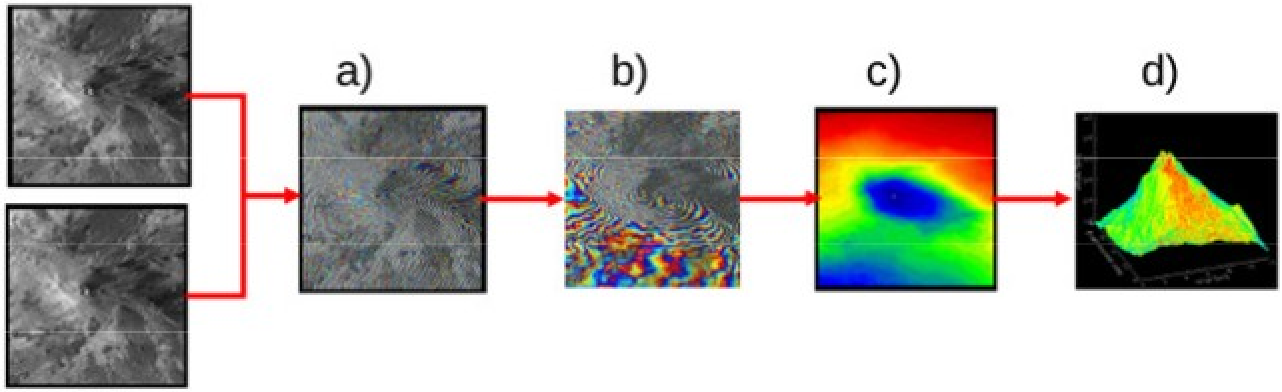
a)
b)
c)
d)

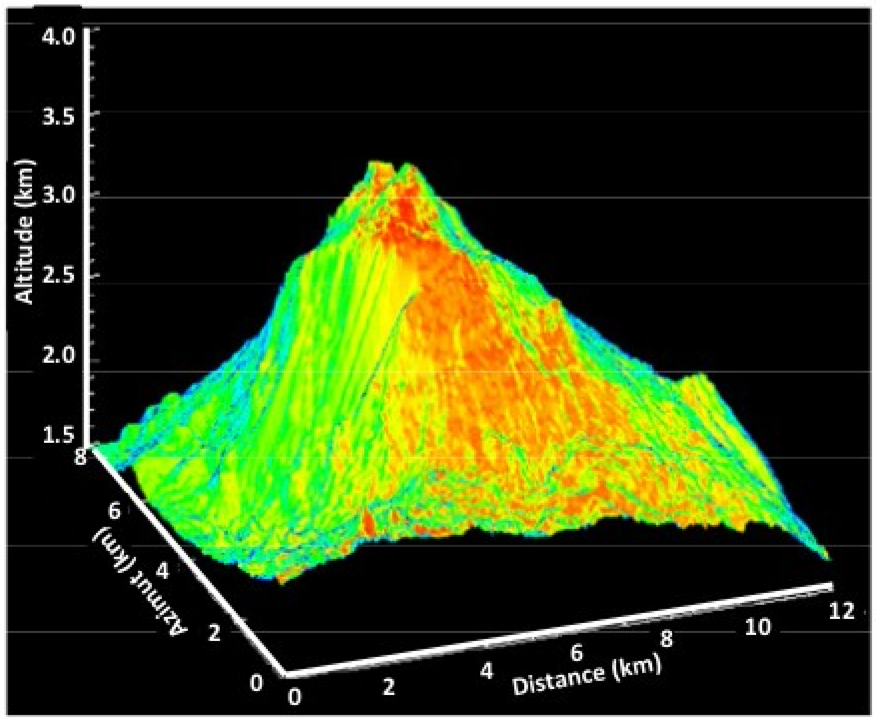
Altitude (km)
4.0
3.5
3.0
2.5
2.0
1.5
Azimut (km)
8
6
4
2
0
Distance (km)
0
2
4
6
8
10
12

Estimation of a single scatterer, M=2 images

InSAR way

$$\begin{aligned} s_1 &= a_c\,\mathrm{e}^{j\xi} \\ s_2 &= a_c\,\mathrm{e}^{j\xi+\Delta\phi} \end{aligned} \Rightarrow \begin{cases} \Delta\hat{\phi} = \arg(s_2 s_1^*) \\ \hat{I} = \frac{|s_1|^2+|s_2|^2}{2} \end{cases}$$

Linear filtering way

$$\mathbf{y} = \begin{bmatrix} s_1 \\ s_2 \end{bmatrix} = a_c\,\mathrm{e}^{j\xi} \begin{bmatrix} 1 \\ \mathrm{e}^{j\Delta\phi} \end{bmatrix}, \mathbf{a}(\phi) = \begin{bmatrix} 1 \\ \mathrm{e}^{j\phi} \end{bmatrix}$$

$$\boxed{f(\phi) = \frac{\mathbf{a}^H(\phi)\mathbf{y}}{2} = \frac{s_1 + s_2\,\mathrm{e}^{-j\phi}}{2} = a_c\,\mathrm{e}^{j\xi}\,\frac{1+\mathrm{e}^{-j(\Delta\phi-\phi)}}{2}}$$

$$\Rightarrow \begin{cases} \Delta\hat{\phi} = \arg\max_\phi |f(\phi)|^2 \\ \hat{I} = |f(\Delta\hat{\phi})|^2 \end{cases}$$

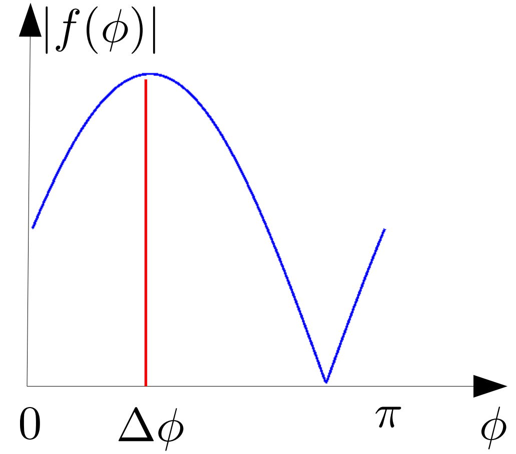

- Phase estimation → linear filtering & search
- Filter output: reflectivity
- $\mathbf{a}(\phi)$ steering vector: **matched filter**

Estimation of several scatterers, M>2 images

Estimation of several scatterers: MB InSAR way

$$\{s_1, \ldots, s_M\}, \quad s_m = \sum_{t=1}^{N_t} a_{c_t}\, e^{j\xi_t}\, e^{jk_{z_m} z_t} \quad \Rightarrow \quad ???$$

Estimation of several scatterers: linear filtering way

$$\mathbf{y} = \begin{bmatrix} s_1 \\ \vdots \\ s_M \end{bmatrix}, \mathbf{a}(z) = \begin{bmatrix} 1 \\ \vdots \\ e^{jk_{z_M} z} \end{bmatrix}$$

$$\boxed{f(z) = \frac{\mathbf{a}^H(z)\mathbf{y}}{M} = \frac{\sum_m s_m\, e^{-jk_{z_m} z}}{M}}$$

$$\Rightarrow \begin{cases} \hat{z}_t = \arg\max_{loc} |f(z)|^2 \\ \hat{I}_t = |f(\hat{z}_t)|^2 \end{cases}$$

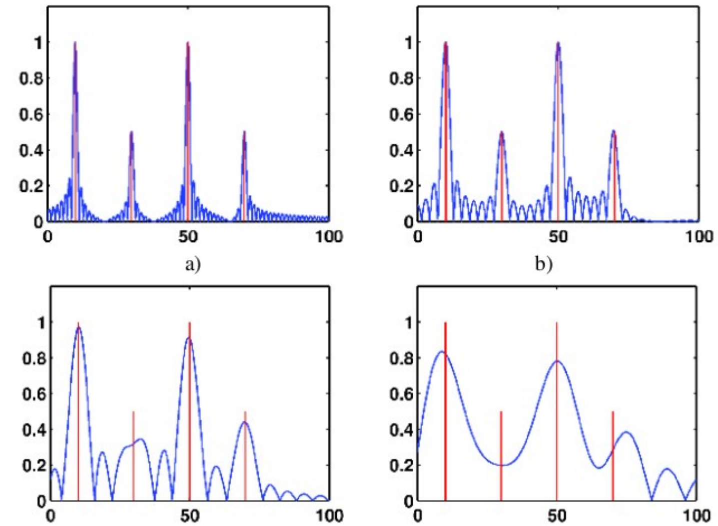

- Matched filter: **Discrete Fourier Transform**
- **Tomographic focusing: spectral estimation problem**
- Estimation quality: depends on MB-inSAR configuration

Tomographic imaging using specan

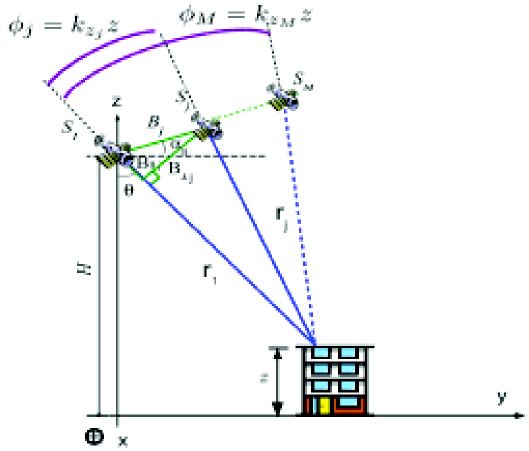

Ideal acquired signal (single scatterer)

$$\mathbf{y} = a_c\,\mathbf{a}(z_0)$$

$$\text{with} \quad \mathbf{a}(z_0) = [1, \mathrm{e}^{jk_{z_2} z_0}, \dots, \mathrm{e}^{jk_{z_M} z_0}]^T$$

Uniform baseline distribution

$$B_{\perp_i} = (i-1)B_\perp \Rightarrow k_{z_i} = (i-1)\mathrm{d}k_z$$

$$\mathbf{a}(z) = [1, \mathrm{e}^{j\mathrm{d}k_z z}, \dots, \mathrm{e}^{j(M-1)\mathrm{d}k_z z}]^T$$

Spectral sampling: $\mathrm{d}k_z = \dfrac{k_c B_\perp}{r \sin\theta}$

Spectral bandwidth: $\Delta k_z = M \mathrm{d}k_z$

$$|f(z)| = |a_c| \frac{|\mathbf{a}^H(z)\mathbf{a}(z_0)|}{M} = \frac{|a_c|}{M} \frac{|\sin(\pi \Delta k_z (z - z_0))|}{|\sin(\pi \mathrm{d}k_z (z - z_0))|}$$

Fast

M times Slower

Periodic oscillating filter output

Tomographic imaging using specan

Uniform baseline sampling $\mathbf{a}(z) = [1, \mathrm{e}^{j\mathrm{d}k_z z}, \ldots, \mathrm{e}^{j(M-1)\mathrm{d}k_z z}]^T$

$$|f(z)| = |a_c| \frac{|\mathbf{a}^H(z)\mathbf{a}(z_0)|}{M} = \frac{|a_c|}{M} \frac{|\sin(\pi \Delta k_z (z - z_0))|}{|\sin(\pi \mathrm{d}k_z (z - z_0))|}$$

Fast → resolution

Slow → ambiguity

Spatial features of a tomogram

- **rapid oscillations: resolution**
- **band-limited: sidelobes**
- **sampled spectrum : spatial ambiguities**

$$\boxed{\delta z = \frac{2\pi}{\Delta k}, z_{amb} = \frac{2\pi}{\mathrm{d}k}, \delta z = \frac{z_{amb}}{M}}$$

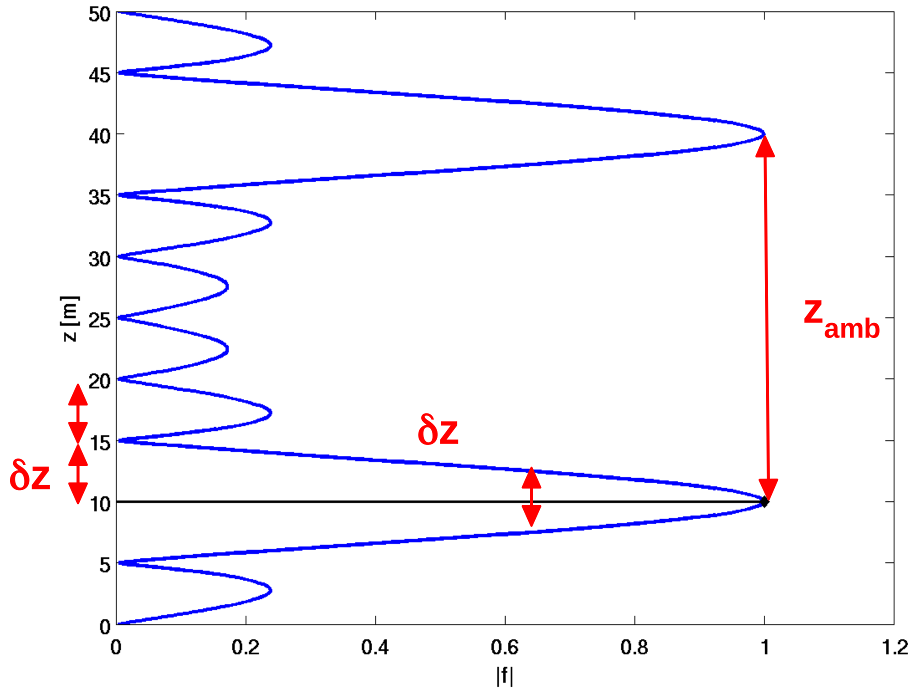

M=6

Tomographic imaging using specan

M=6

$$\Delta k_z \propto M B_\perp$$

$$\mathrm{d}k_z = \frac{\Delta k_z}{M}$$

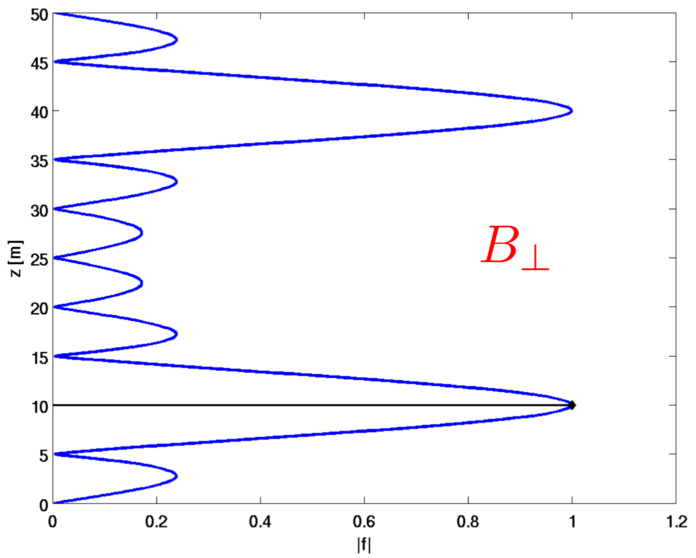

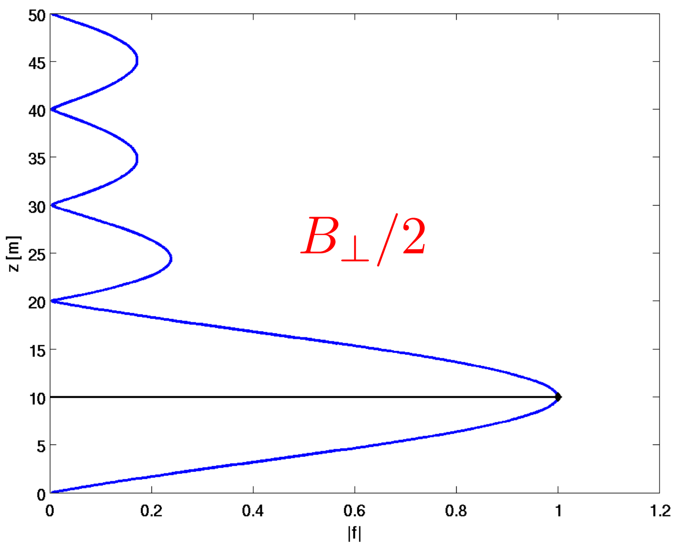

- **Reduced resolution**
- **Improved ambiguity**

Tomographic imaging using specan

M=6

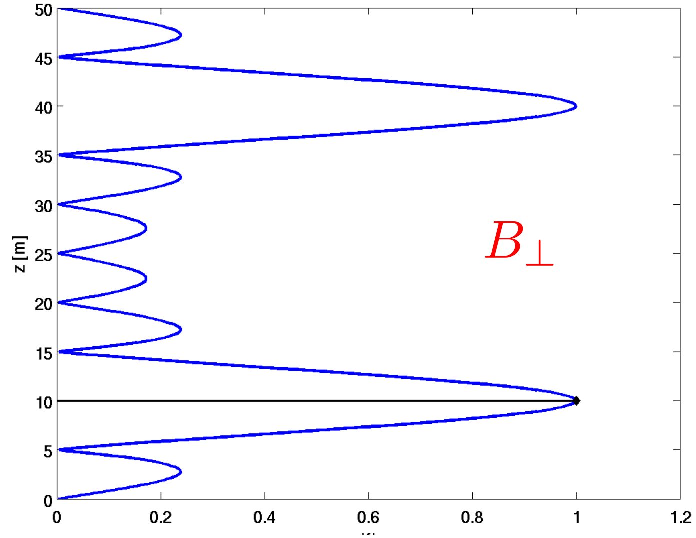

$$\boxed{\begin{aligned}\Delta k_z &\propto M B_\perp \\ \mathrm{d}k_z &= \frac{\Delta k_z}{M}\end{aligned}}$$

M=12

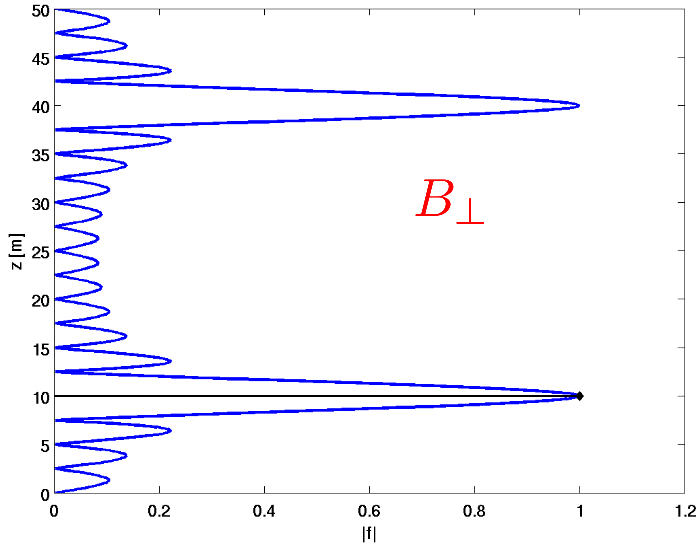

- **Improved resolution**
- **Unchanged ambiguity**

Tomographic imaging using specan

M=6

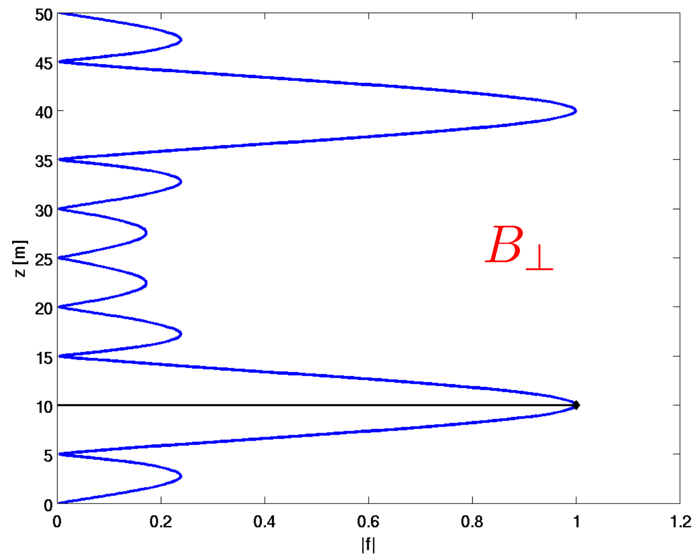

$$\Delta k_z \propto M B_\perp$$
$$\mathrm{d}k_z = \frac{\Delta k_z}{M}$$

M=12

- **Unchanged resolution**
- **Improved ambiguity**

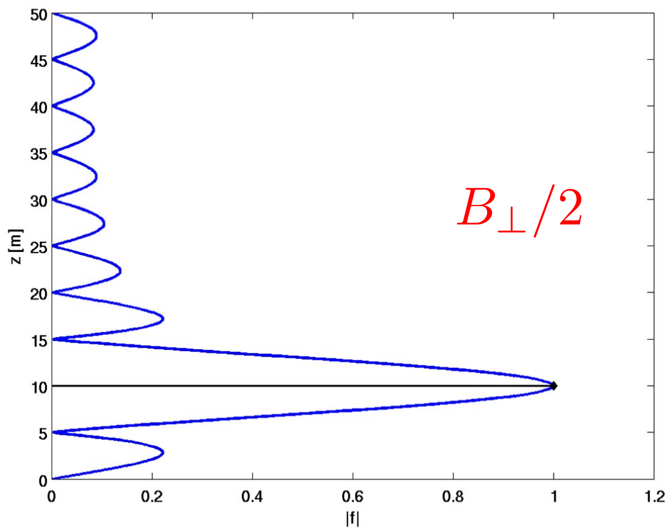

Tomographic imaging using specan

M=6

$$\Delta k_z \propto M B_\perp$$

$$\mathrm{d}k_z = \frac{\Delta k_z}{M}$$

M=12

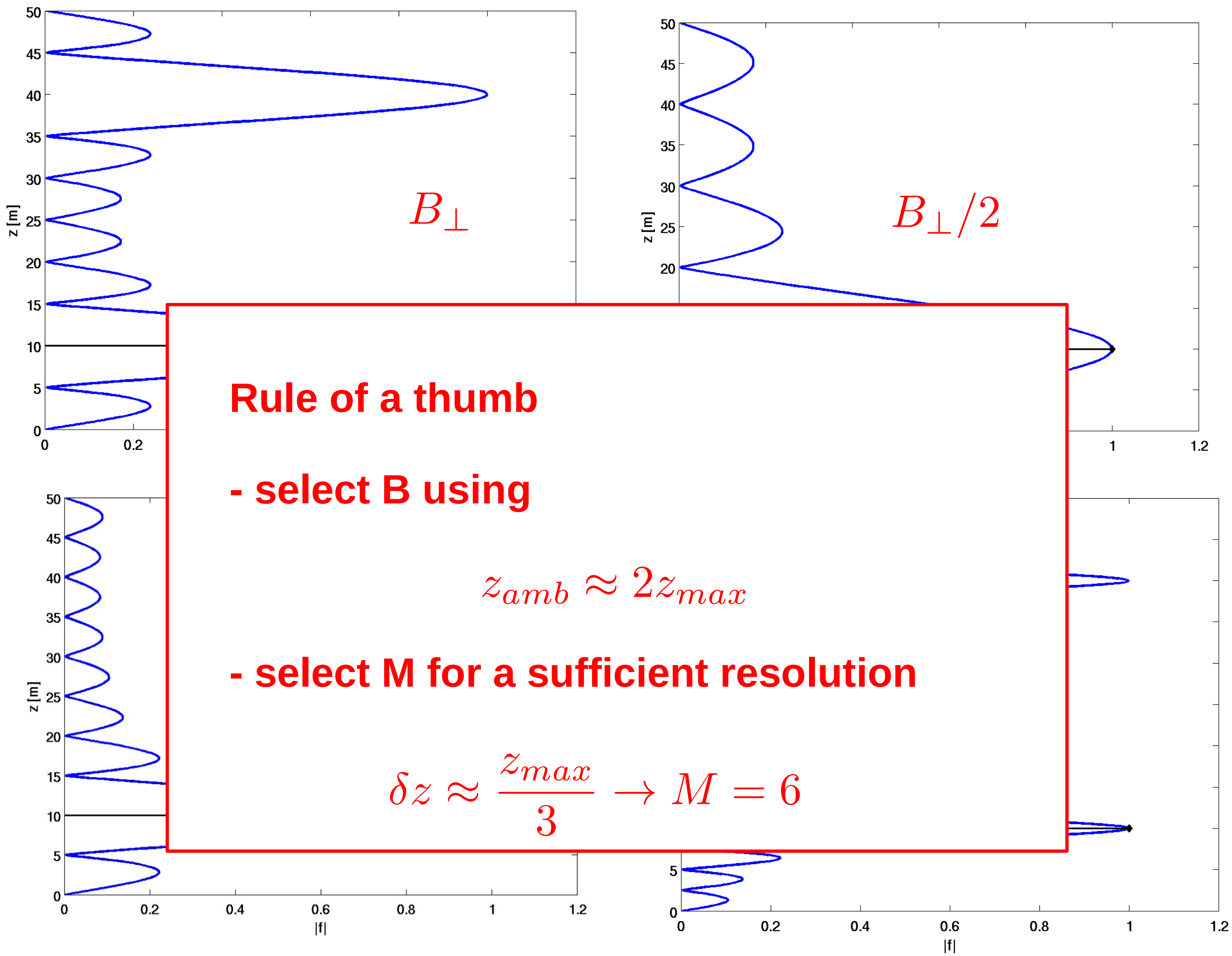

Rule of a thumb

- select B using

$$z_{amb} \approx 2 z_{max}$$

- select M for a sufficient resolution

$$\delta z \approx \frac{z_{max}}{3} \rightarrow M = 6$$

Tomographic imaging using specan

Single-look tomograms

$$\hat{I}(z) = \left| \frac{\mathbf{a}^H(z)\mathbf{y}}{M} \right|^2$$

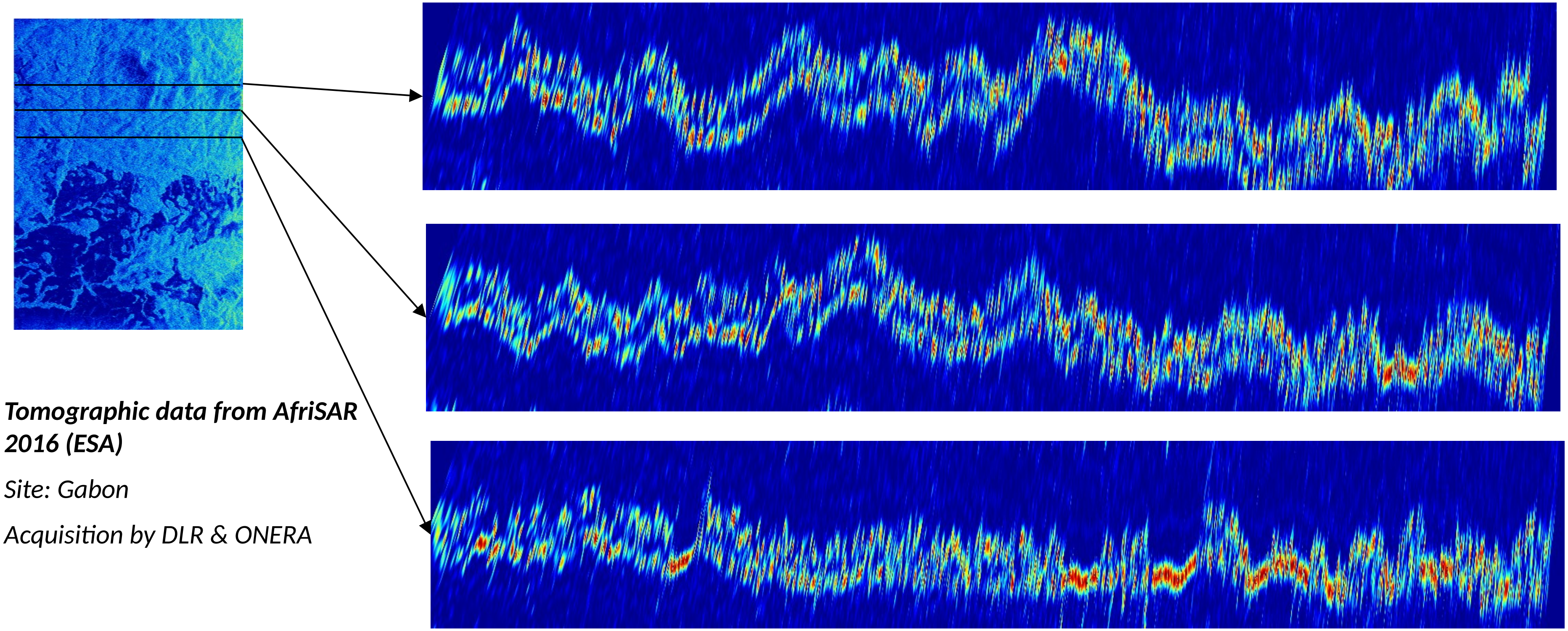

Tomographic data from AfriSAR 2016 (ESA)

Site: Gabon

Acquisition by DLR & ONERA

Noisy aspect due to speckle

TomoSAR imaging
Using multilook
Specan methods

Speckle effect

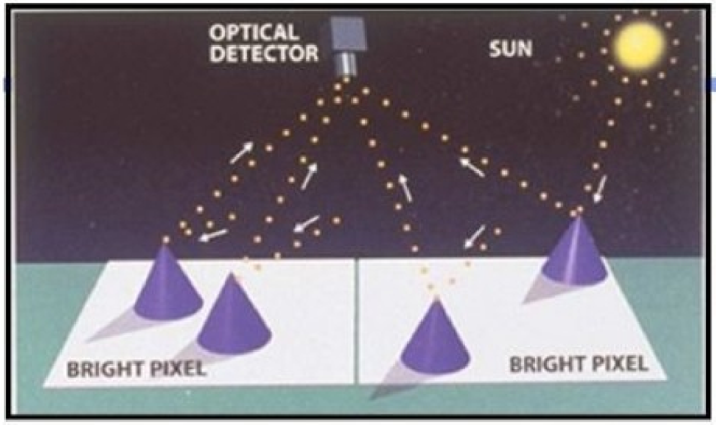

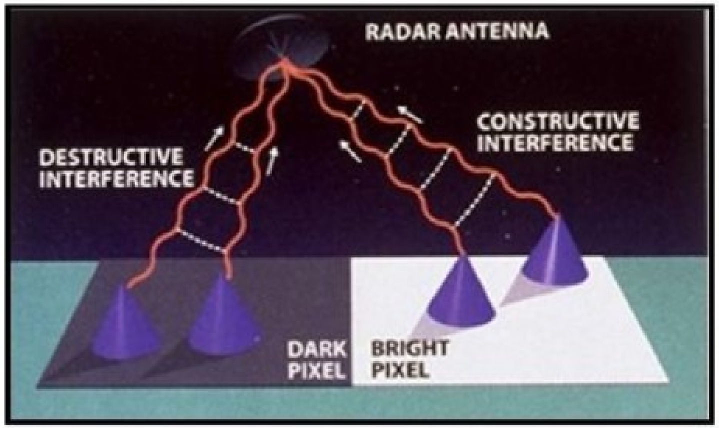

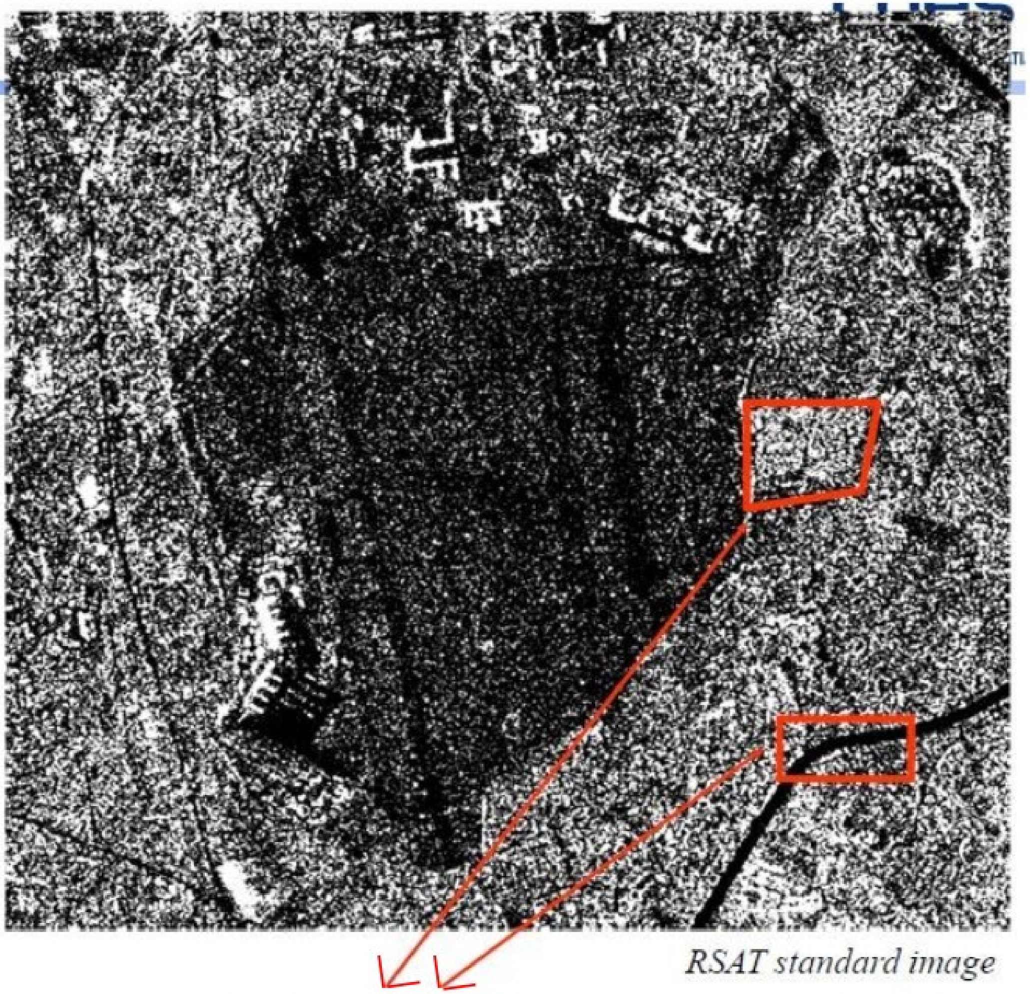

RSAT standard image

Speckle: coherent effect that appears as a Multiplicative noise

Speckle effect

$$s(x,r) \approx \int_{\mathcal{C}} a_c(x,r,\nu)\, \mathrm{e}^{-jk_c r(\nu)}\, \mathrm{d}\nu$$

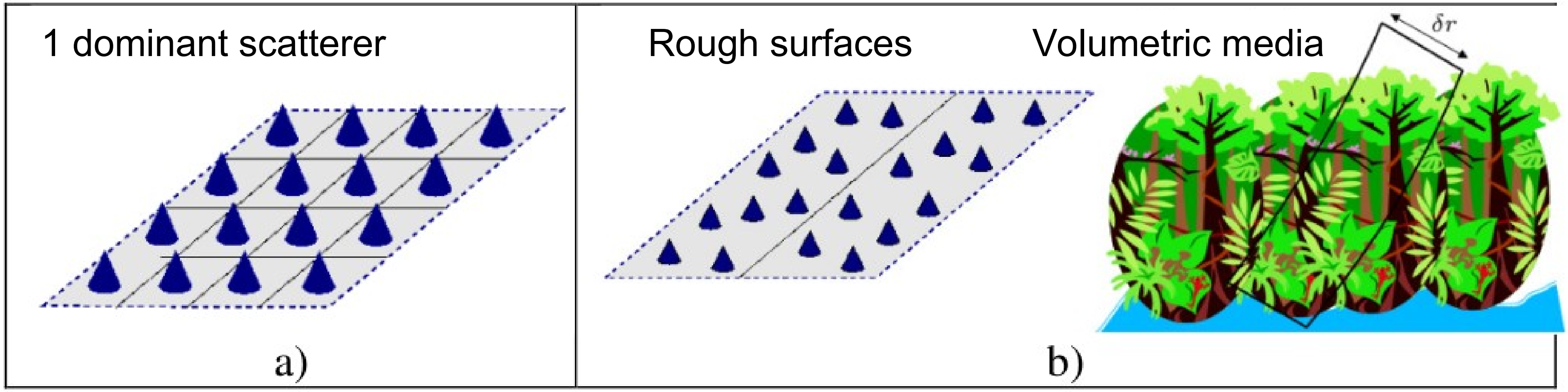

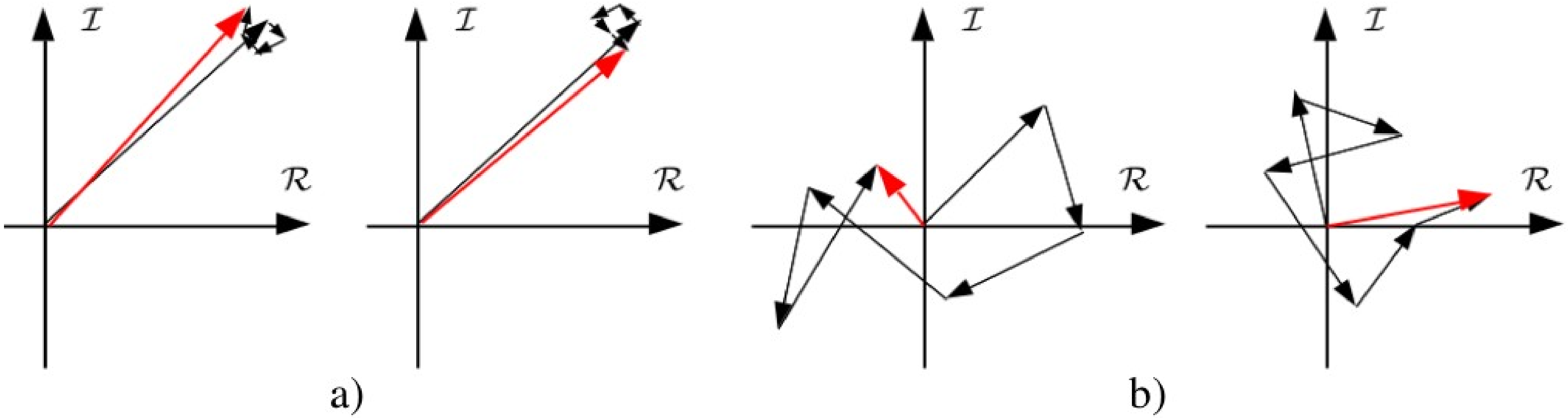

Two realizations in both cases

Speckle filtering

Unfiltered intensity image: exponential distribution

$$\hat{I} = |s(l)|^2, \quad E(\hat{I}) = I, \quad \mathrm{var}(\hat{I}) = I^2$$

L independent samples (looks): ML estimate has chi2 distribution

$$\boxed{\hat{I} = \frac{1}{L}\sum_{l=1}^{L} |s(l)|^2}, \quad E(\hat{I}) = I, \mathrm{var}(\hat{I}) = \frac{I^2}{L}$$

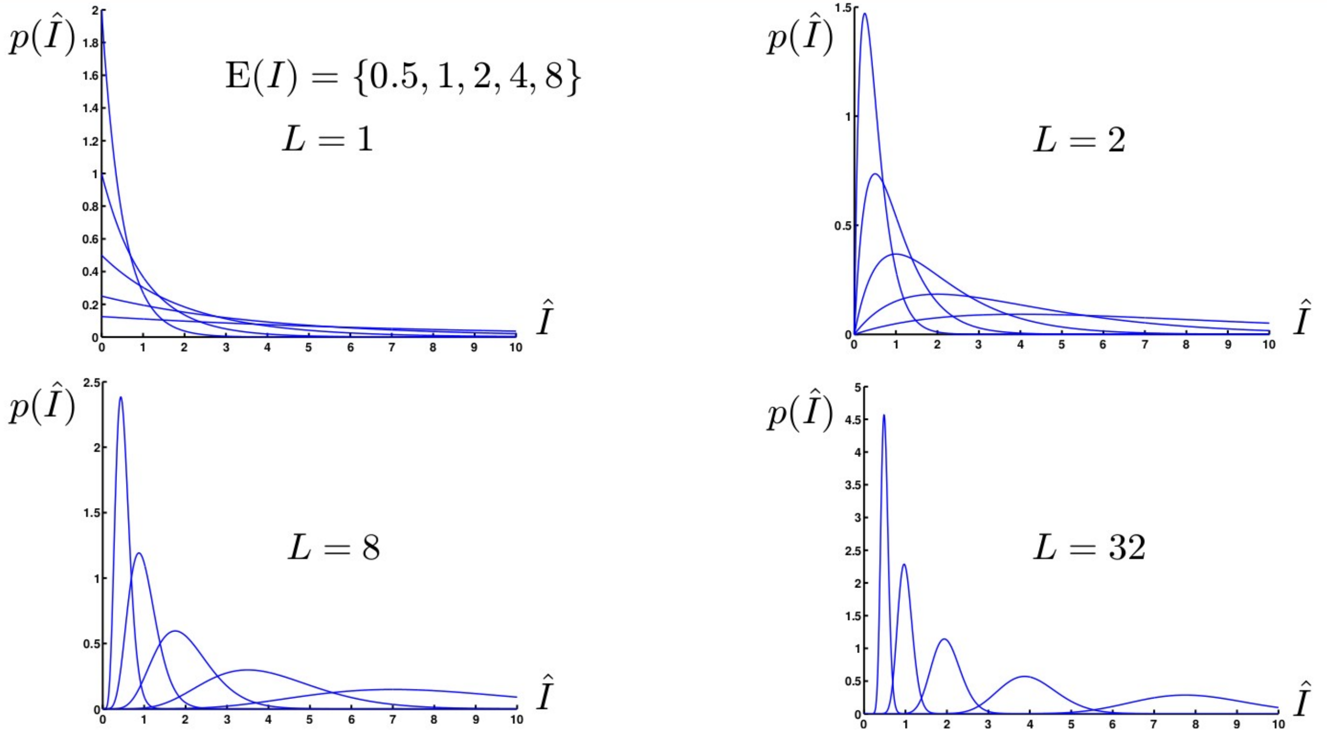

Speckle filtering

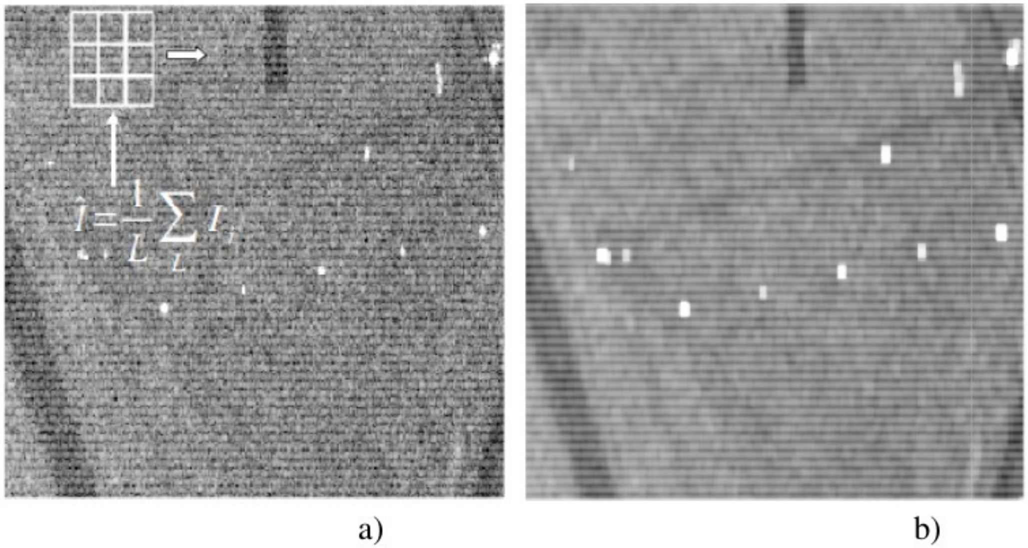

Equivalent Number of Looks

$$ENL = \frac{\mathrm{E}(\hat{I})^2}{\mathrm{var}\,\hat{I}}$$

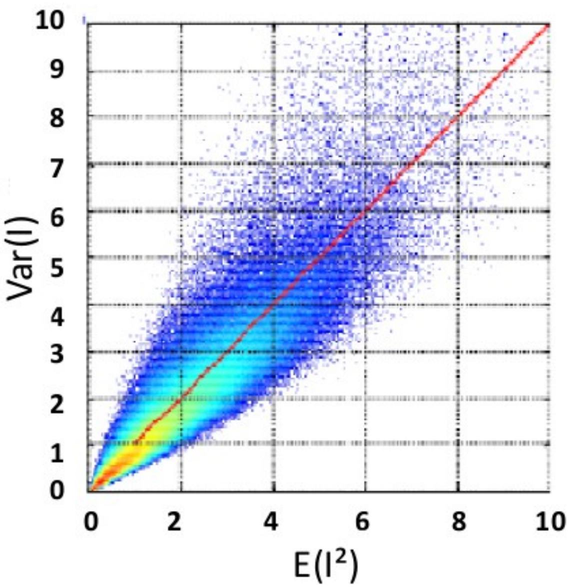

Speckle filtering

Intensity image

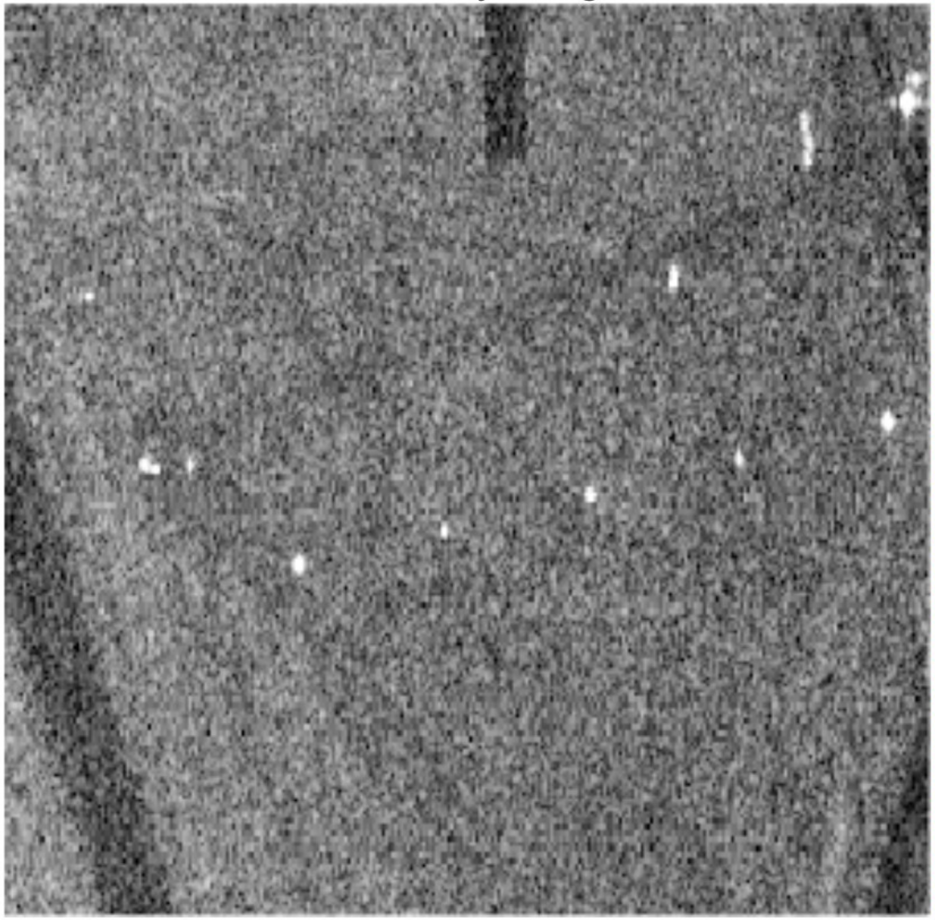

Phase image

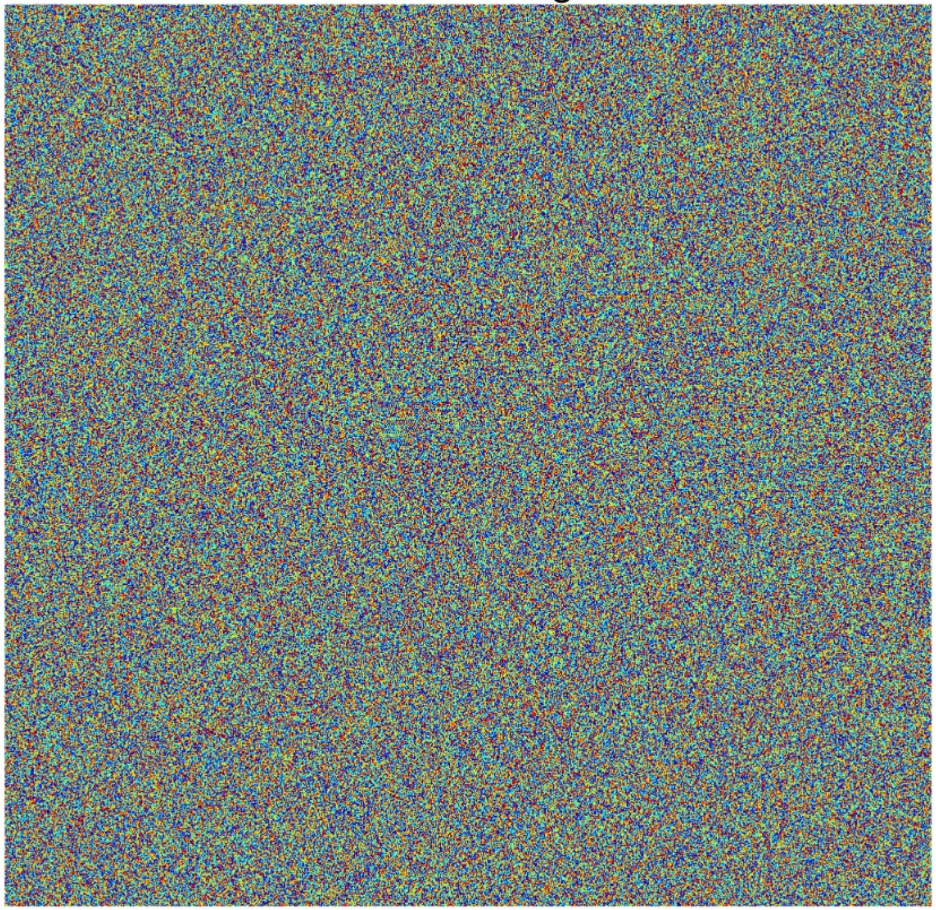

Speckle filtering

Intensity images

$$\hat{I} = \frac{1}{L}\sum_{L} I_i$$

Single look image

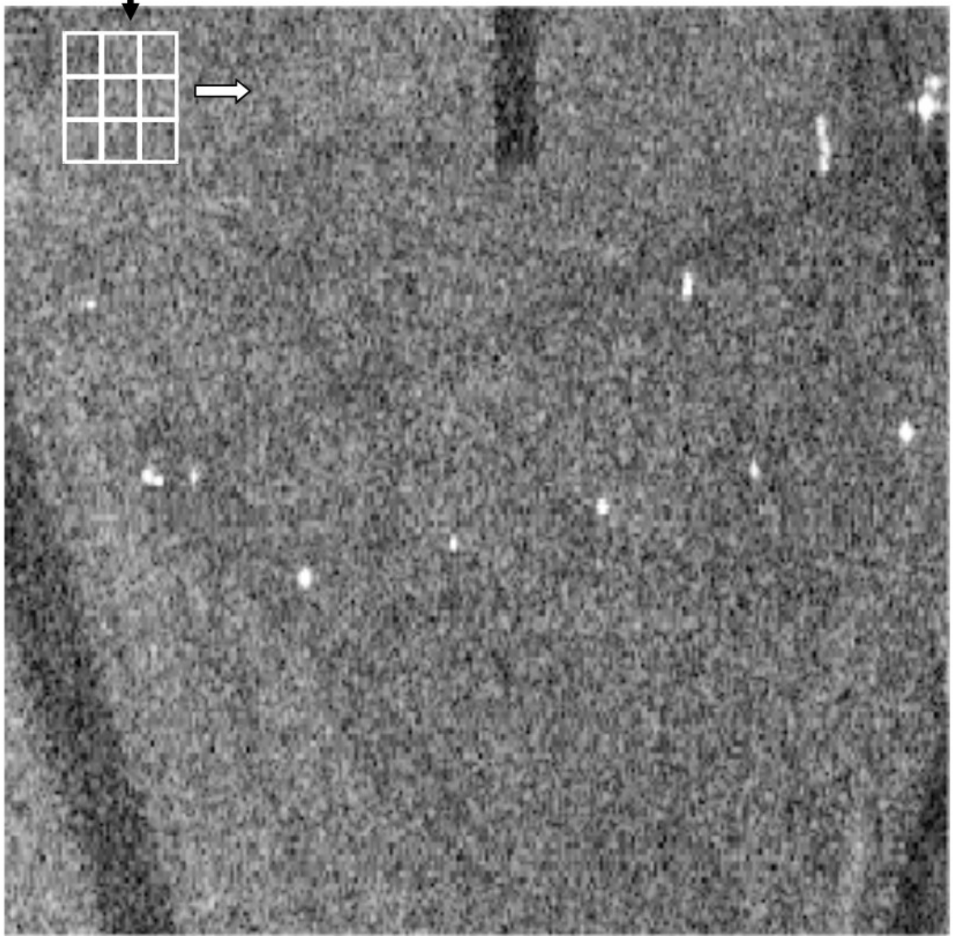

After spatial filtering (N*N boxcar)

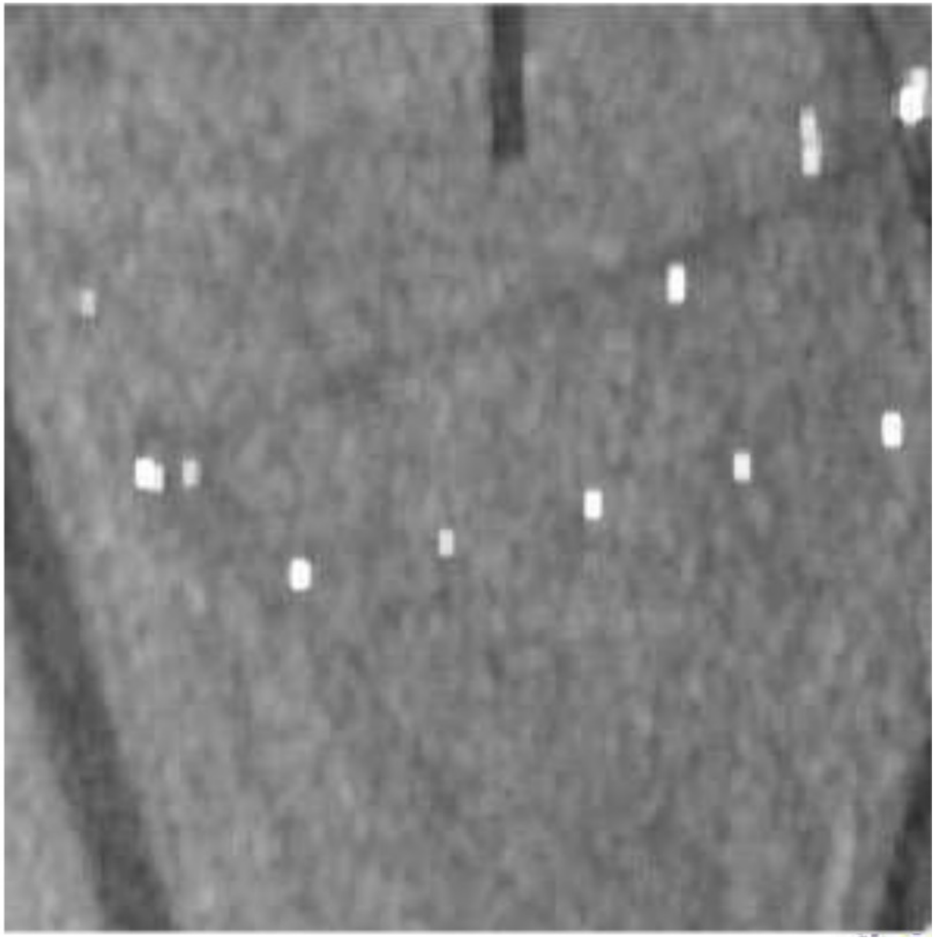

Speckle filtering

Single look image

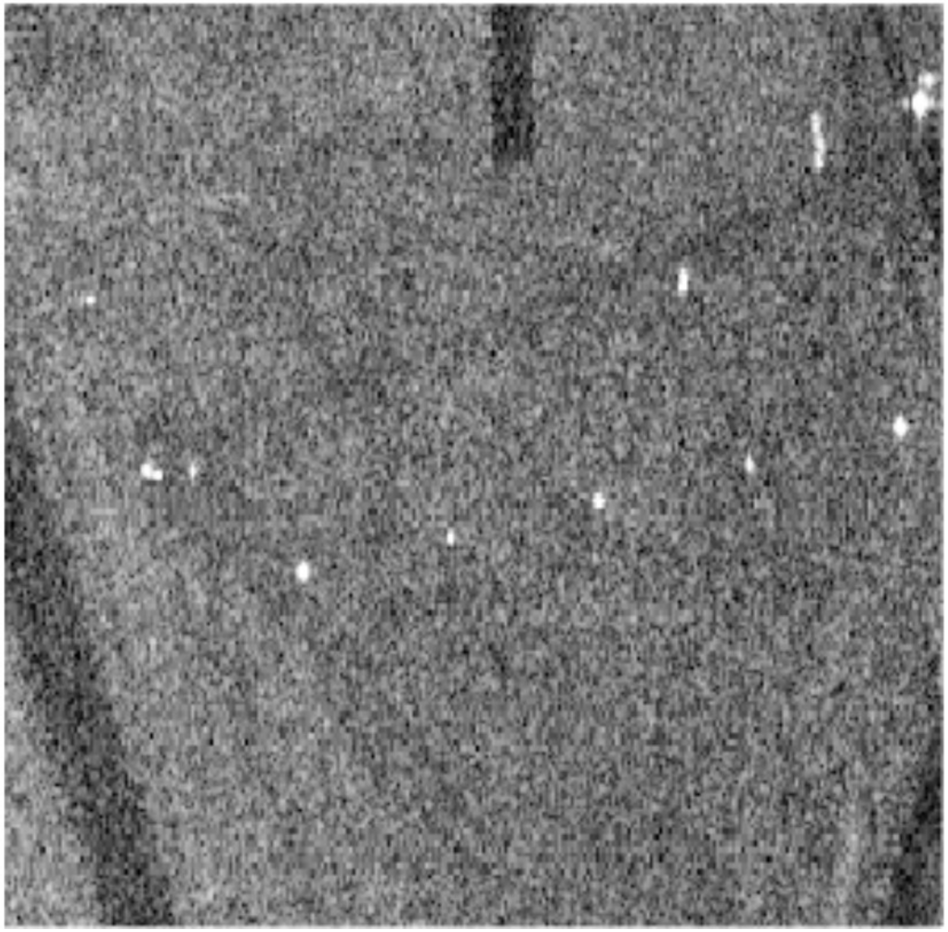

After spatial filtering (N*N Lee filter)

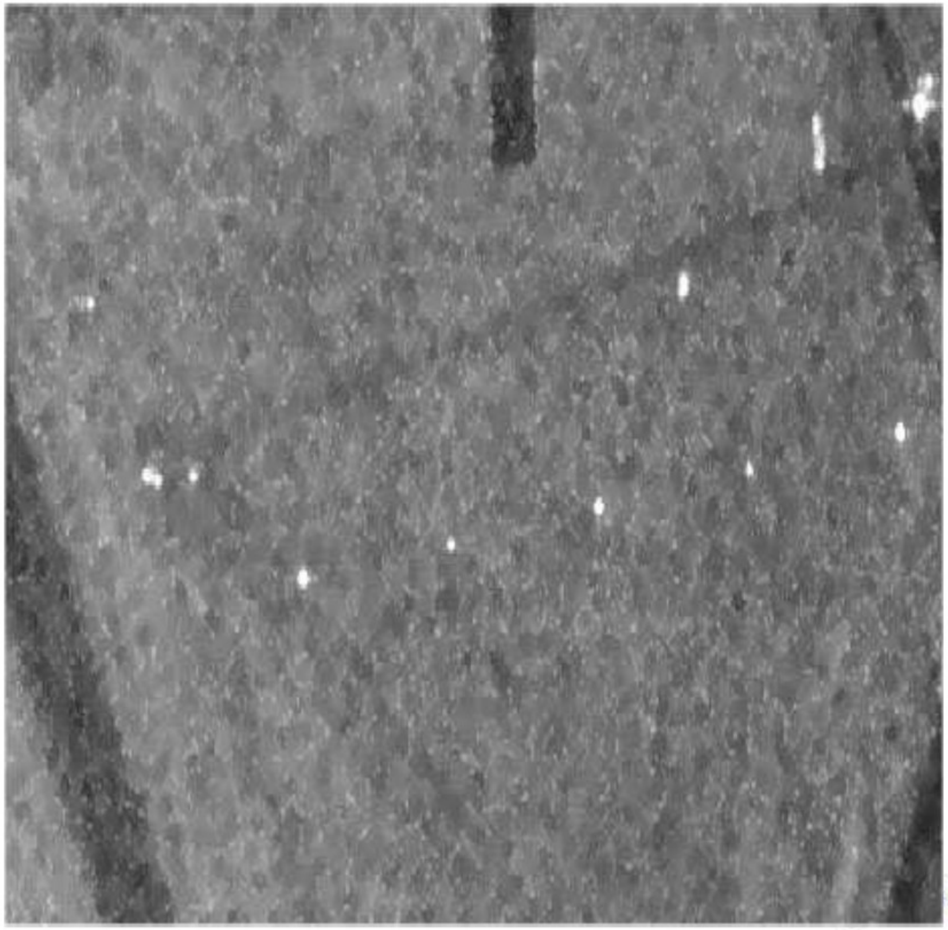

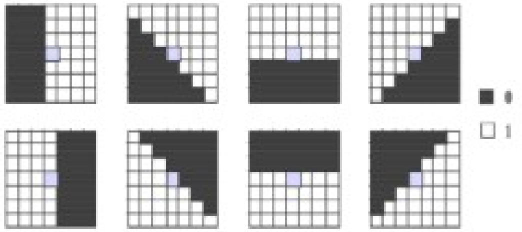

Speckle filtering

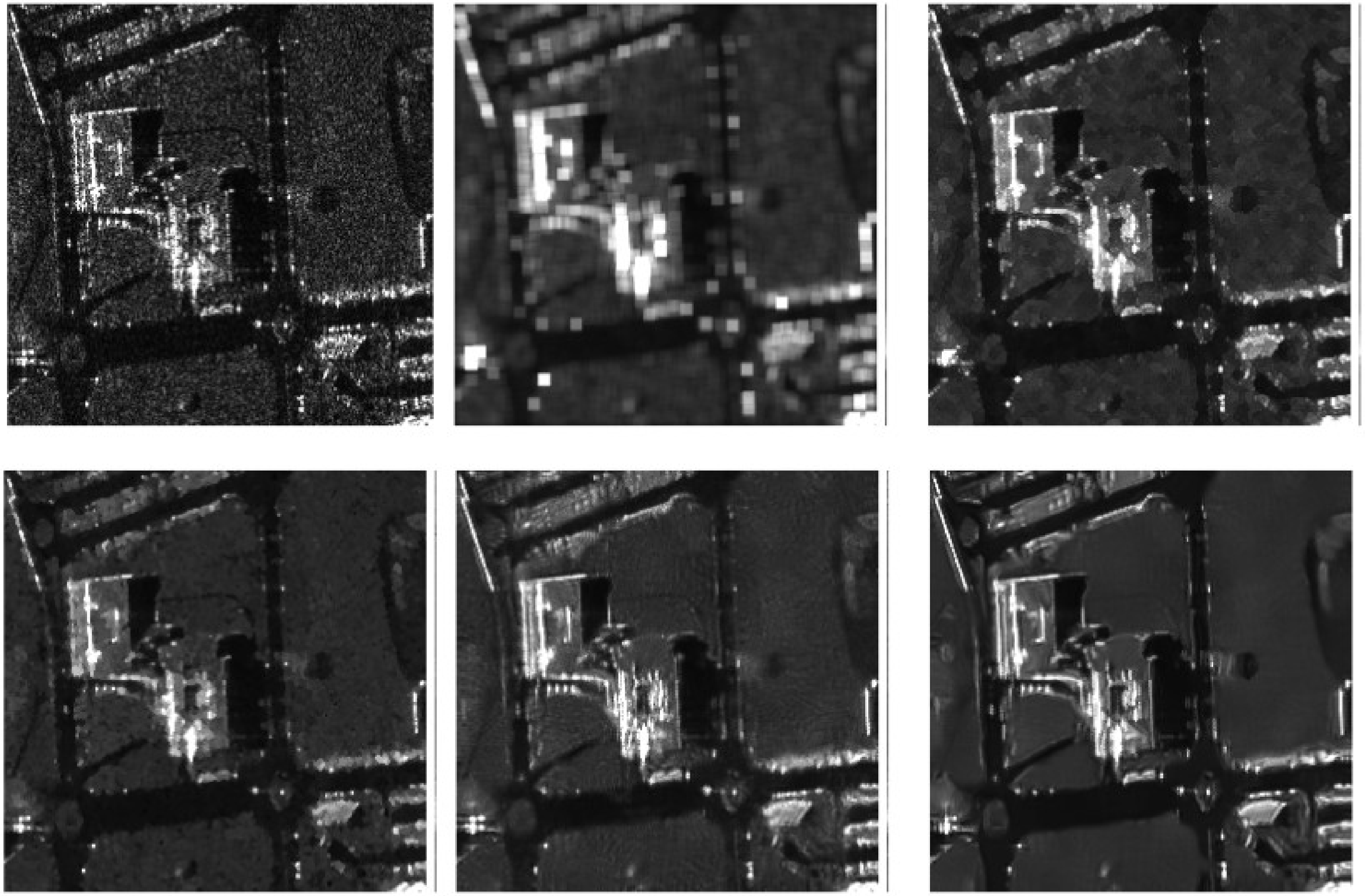

Non local speckle filtering

Speckle filtering with tomographic data

Speckle filtering for monovariate SLC SAR images

$$\boxed{\hat{I} = \frac{1}{L}\sum_{l=1}^{L} |s(l)|^2}, \quad \mathrm{E}(\hat{I}) = I, \quad \mathrm{var}(\hat{I}) = \frac{I^2}{L}$$

Speckle filtering for multivariate SLC MB-InSAR images

$$\mathbf{y} = \begin{bmatrix} s_1 \\ \vdots \\ s_M \end{bmatrix}, \mathbf{a}(z) = \begin{bmatrix} 1 \\ \vdots \\ \mathrm{e}^{jk_{z_M} z} \end{bmatrix} \qquad f(z) = \frac{\mathbf{a}^H(z)\mathbf{y}}{M} = \frac{1}{M}\sum_m s_m \, \mathrm{e}^{-jk_{z_m} z}$$

$$\hat{I}(z) = \frac{1}{L}\sum_{l=1}^{L} |f(z,l)|^2 = \frac{1}{M^2}\mathbf{a}^H(z)\widehat{\mathbf{R}}\mathbf{a}(z)$$

L-look (ML) estimate of the TomoSAR covariance matrix

$$\boxed{\widehat{\mathbf{R}} = \frac{1}{L}\sum_{l=1}^{L} \mathbf{y}(l)\mathbf{y}^H(l) \quad \mathrm{E}(\widehat{\mathbf{R}}) = \mathbf{R}}$$

TomoSAR covariance matrix

$$\boxed{\widehat{\mathbf{R}} = \frac{1}{L}\sum_{l=1}^{L}\mathbf{y}(l)\mathbf{y}^{H}(l) \quad \mathrm{E}(\widehat{\mathbf{R}}) = \mathbf{R}}$$

$$\widehat{\mathbf{R}} = \frac{1}{L}\sum_{l=1}^{L}\mathbf{y}(l)\mathbf{y}^{H}(l) = \begin{bmatrix} R_{11} & R_{12} & \dots & R_{1M} \\ R_{12}^{*} & R_{22} & \dots & R_{2M} \\ & & \ddots & \\ R_{1M}^{*} & R_{2M}^{*} & \dots & R_{MM} \end{bmatrix}$$

$$\hat{R}_{ii} = \frac{1}{L}\sum_{l=1}^{L} y_i(l)y_i^{*}(l) = \hat{I}_i \qquad \hat{R}_{ij} = \frac{1}{L}\sum_{l=1}^{L} y_i(l)y_j^{*}(l) = \sqrt{\hat{I}_i\hat{I}_j}\,\hat{\gamma}_{ij}$$

Interferometric coherence estimate

$$\hat{\gamma}_{ij} = \frac{\hat{R}_{ij}}{\sqrt{\hat{I}_i\hat{I}_j}} \qquad \hat{\phi}_{ij} = \arg(\hat{\gamma}_{ij}) \qquad |\hat{\gamma}_{ij}| \leq 1$$

Beamformer <u>is</u> Fourier imaging

$$\boxed{\hat{I}_{BF}(z) = \frac{1}{M^2}\mathbf{a}^H(z)\widehat{\mathbf{R}}\,\mathbf{a}(z)}$$

- Excellent (optimal) statistical accuracy
- Fourier resolution: $\delta z = \dfrac{2\pi}{\Delta k}$
- Cannot handle closely spaced scatterers
- High sidelobes

Capon's solution: constrained beamformer

Objective: minimize output power, with unitary gain at the height of interest

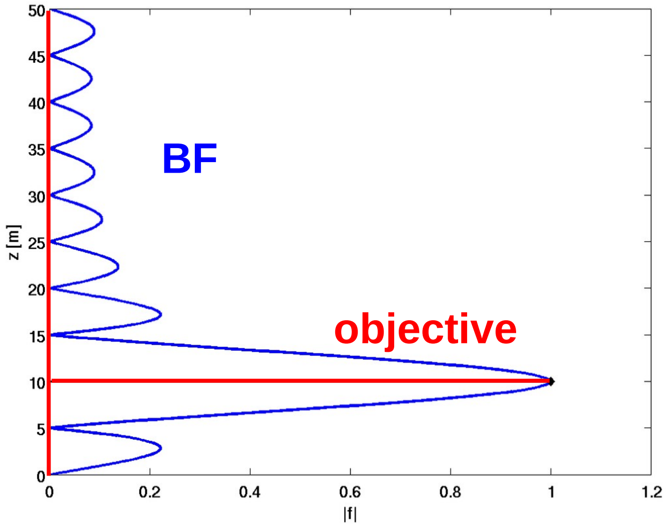

$$\mathbf{v}_{CP}(z) = \arg\min_{\mathbf{v}} \mathrm{E}(|\mathbf{v}^H\mathbf{y}|^2) \quad \text{s.t,} \quad \mathbf{v}^H\mathbf{a}(z) = 1$$

Solution: $$\boxed{\hat{I}_{CP} = \frac{1}{\mathbf{a}^H(z)\widehat{\mathbf{R}}^{-1}\mathbf{a}(z)}}$$

Tomographic imaging using specan

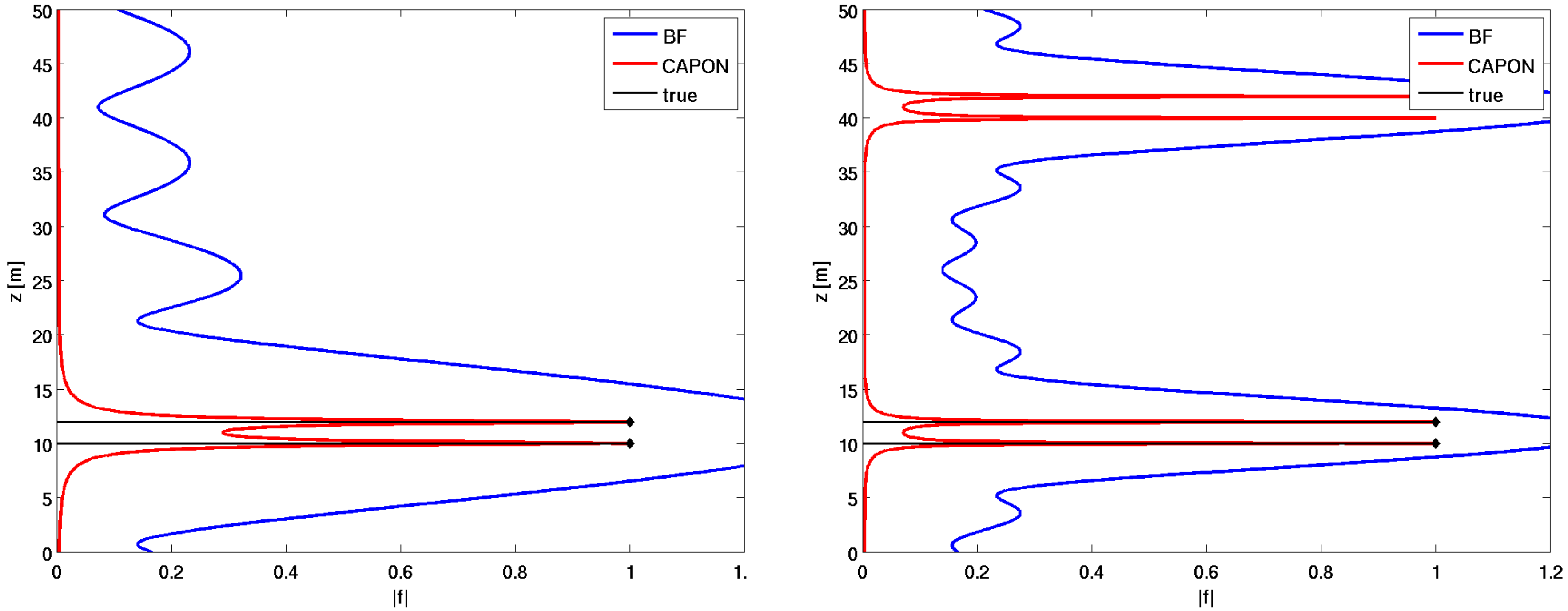

- **Capon: significantly improved resolution**
- **Resolution improvement is a function of the Signal to Noise Ratio (SNR)**
- **For regular baselines, BF & Capon are equally affected by ambiguities**

Irregular baseline sampling: logscale distribution

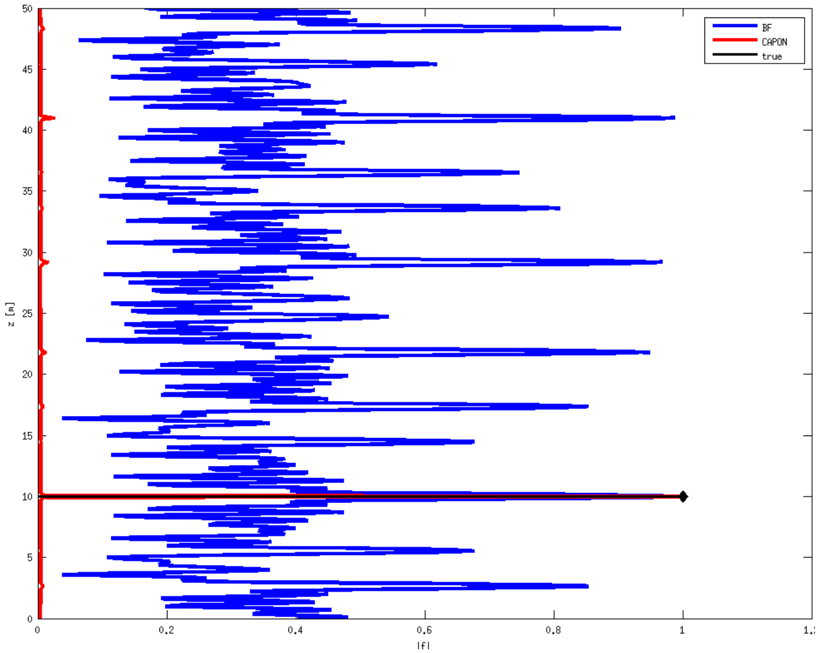

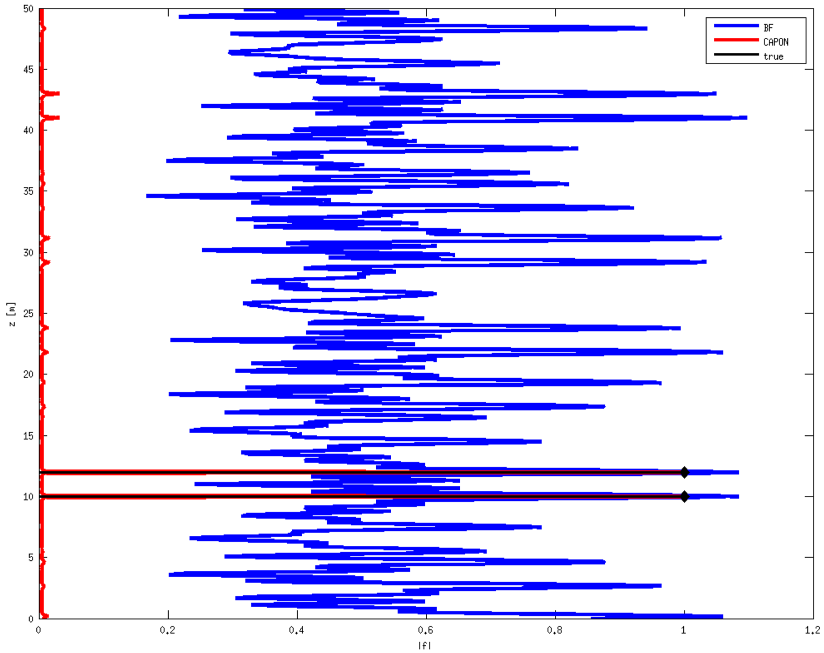

- BF: strongly affected by ambiguities
- CAPON: asynchronous ambiguities are considered as perturbations and filtered (may be dangerous!). Good resolution performance preserved

Practical implementation

- Asymptotic (L→ +∞) estimators

$$\boxed{I_{BF}(z) = \frac{\mathbf{a}^H(z)\mathbf{R}\mathbf{a}(z)}{M^2}} \qquad \boxed{I_{CP}(z) = \frac{1}{\mathbf{a}^H(z)\mathbf{R}^{-1}\mathbf{a}(z)}}$$

- In practice, spatial averaging

$$\mathbf{R} \to \widehat{\mathbf{R}} = \frac{1}{L}\sum_{l=1}^{L}\mathbf{y}(l)\mathbf{y}^H(l)$$

- BF: quite stable w.r.t L
- Capon may suffer from a poor covariance matrix conditioning: sufficient ENL needed

⇒ Diagonal Loading $\widetilde{\mathbf{R}} = \widehat{\mathbf{R}} + \alpha\mathbf{I}_M, \quad \alpha \geq 0$

For large α (low SNR): CP → BF

Tomographic imaging using specan

Tropical forest profile at P band with residual phase errors

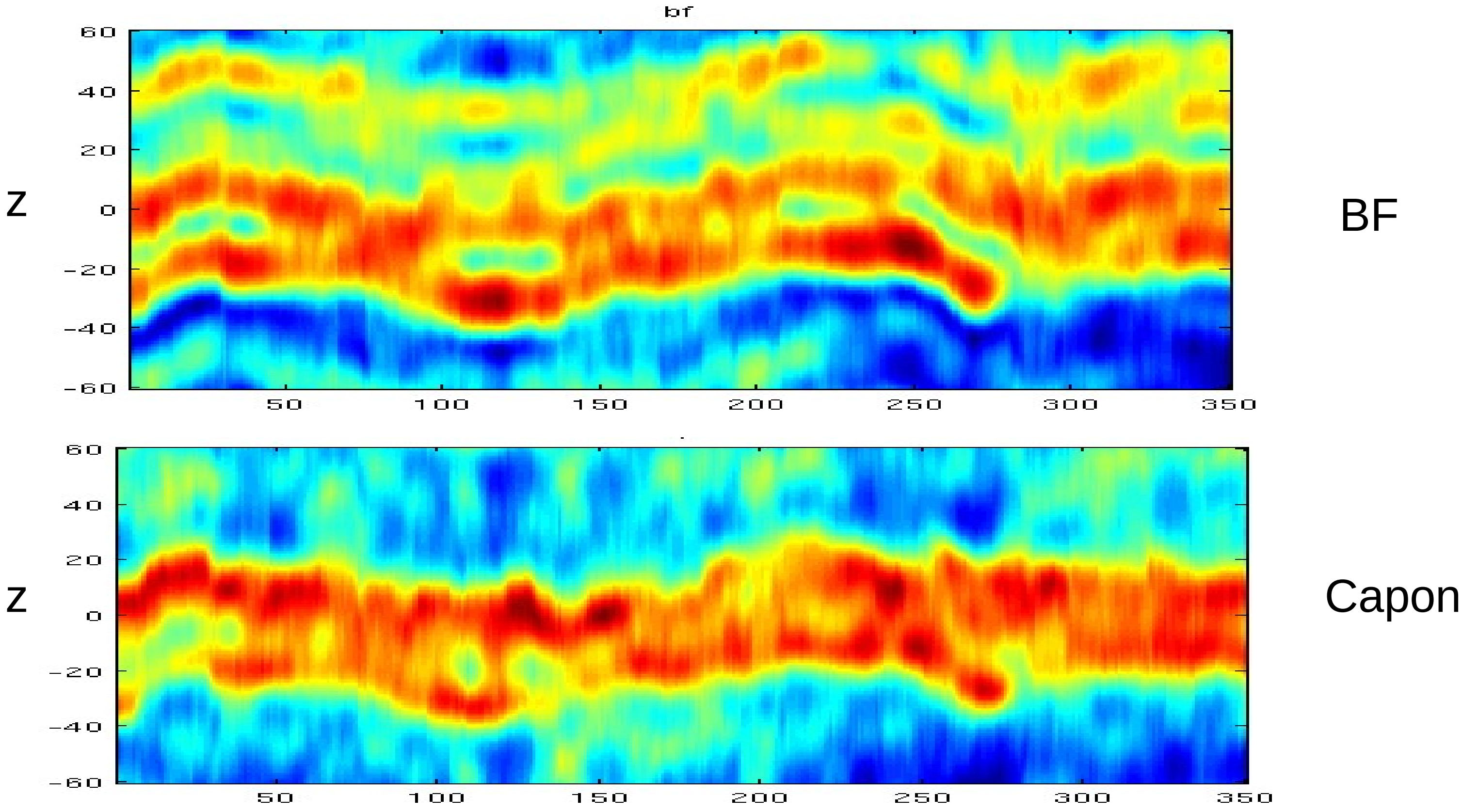

Tomographic imaging using specan

P band tomogram (Tomosense campaign) with residual phase errors

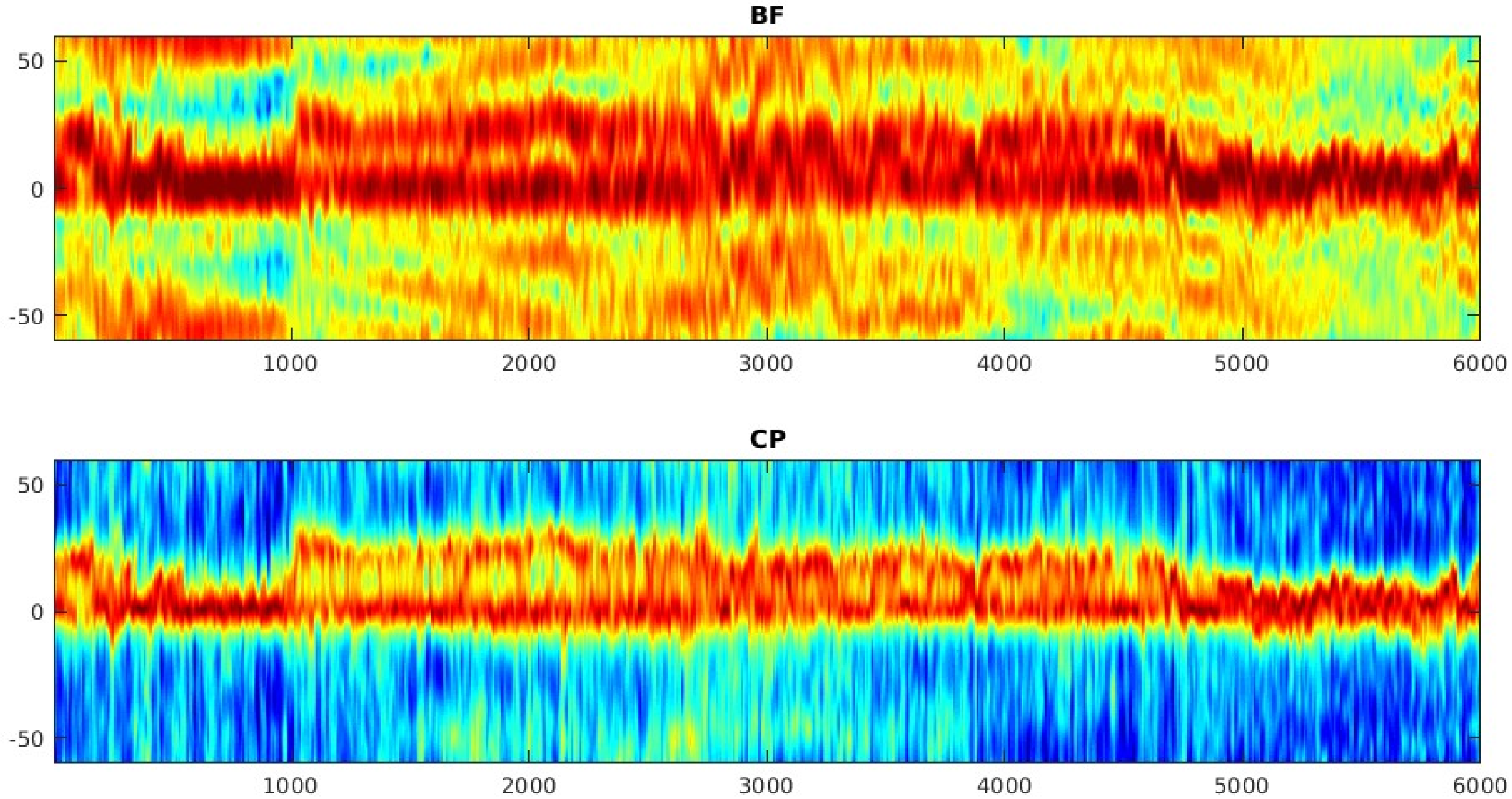

Case study: BIOSAR 2 data

Forest height

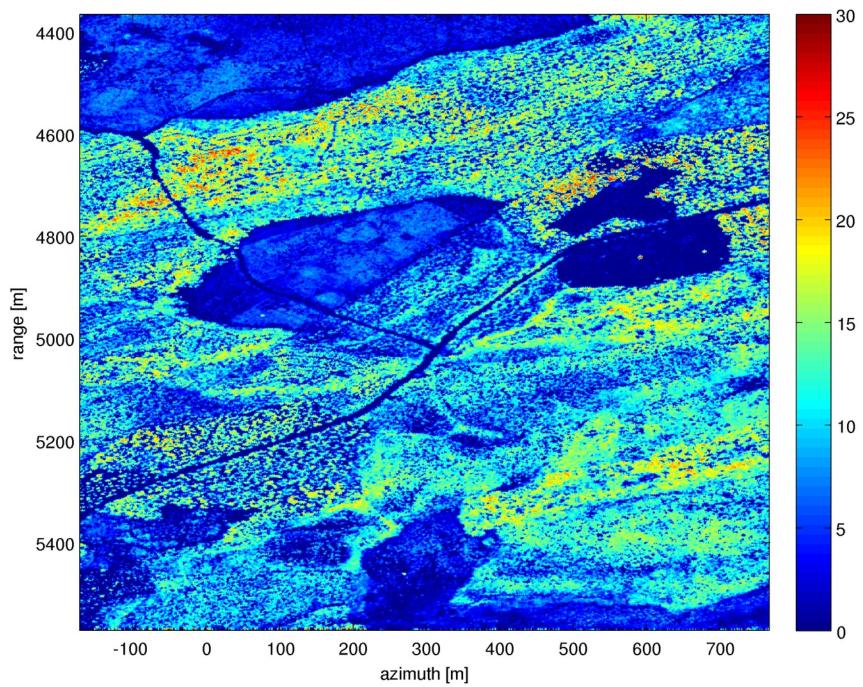

HH intensity

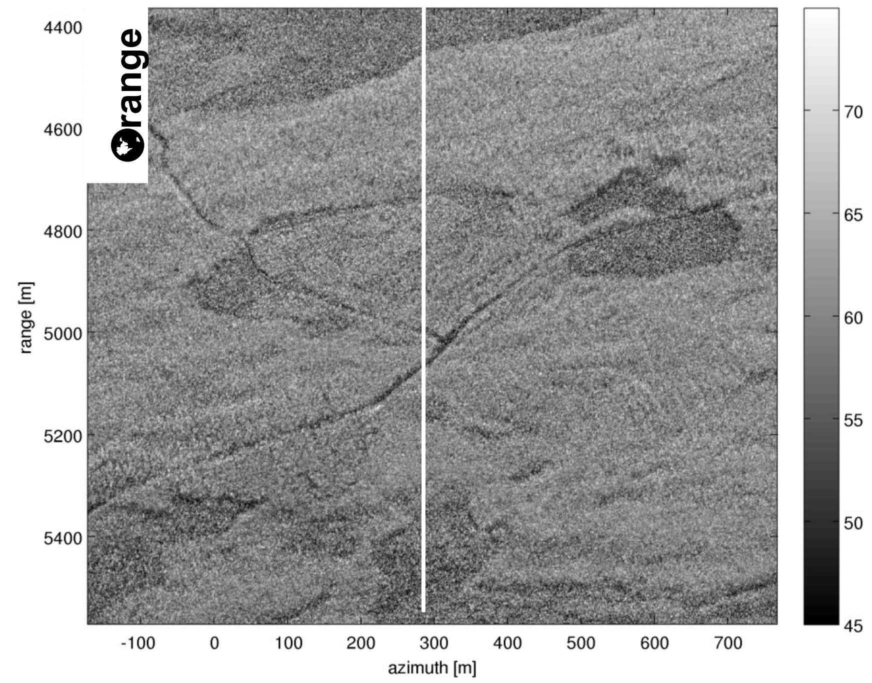

DEM

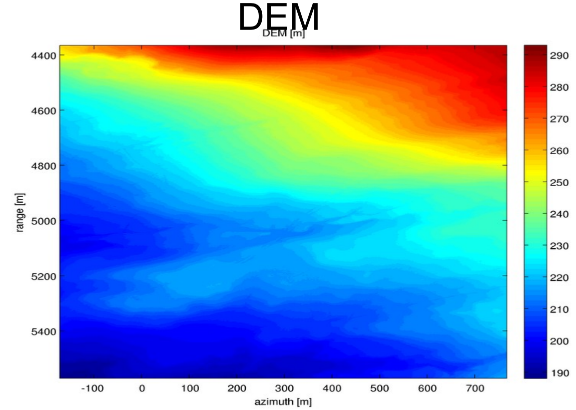

Case study: BIOSAR 2 data

BF

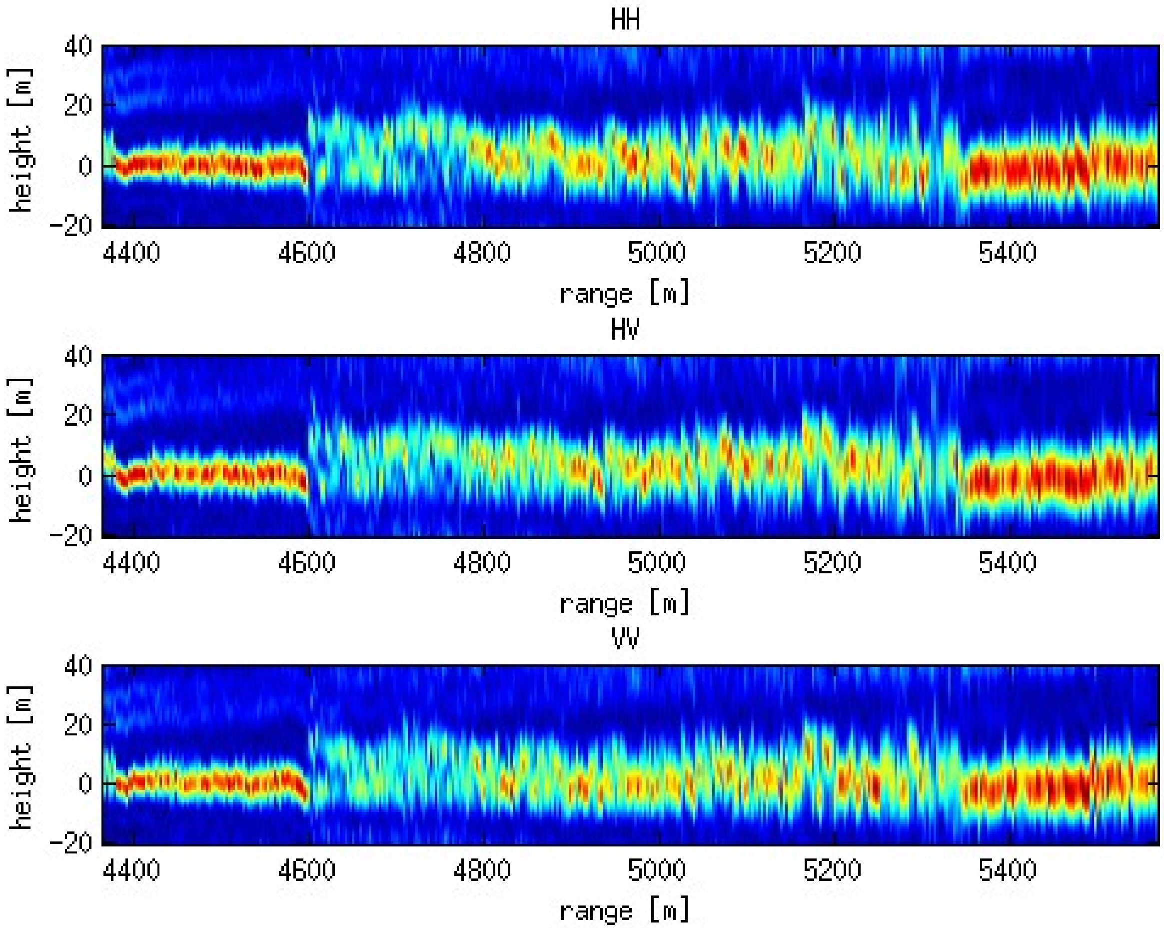

CAPON: processing OK ?

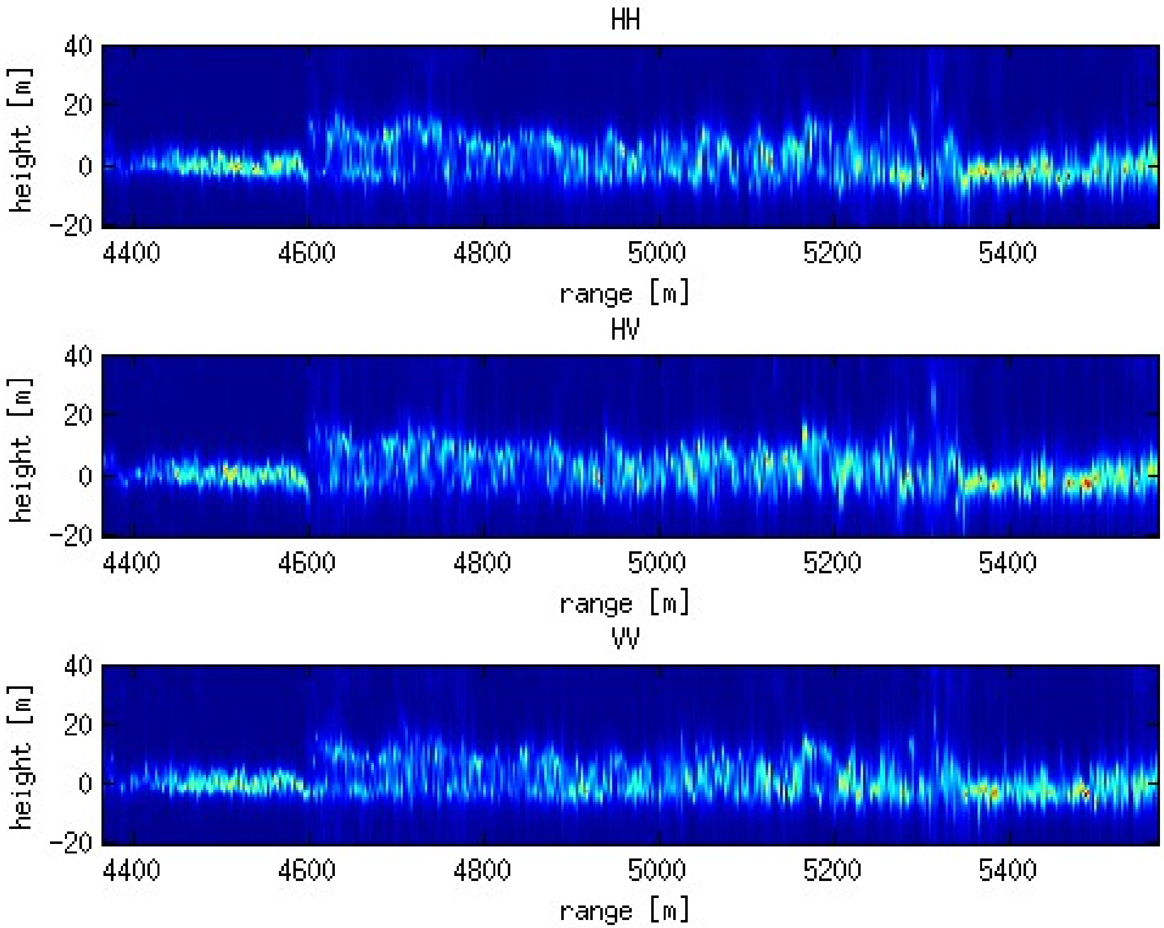

Advanced

TomoSAR imaging

Using Specan methods

3-D imaging of an urban area using a minimal configuration

Urban area test site

- Images over Dresden, 2000
- DLR's E-SAR at L-Band
- Resolution : 0.5 m × 2.5 m
- Fully polarimetric
- Dual-baseline InSAR

Baselines	H_{am}
10 m	55-73 m
40 m	14-18 m

3 PolSAR images

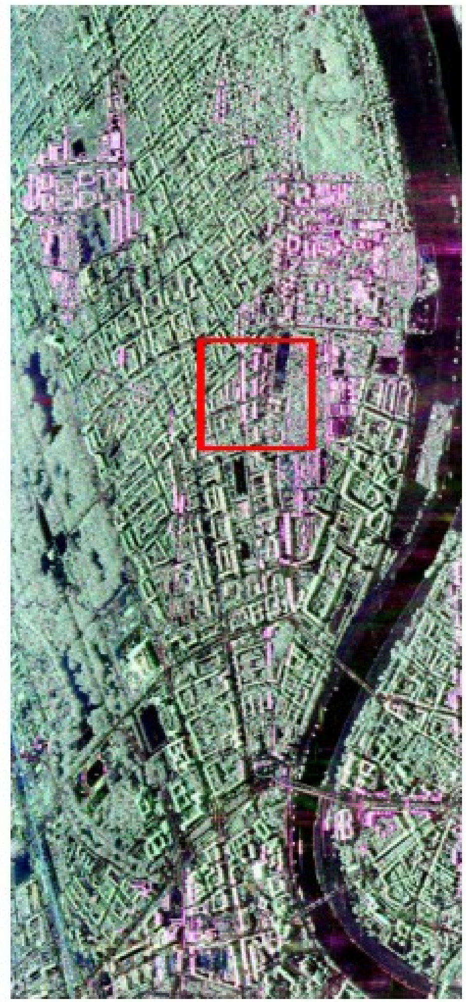

Pauli-coded SAR image

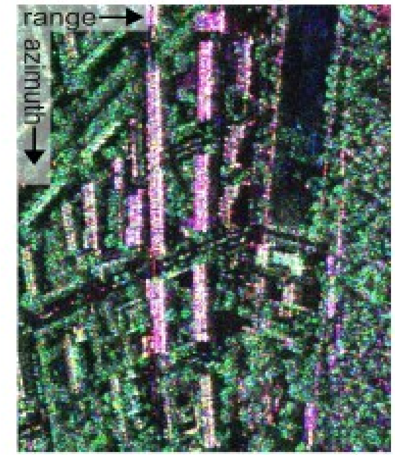

Optical image

SAR tomography over urban areas

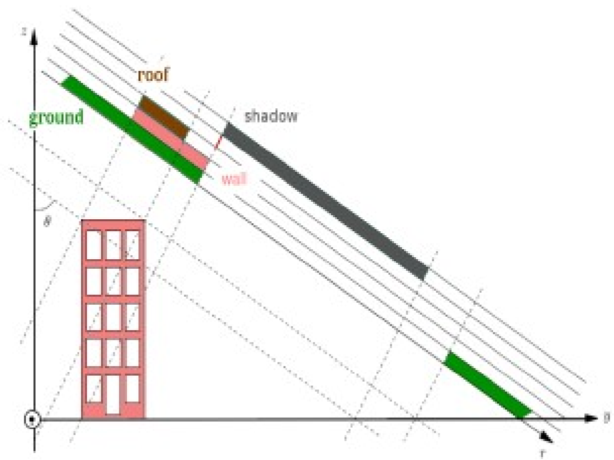

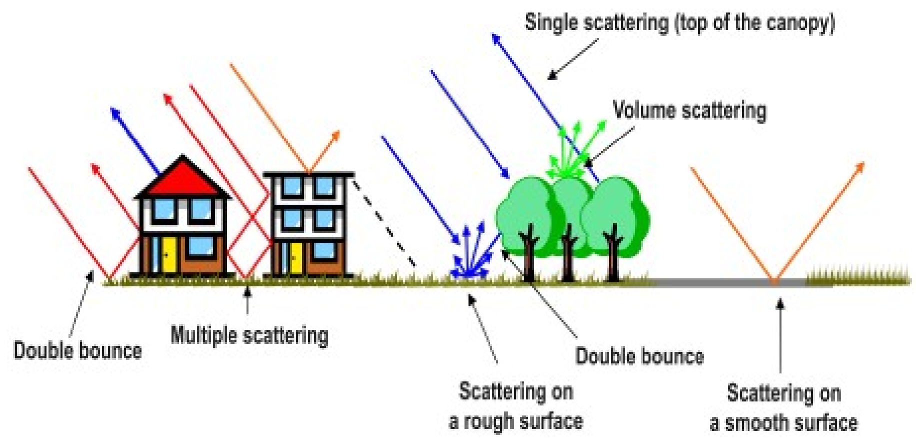

- L-band intermediate-resolution data sets
  $\Rightarrow$ High-Resolution (HR) tomographic estimators
- 3 images
  $\Rightarrow N_s = 2$

Tomographic imaging using specan

Critical configuration **(3 images)** in an urban environment at L band

(a) Optical image (b) SAR

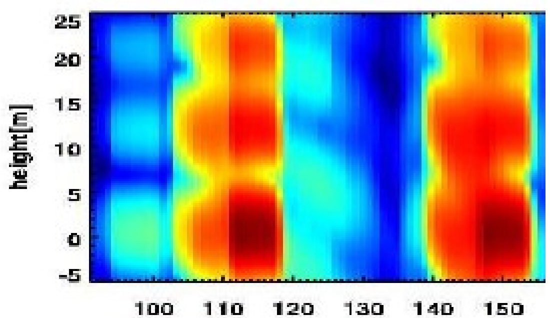

BF

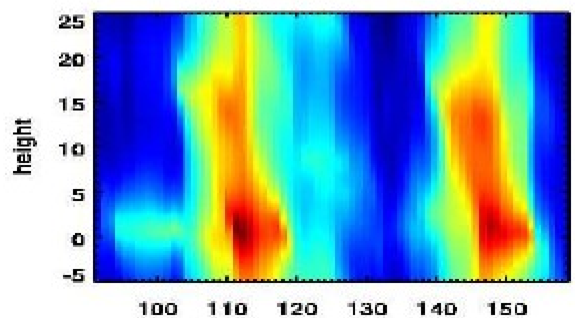

CAPON

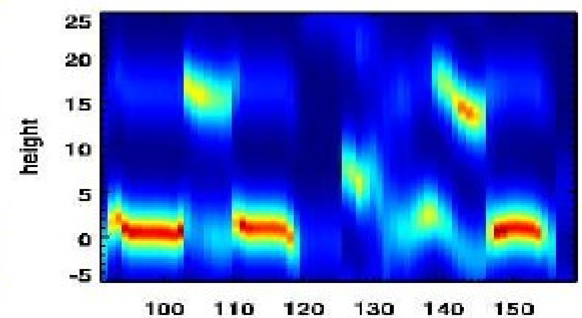

MUSIC

- Strictly speaking, Capon's technique is not HR, but is very convenient
- MUSIC (and some other techniques) is HR

Polarimetric SAR tomography over urban areas

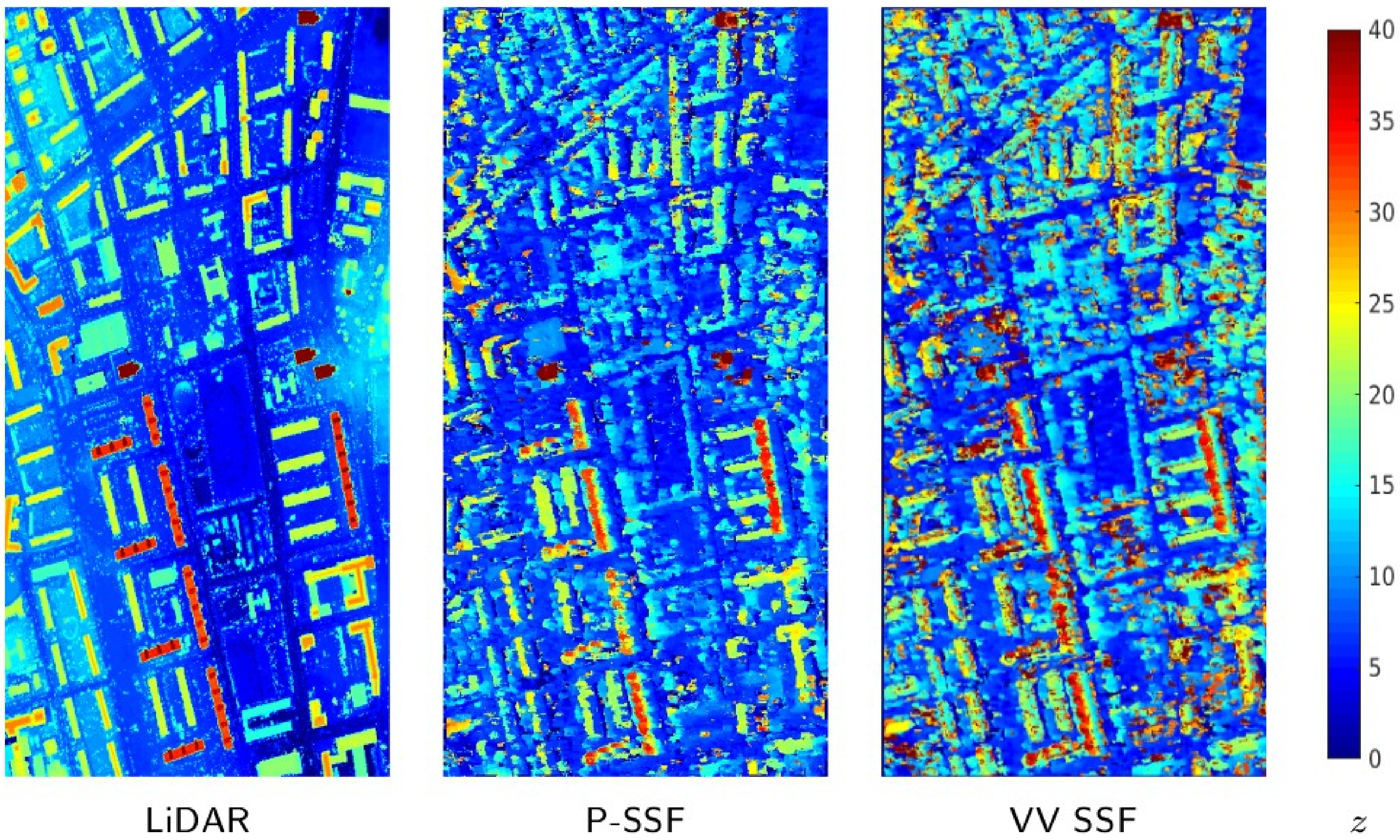

Polarimetric SAR tomography over urban areas

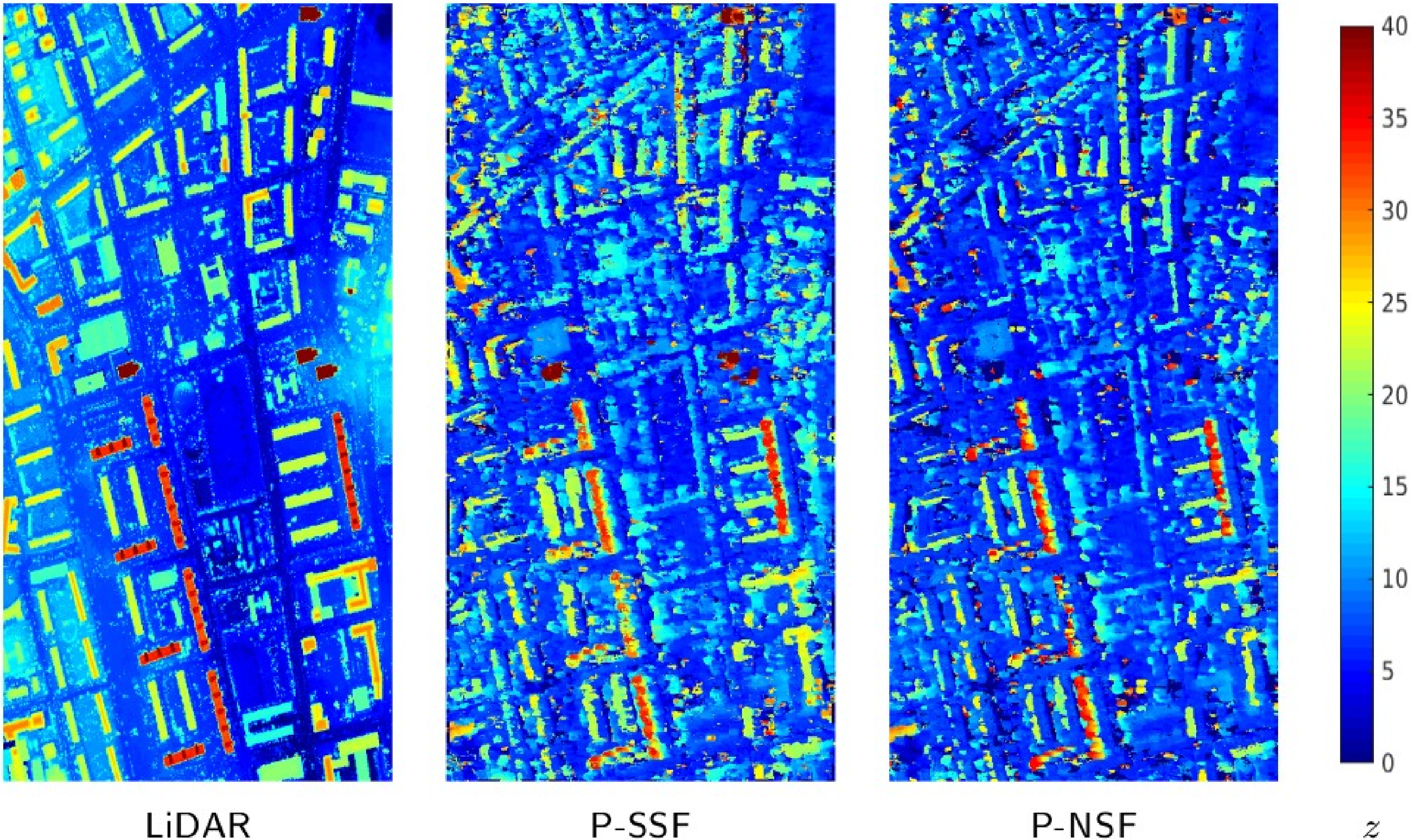

Polarimetric SAR tomography over urban areas

Building reconstruction

Google map

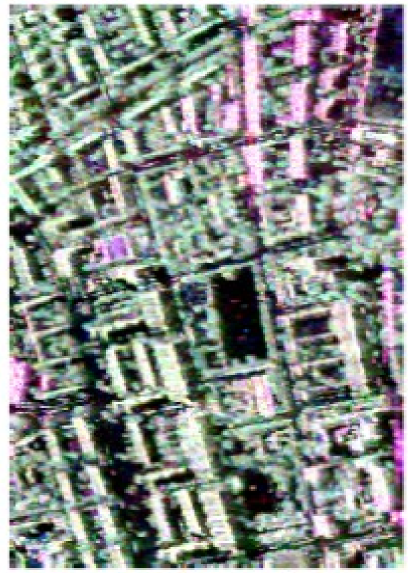

Pauli-coded

LiDAR

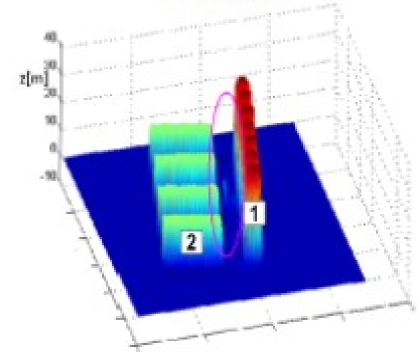

Estimated by FP-NSF
($N_s = 2$)

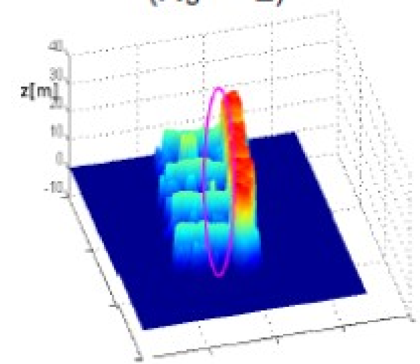

Difference between LiDAR and estimated surface

- projection of SAR imaging
- vegetation between B1 and B2

Polarimetric SAR tomography over urban areas

Building reconstruction

Google map

Bing map

LiDAR

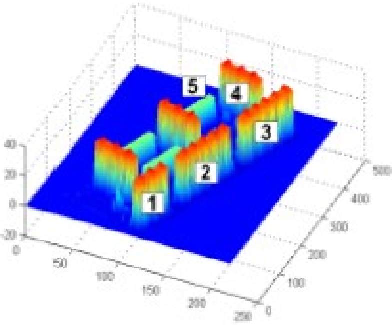

Estimated by FP-NSF ($N_s = 2$)

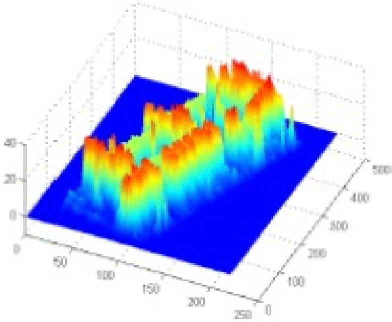

Averaged z[m]	B1	B2	B3	B4	B5
LIDAR	30.0	30.2	30.1	30.8	16.3
Estimated	27.5	27.8	27.5	27.3	16.1

Tropical forest characterization

Tropical forest test site and objectives

- TropiSAR Campaign, 2009
- ONERA SETHI
- P-Band
- 6 tracks
- $\delta_{az} = 1.245m$
  $\delta_{rg} = 1m$
- $\delta_z = 12.5m$
- Ground truth
  - LiDAR data
  - Biomass measurements for 16 ROIs

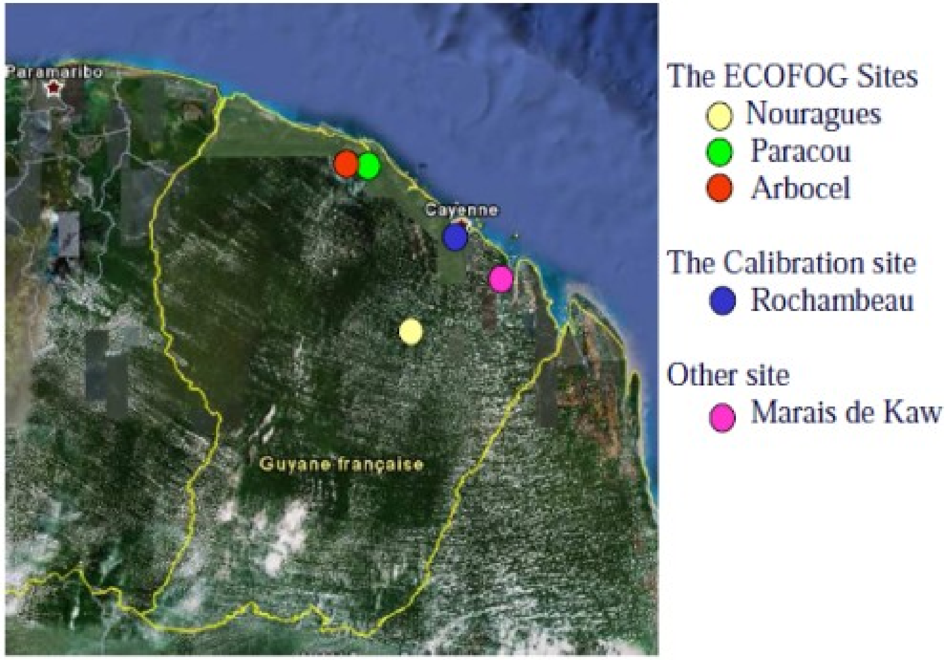

Courtesy ONERA

Objectives

- Tree height,underlying ground topography estimation
- Forest vertical structure characterization
- Biomass monitoring

Tropical forest characterization

Tropical forest test site : Paracou

Optical image

SAR image

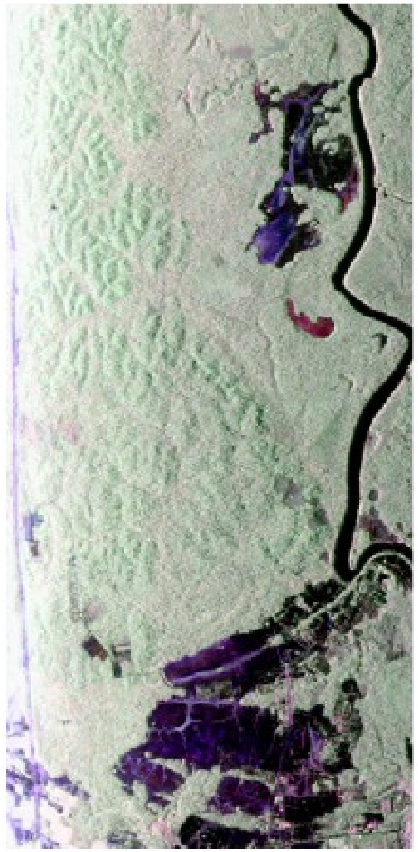

LiDAR z_g

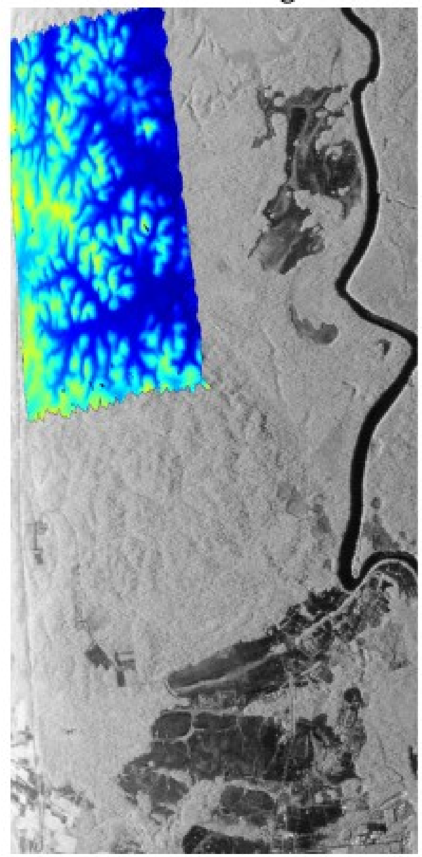

LiDAR z_{top}

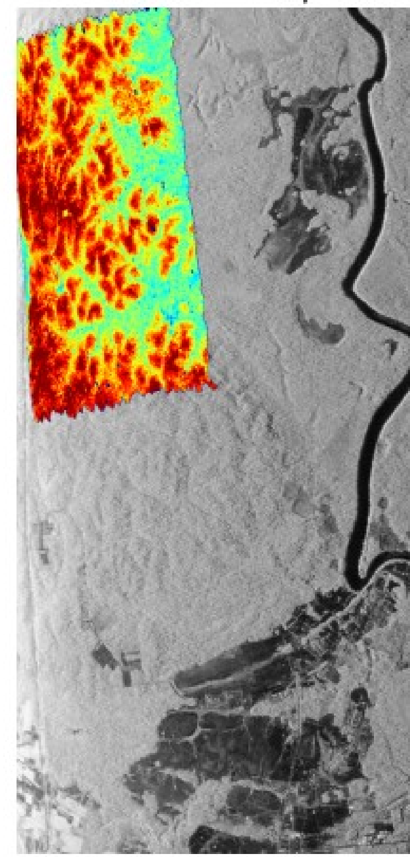

- Tropical forest environments
(savannah, undisturbed forests, logged plots...)

- Highly varying ground topography

Tropical forest characterization

Tree height and ground topography estimation

Hybrid spectral approach

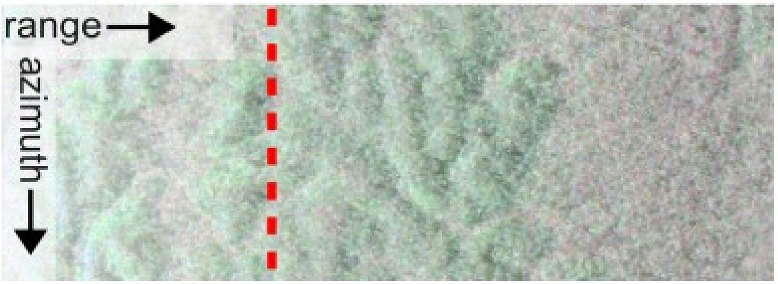

- Estimated profiles match LiDAR
- HH profiles : similar to FP case

LiDAR TomSAR

HH

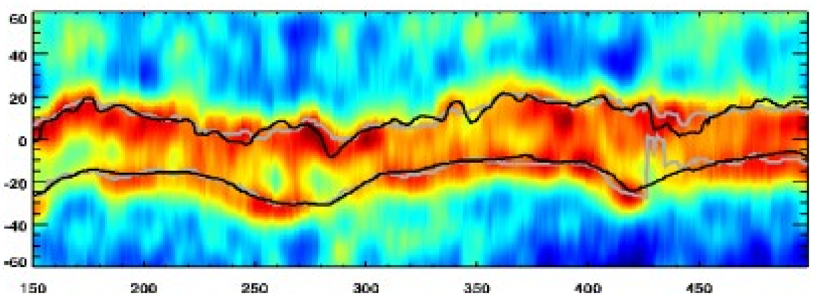

VV

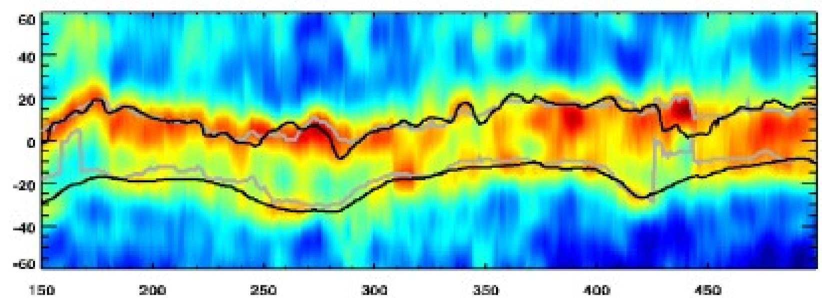

HV

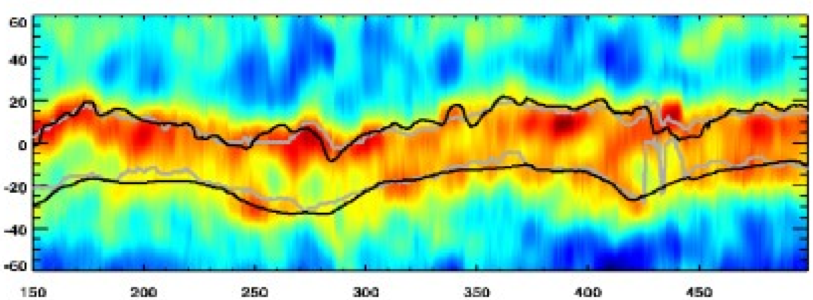

FP

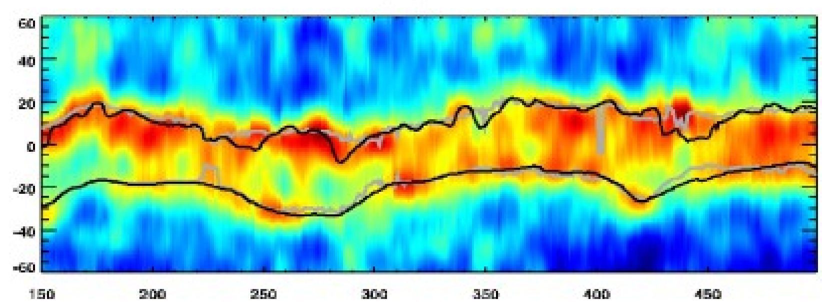

Tropical forest characterization

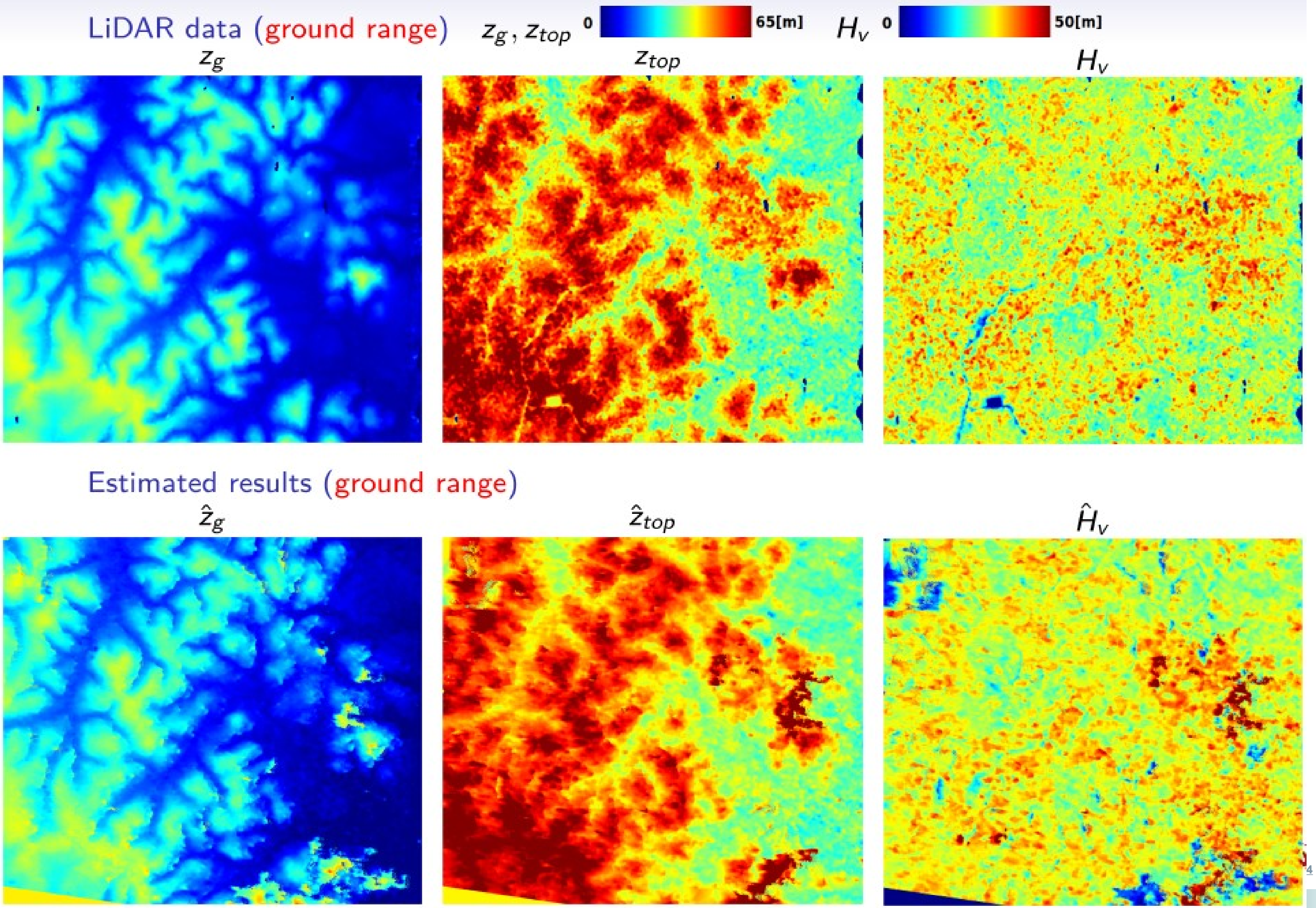

Tropical forest characterization

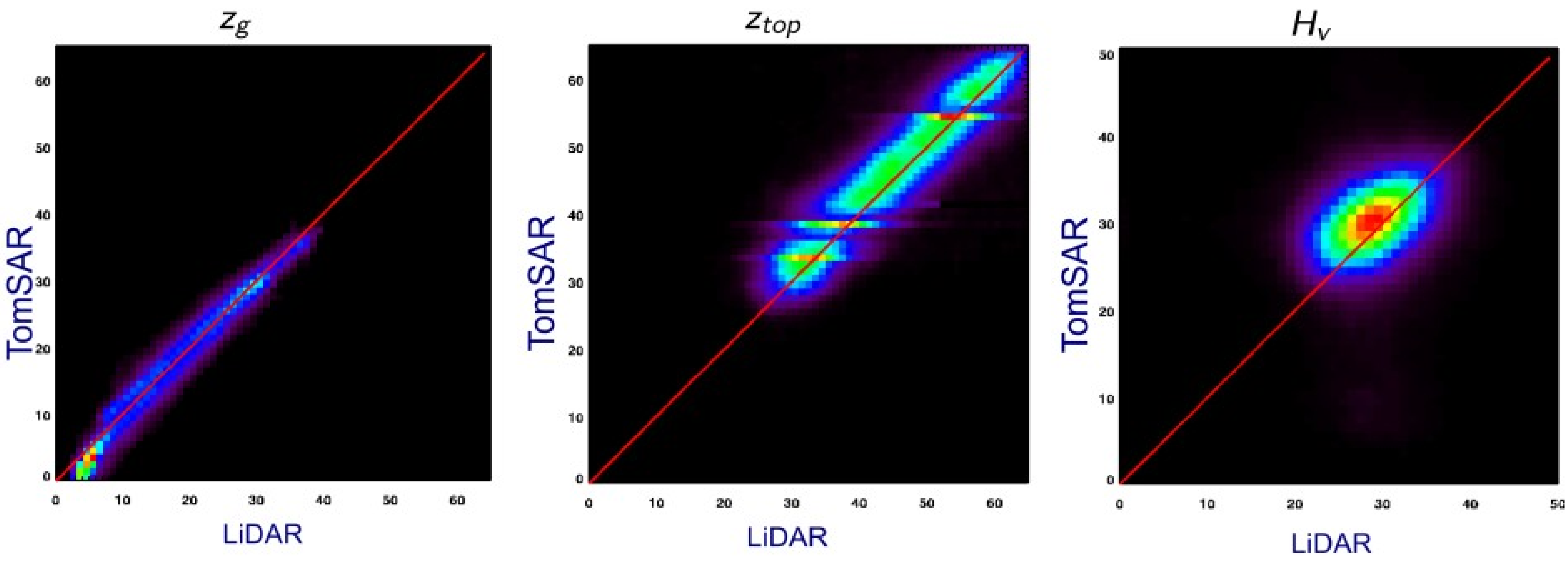

TomoSAR imaging of concealed objects

Above ground and under foliage objects observed at L band

- DLR E-SAR image over Dornstetten, Germany
- L-Band
- 21 tracks : average baseline 20m
- $\delta_z = 2\text{m}$

Horizontal baseline distribution

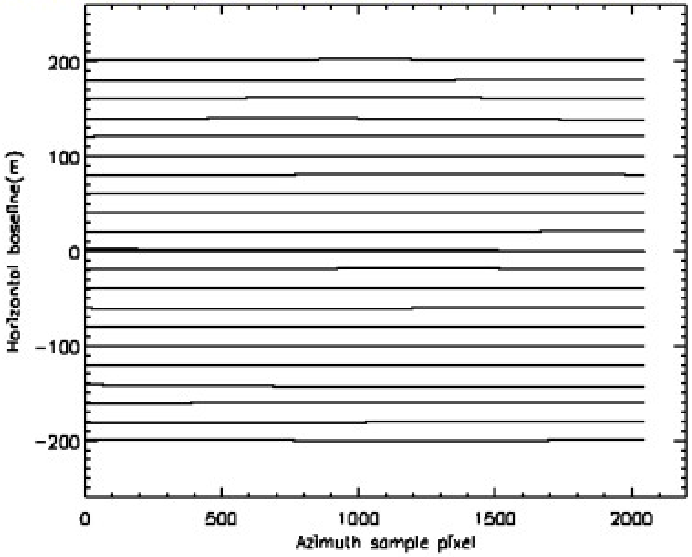

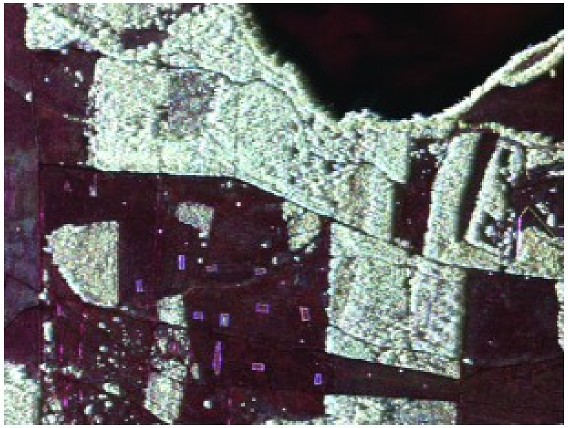

Huang, Y.; Ferro-Famil, L. & Reigber, A. "Under-Foliage Object Imaging Using SAR Tomography and Polarimetric Spectral Estimators", IEEE TGRS 2011

TomoSAR imaging of concealed objects

VV refectivity tomograms

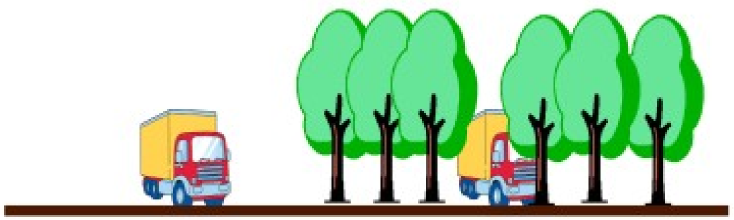

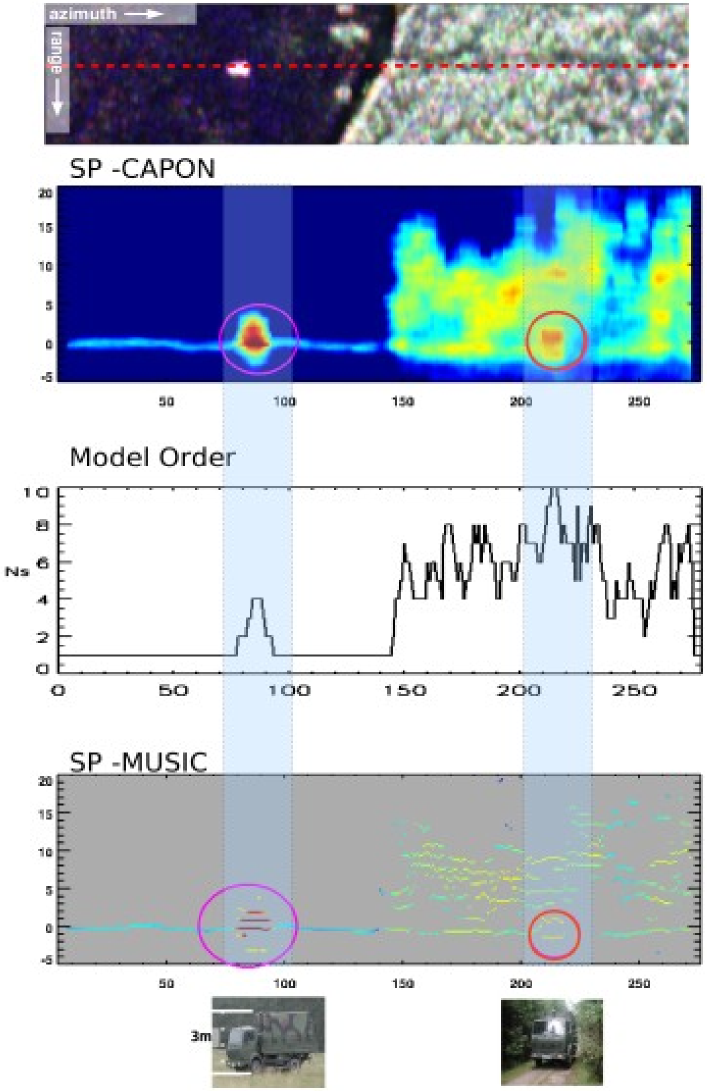

Capon :

limited resolution

$\Rightarrow$ overestimated H_{truck}

MUSIC :

- ☺ Sub-canopy truck
  $\Rightarrow$ hybrid scatterer
- ☹ Uncovered
  $\Rightarrow$ coherent scatterer
- ☹ Spurious sidelobes.

TomoSAR imaging of concealed objects

High Resolution tomograms of underfoliage objects

SSF : shape and reflectivity

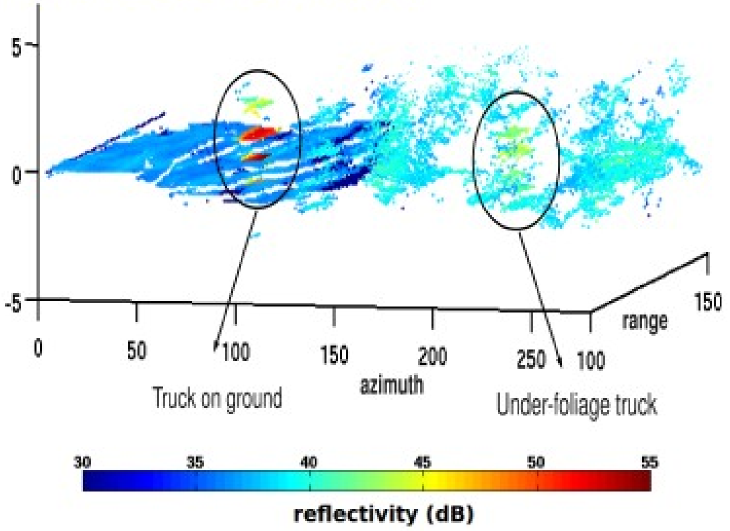

FP-NSF : scattering mechanisms

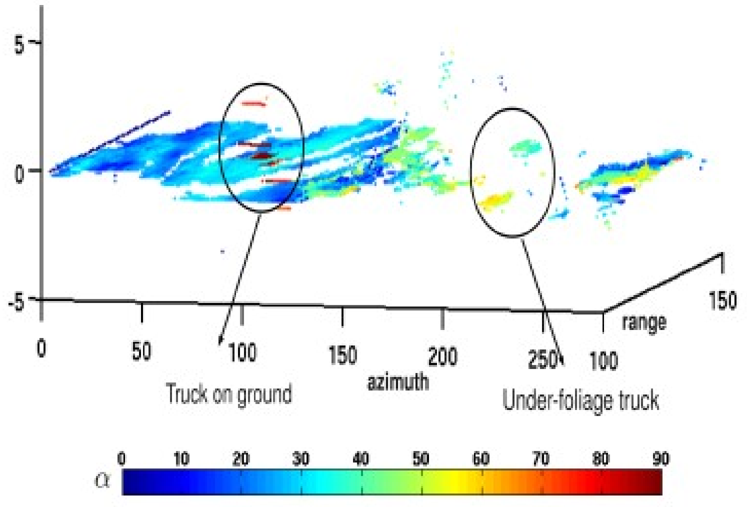

Sparse (compressive) sensing solution

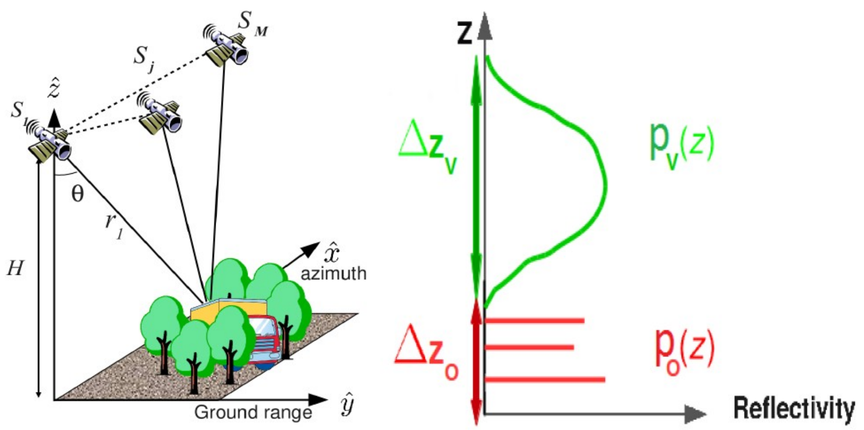

- a few wavelet components

- a few discrete contributions

$$\min_{\mathbf{p}} ||\mathbf{B}\mathbf{p}||_1 \text{ subject to } \quad ||\mathbf{R} - \widehat{\mathbf{R}}||_F \leq \epsilon \qquad \widehat{\mathbf{R}} = \mathbf{A}(\mathbf{z})\, \mathrm{diag}(\mathbf{p}) \mathbf{A}^H(\mathbf{z})$$

$$\mathbf{B} = \begin{bmatrix} \mathbf{I}_{(N_o \times N_o)} & \mathbf{0} \\ \mathbf{0} & \mathbf{\Psi}_{(N_v \times N_v)} \end{bmatrix} \in \mathbb{R}^{(N_s \times N_s)} \qquad \mathbf{p} = [\mathbf{p}_o^T \quad \mathbf{p}_v^T]^T \in \mathbb{R}^{+N_s \times 1}$$

TomoSAR imaging of concealed objects

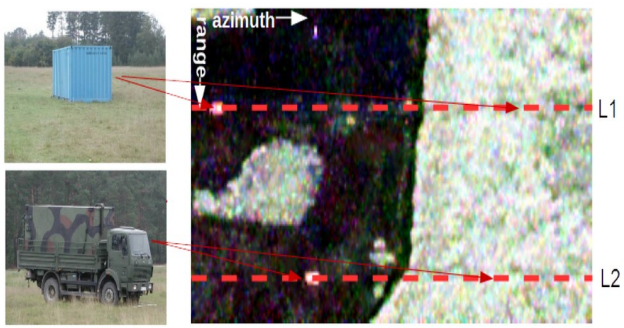

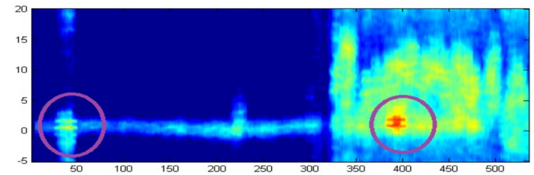
(a) Capon

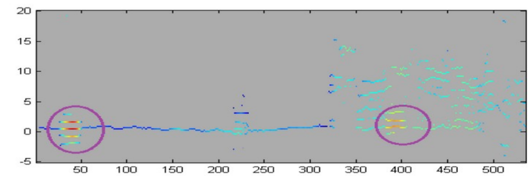
(b) MUSIC

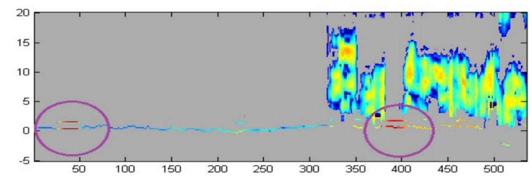
(c) Proposed method with merging

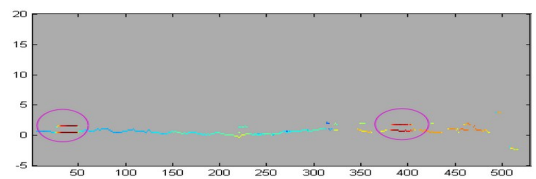
(d) Ground and underfoliage scattering ($\mathbf{p}_o$) estimated by proposed method with merging

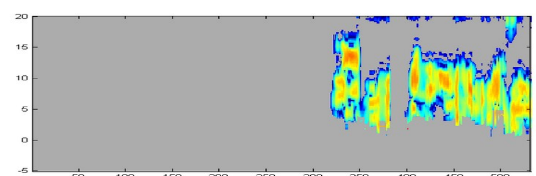
(e) Canopy power ($\mathbf{p}_v$) estimated by proposed method with merging

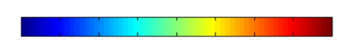
(f) dB

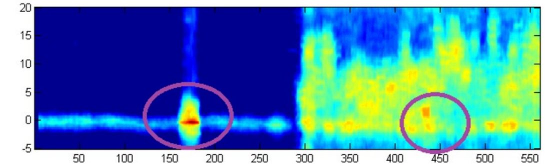
(a) Capon

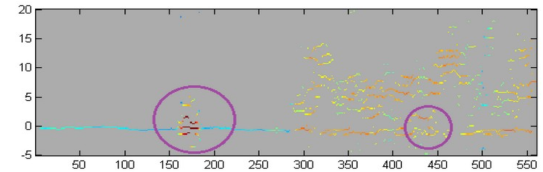
(b) MUSIC

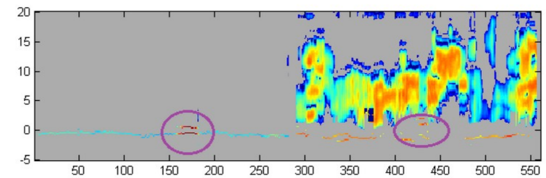
(c) Proposed method with merging

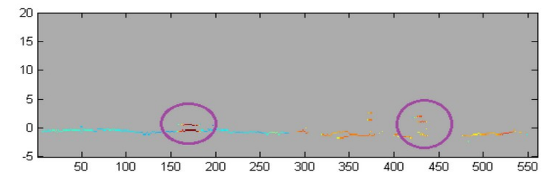
(d) Ground and underfoliage scattering ($\mathbf{p}_o$) estimated by proposed method with merging

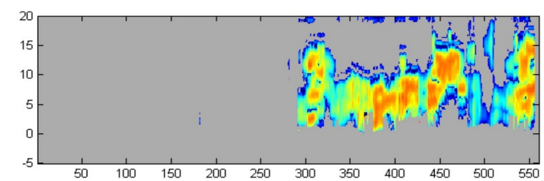
(e) Canopy power ($\mathbf{p}_v$) estimated by proposed method with merging

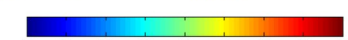
(f) dB

InSAR coherence analysis

and

TomoSAR modeling

InSAR coherence analysis

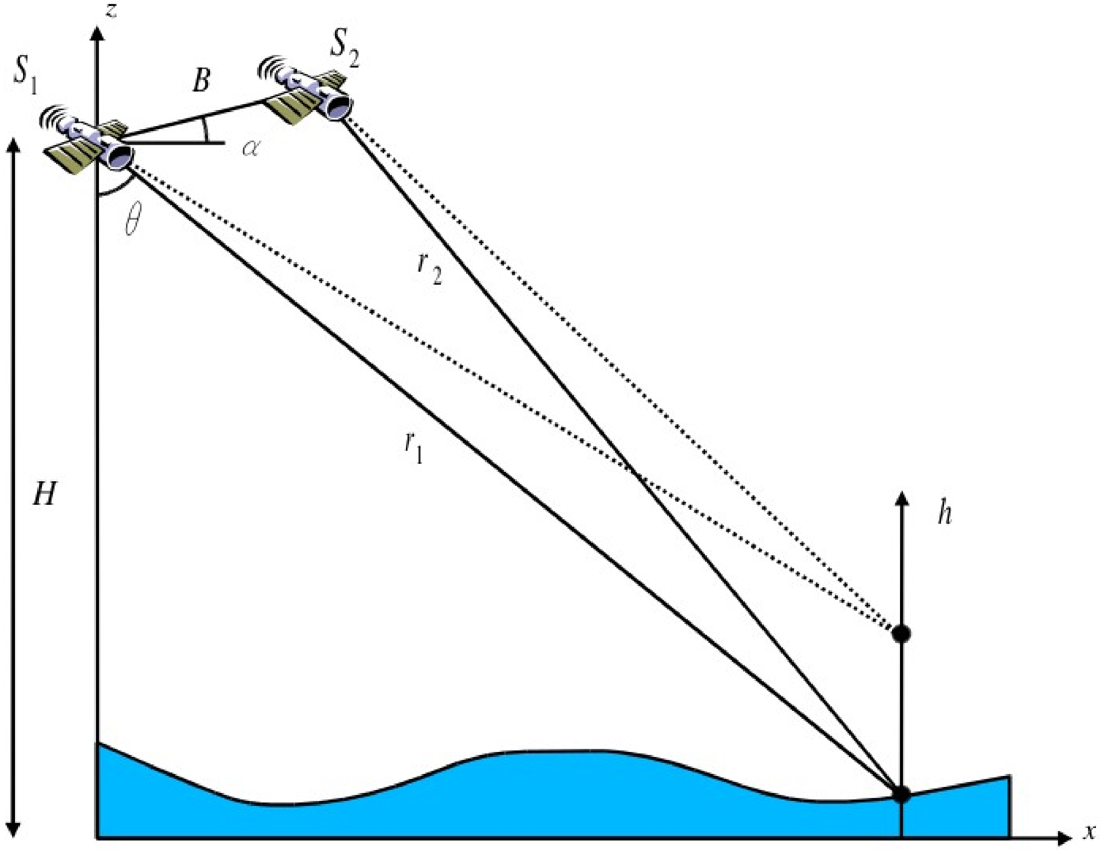

Coherent SAR image pair

$$s_1 = \sqrt{I_1}\, e^{j\phi_1} = \sqrt{I_1}\, e^{j(-kr_1+\phi_{obj1})}$$

$$s_2 = \sqrt{I_2}\, e^{j\phi_2} = \sqrt{I_2}\, e^{j(-kr_2+\phi_{obj2})}$$

Assumptions

$$I_1 \approx I_2 \quad \text{and} \quad \phi_{obj1} \approx \phi_{obj2}$$

Interferometric phase difference

$$\Delta\phi_{12} = \arg(s_1 s_2^*)$$

S_1 and S_2 are random variables

⇨ assumptions may not be fully verified

⇨ the interferometric phase difference is a random variable

InSAR coherence analysis

Interferometric coherence

Joint interferometric representation

$$\mathbf{k} = \begin{bmatrix} s_1 \\ s_2 \end{bmatrix} \sim \mathcal{N}_c(\mathbf{0}, \mathbf{C})$$

with $$\mathbf{C} = \mathrm{E}(\mathbf{k}\mathbf{k}^\dagger) = \begin{bmatrix} \mathrm{E}(s_1 s_1^*) & \mathrm{E}(s_1 s_2^*) \\ \mathrm{E}(s_1^* s_2) & \mathrm{E}(s_2 s_2^*) \end{bmatrix} = \begin{bmatrix} \overline{I_1} & \gamma \sqrt{\overline{I_1}\,\overline{I_2}} \\ \gamma^* \sqrt{\overline{I_1}\,\overline{I_2}} & \overline{I_2} \end{bmatrix}$$

Interferometric coherence : normalized correlation coefficient

$$\gamma = \frac{\mathrm{E}(s_1 s_2^*)}{\sqrt{\overline{I_1}\,\overline{I_2}}} = |\gamma|\,\mathrm{e}^{j\phi}$$

$|\gamma| \leq 1$ Cauchy-Schwarz inequality

$|\gamma| = 1 \Rightarrow \phi = \Delta\phi_{12}$ interferometric assumptions are fulfilled

$|\gamma| = 1 \Rightarrow \phi = ?$ interferometric images are totally uncorrelated

$|\gamma|$ is an indicator of the interferometric information (and phase) quality

InSAR coherence analysis

Phase pdf

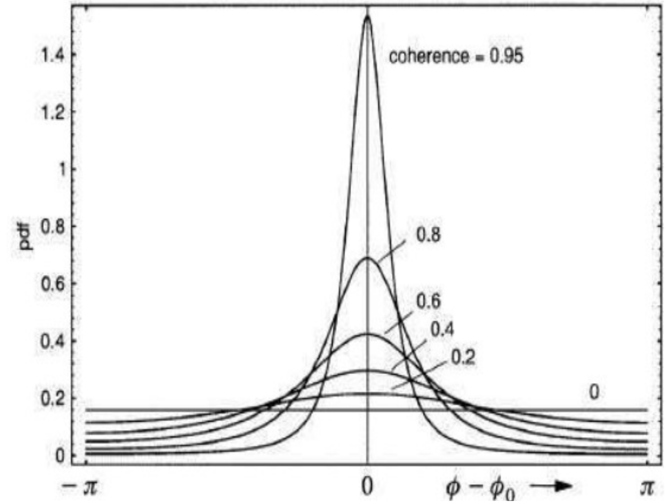

$|\gamma|$: indicator of phase quality

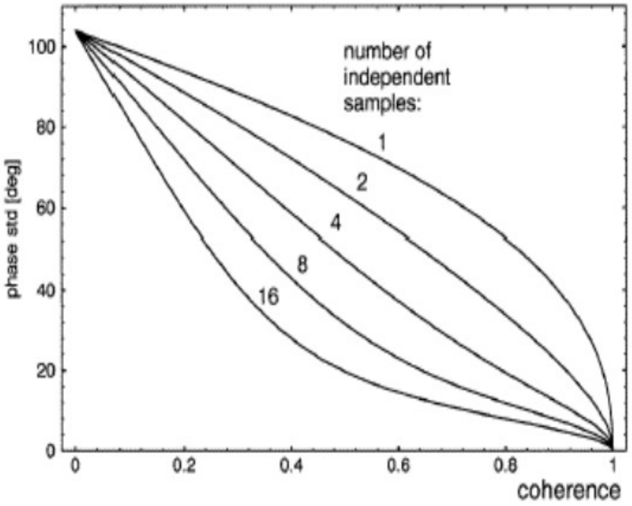

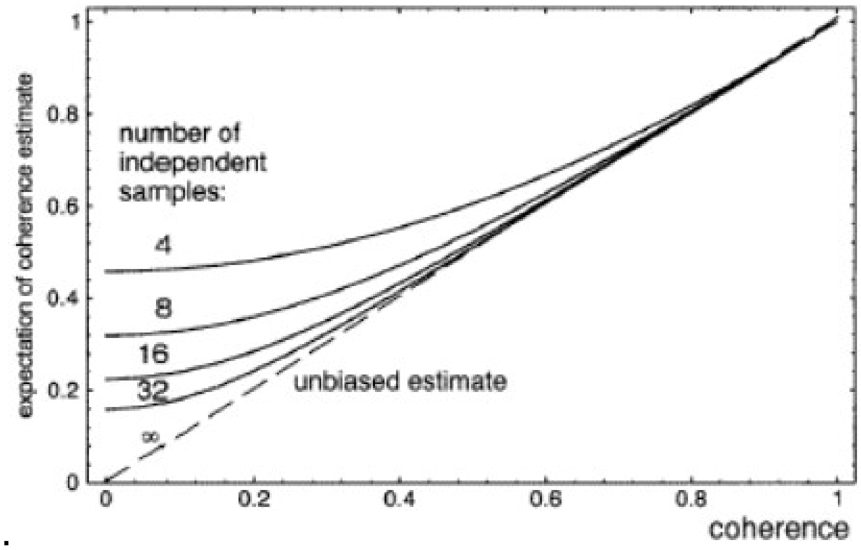

Large number of looks required to reduce:

$$\sigma_{\hat{\phi}} \text{ as } |\gamma| \to 0$$

$$\text{bias: } |\gamma| - \mathrm{E}(|\hat{\gamma}|) \geq 0$$

InSAR coherence analysis

Single-look inSAR phase

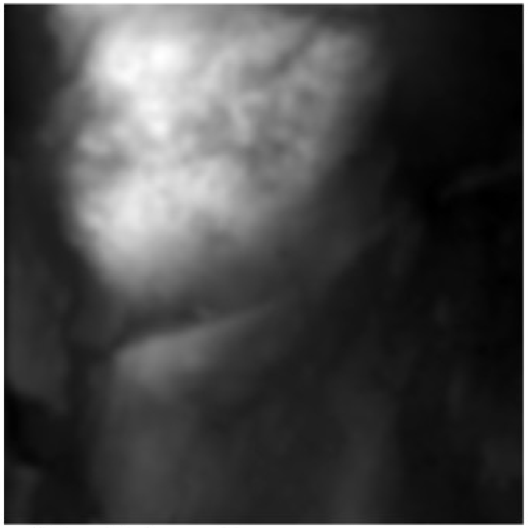

Absolute «True » Phase

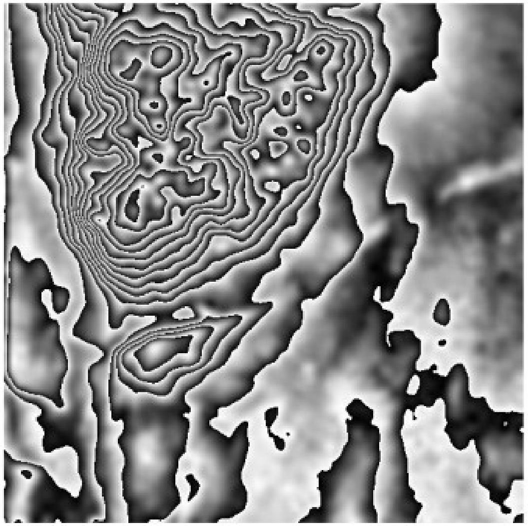

Coherence=1.0 L=1

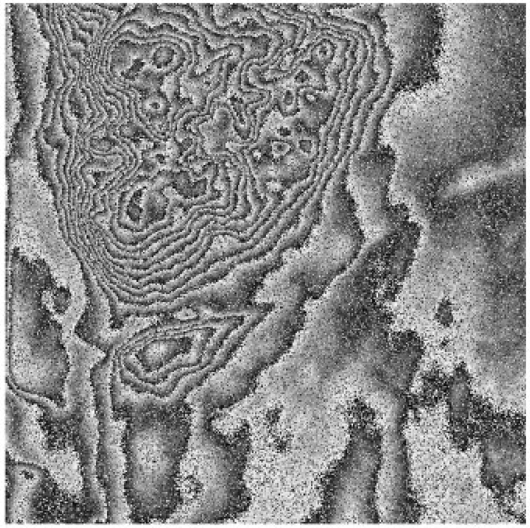

Coherence=0.8 L=1

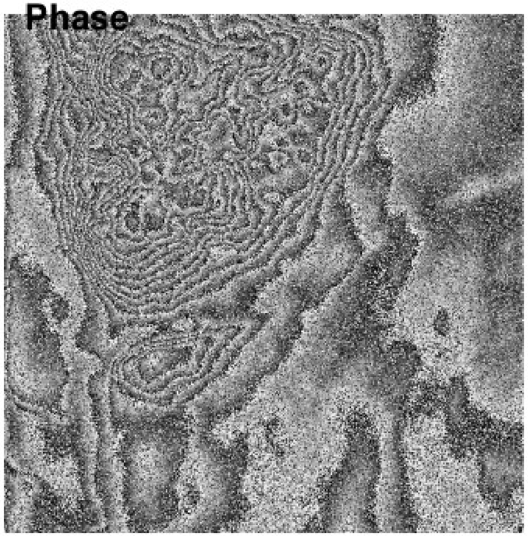

Coherence=0.6 L=1

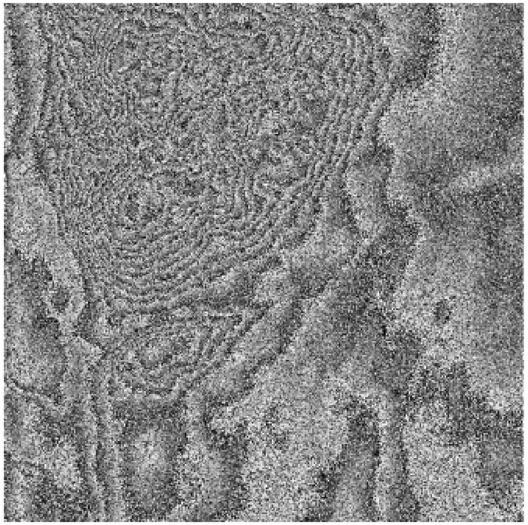

Coherence=0.4 L=1

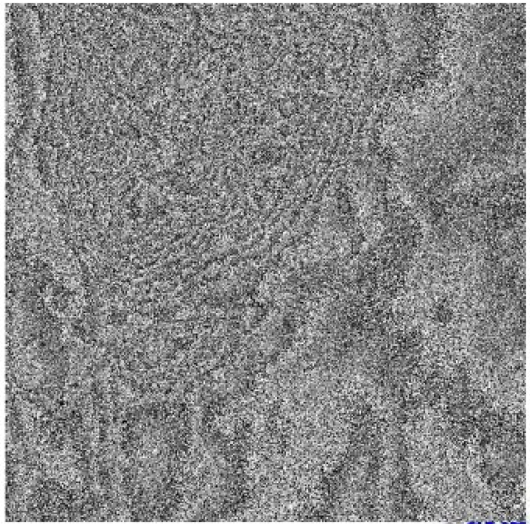

Coherence=0.2 L=1

InSAR coherence analysis

Multi-look inSAR phase

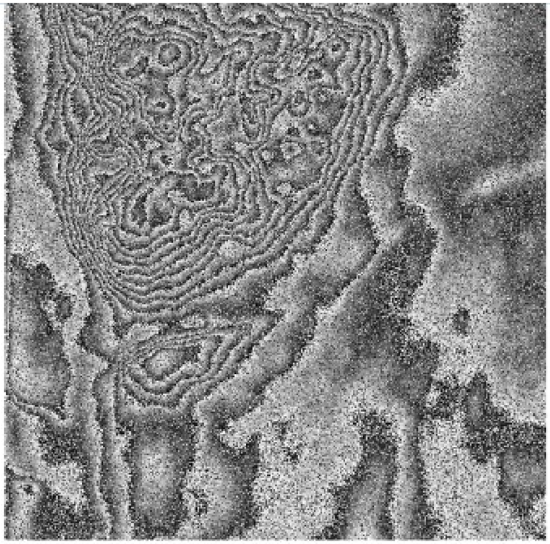

Coherence = 0.7 L=1

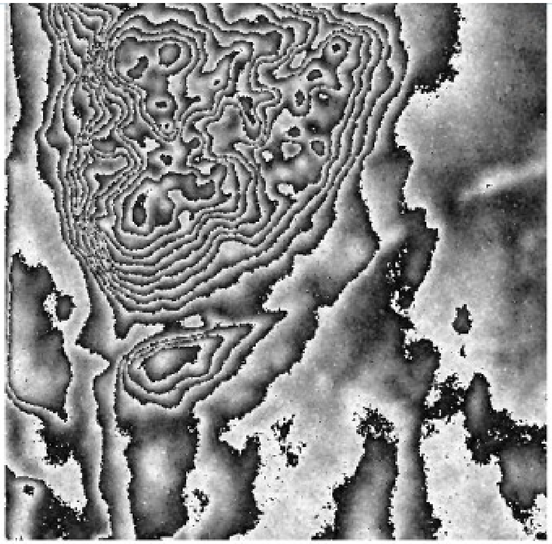

Coherence = 0.7 L=8

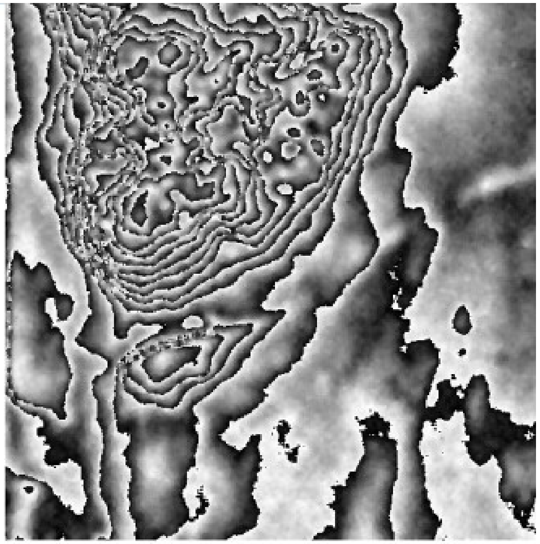

Coherence = 0.7 L=1

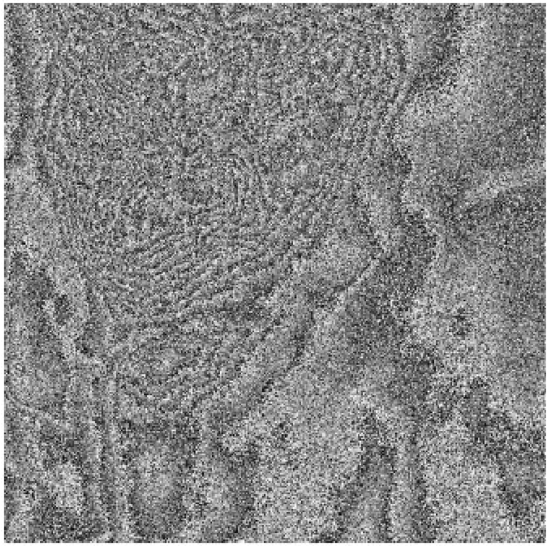

Coherence = 0.3 L=1

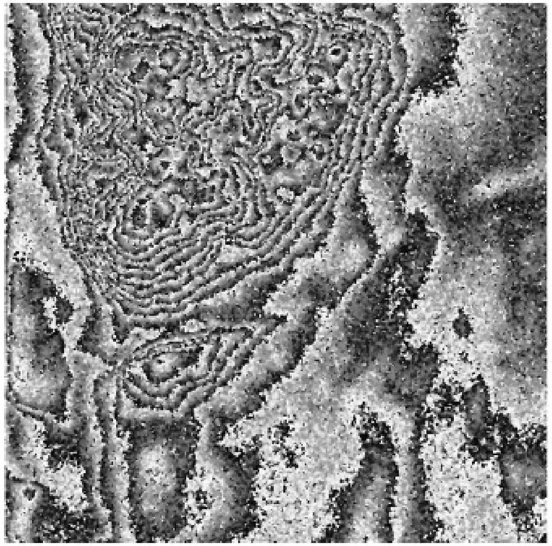

Coherence = 0.3 L=8

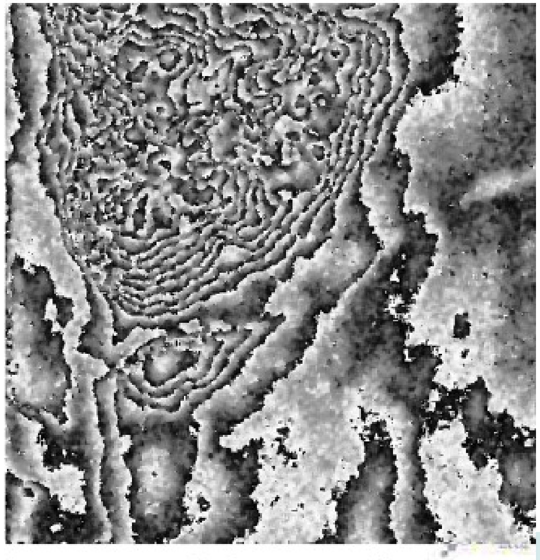

Coherence = 0.3 L=16

InSAR coherence decomposition

The true value of the coherence, γ , is fixed by a set of external sources :

Thermal or system noise : SAR amplifiers, ADC, antennas …

Geometric decorrelation : Baseline, squint …

Volume decorrelation : Volumetric media e.g. forest …

Temporal variations : wind, flowing or plowing, building …

Processing errors : coregistration, interpolation …

$$\gamma = \gamma_{th} \cdot \gamma_{geom} \cdot \gamma_{vol} \cdot \gamma_{temp} \cdot \gamma_{proc}$$

InSAR coherence decomposition

Thermal or system decorrelation

Intensity image

Coherence image

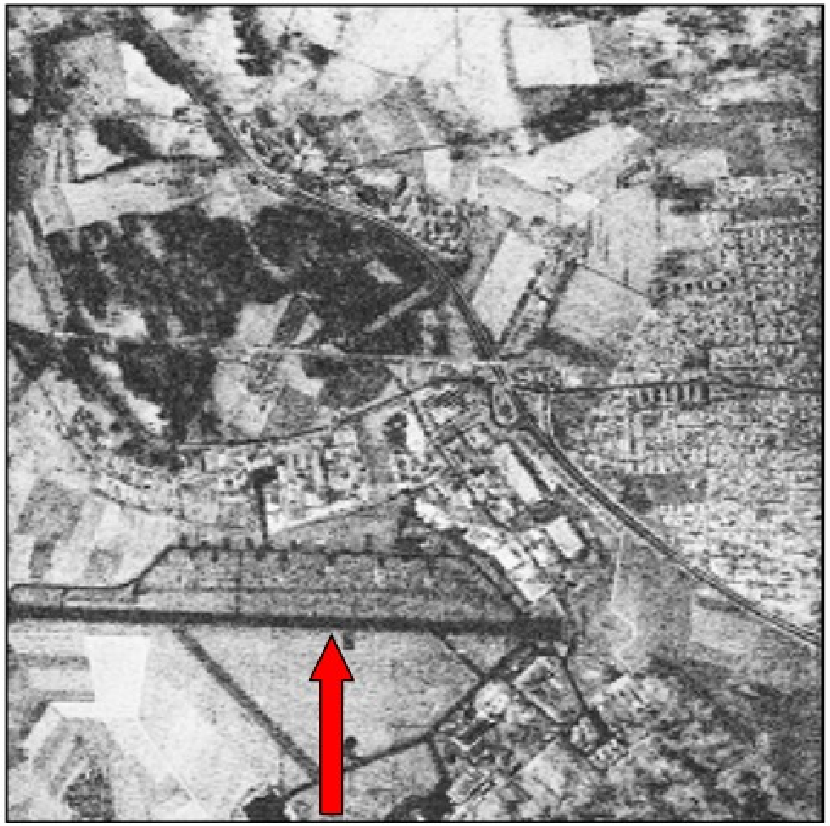

InSAR coherence decomposition

Temporal decorrelation

1 hour, 20m baseline

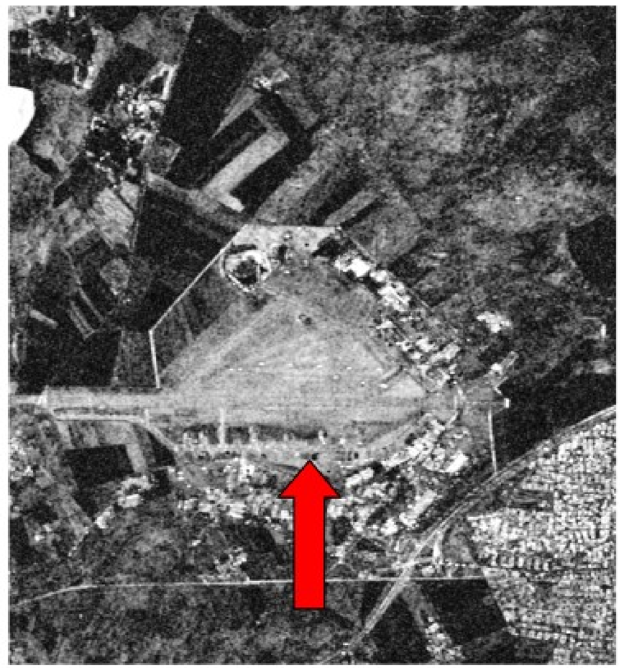

3 months, 0m baseline

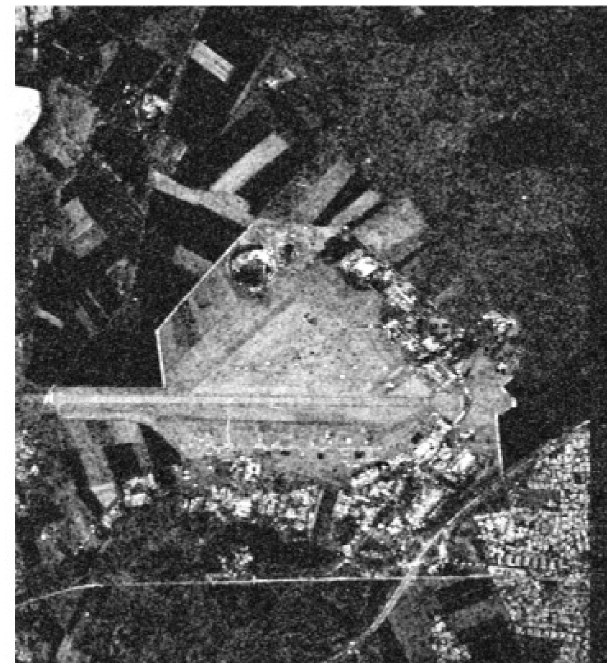

1 year, 0m baseline

Temporal decorrelation

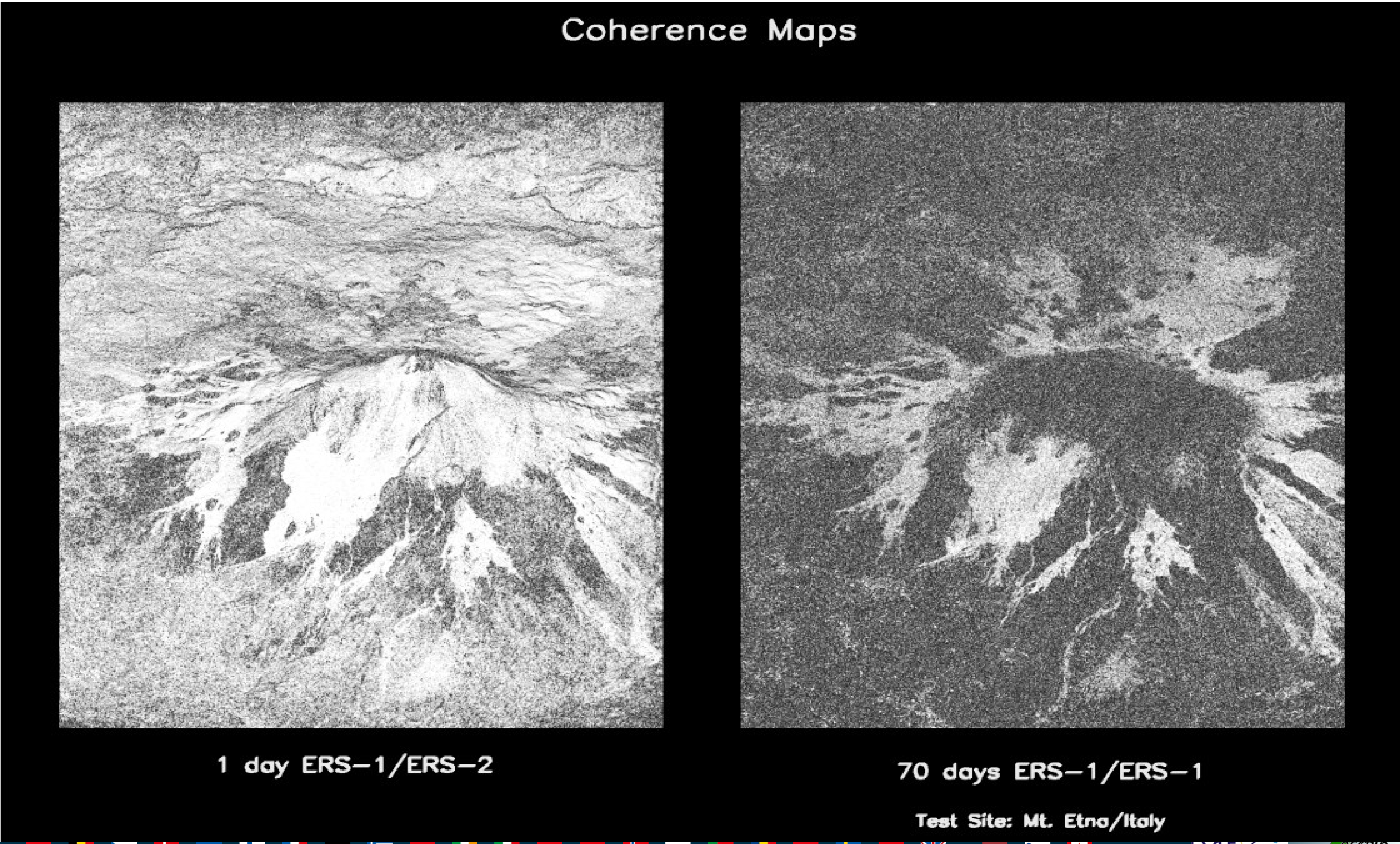

InSAR coherence decomposition

Volume decorrelation

1 hour, 20 baseline

Volumetric media inSAR response modeling

- Vertical reflectivity structure $\sigma_{v_e}(\vec{r}) = \sigma_{v_e}(z) = A_{v_e} f(z)$

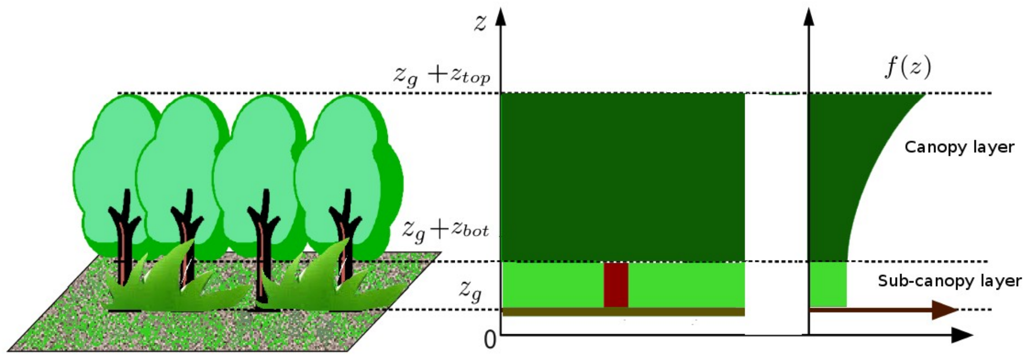

- InSAR coherence $\gamma = \gamma_{th} \quad \gamma_{proc} \quad \gamma_{temp} \quad \gamma_{surf} \quad \gamma_z$

- Decorrelation due to vertical structure :

$$\boxed{\gamma_z = \frac{\int \sigma_{v_e}(z)\, \mathrm{e}^{jk_z z}\, \mathrm{d}z}{\int \sigma_{v_e}(z) \mathrm{d}z}} \qquad k_z = \frac{k_c B_\perp}{r \sin\theta}$$

- Fourier transform-like **coherence-structure relationship**

$$\boxed{\gamma_z \overset{FT}{\longleftrightarrow} \sigma_{v_e}(z)}$$

InSAR RVOG model

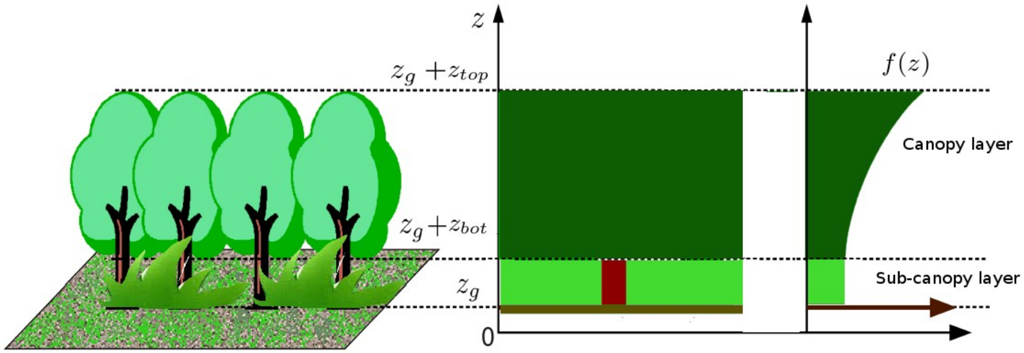

Modeling at order 1

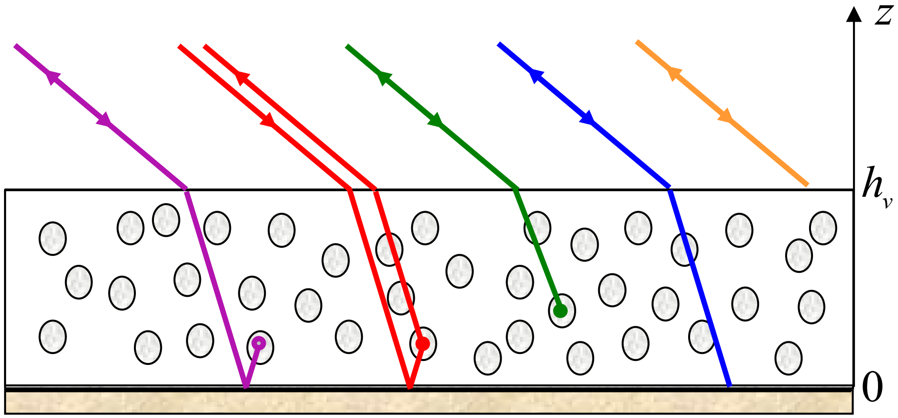

Parameter Estimation

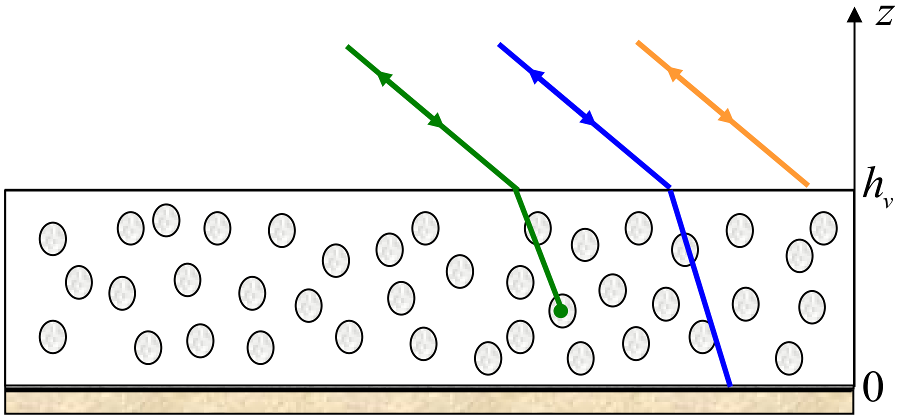

Parameter estimation often requires to simplify models

- omitting negligible terms
- merging contributions that cannot be discriminated (e.g. ground and double-bounce)

InSAR RVOG model

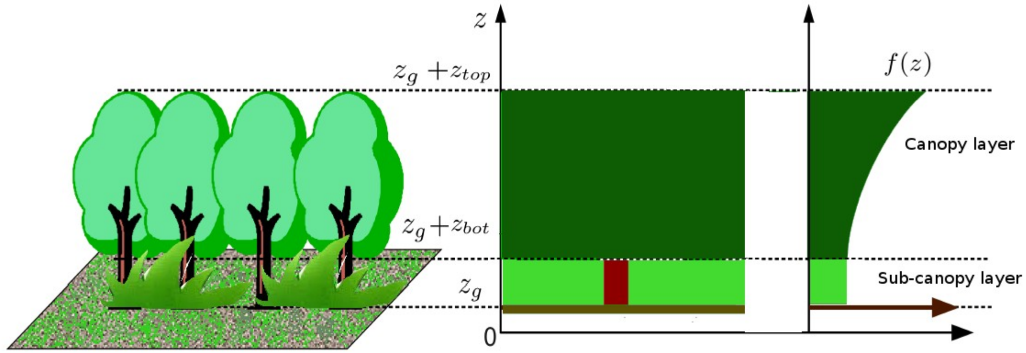

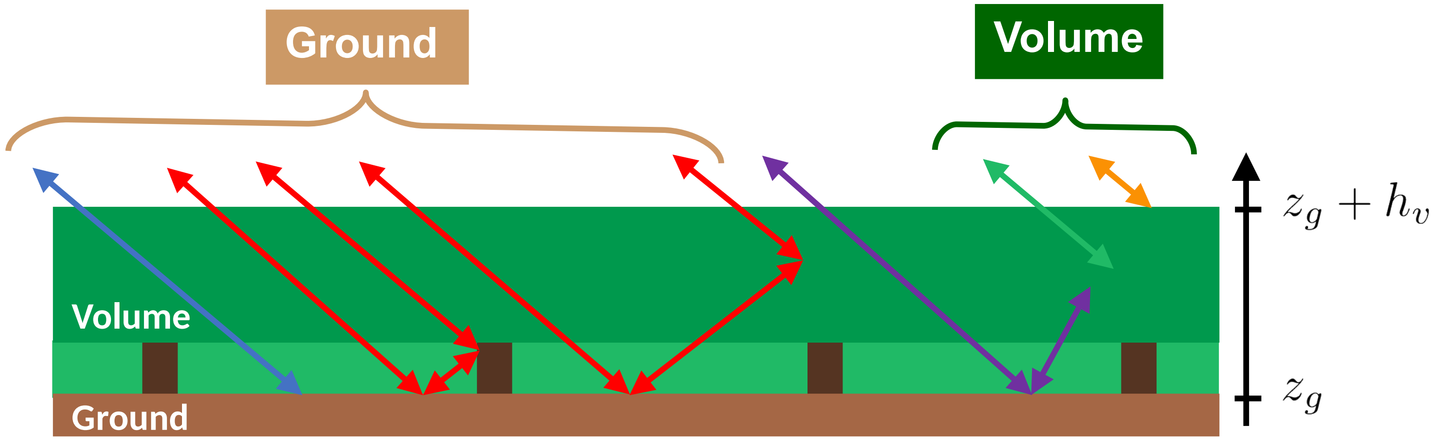

- 2 significant and uncorrelated mechanisms :

  ⇨ volume + underlying ground

- low density medium

  ⇨ no refraction

InSAR RVOG analysis

Ground only

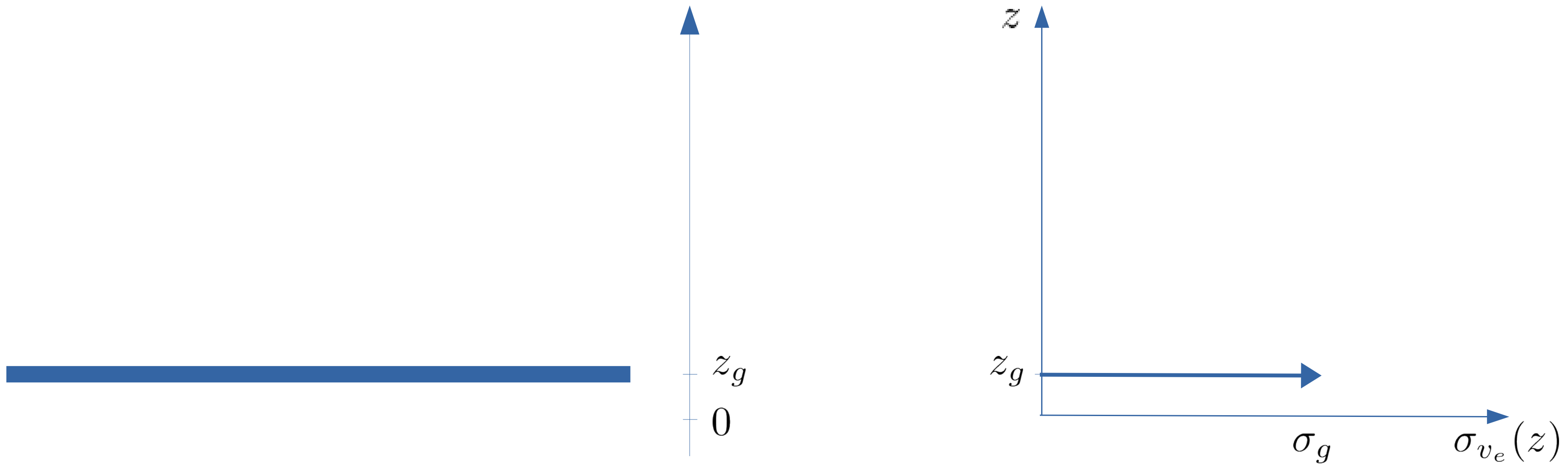

$$\gamma_z = \frac{\int \sigma_{v_e}(z)\, \mathrm{e}^{jk_z z}\, \mathrm{d}z}{\int \sigma_{v_e}(z)\mathrm{d}z}$$

$$\sigma_{v_e}(z) = \sigma_g \delta(z - z_g) \quad \Rightarrow \quad \gamma_z = \mathrm{e}^{jk_z z_g}$$

InSAR well adapted to topography estimation

Non attenuating random volume only

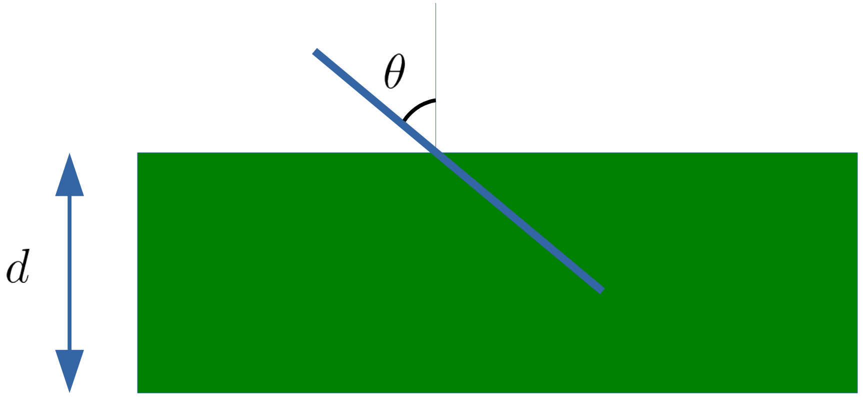

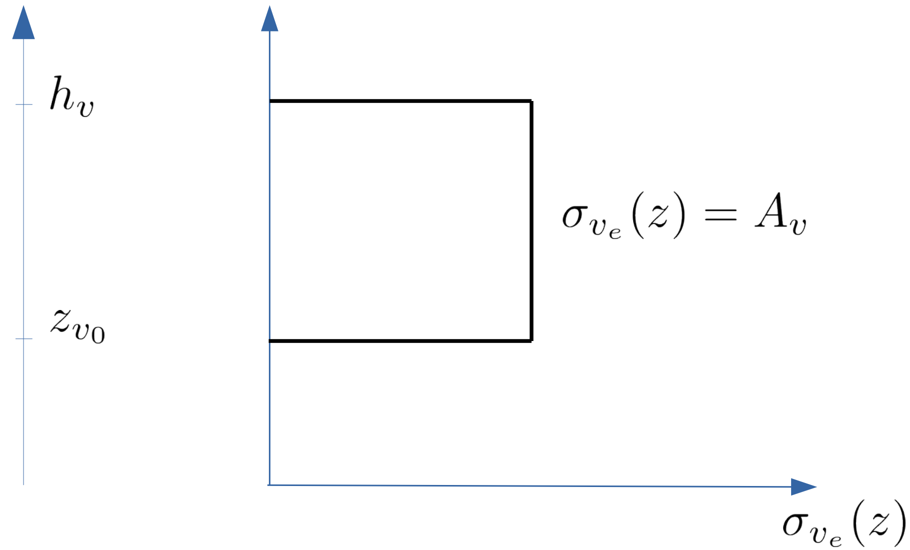

$$\gamma_z = \frac{\int \sigma_{v_e}(z)\, \mathrm{e}^{jk_z z}\, \mathrm{d}z}{\int \sigma_{v_e}(z) \mathrm{d}z}$$

No underlying ground

Null extinction: $\sigma_{v_e}(z) = A_v$

$$\gamma_z = \frac{1}{d} \int_{z_{v0}}^{h_v} \mathrm{e}^{jk_z z}\, \mathrm{d}z$$

$$\gamma_z = \mathrm{e}^{jk_z \frac{h_v + z_{v0}}{2}} \operatorname{sinc}\left(\frac{k_z d}{2}\right)$$

InSAR RVOG analysis

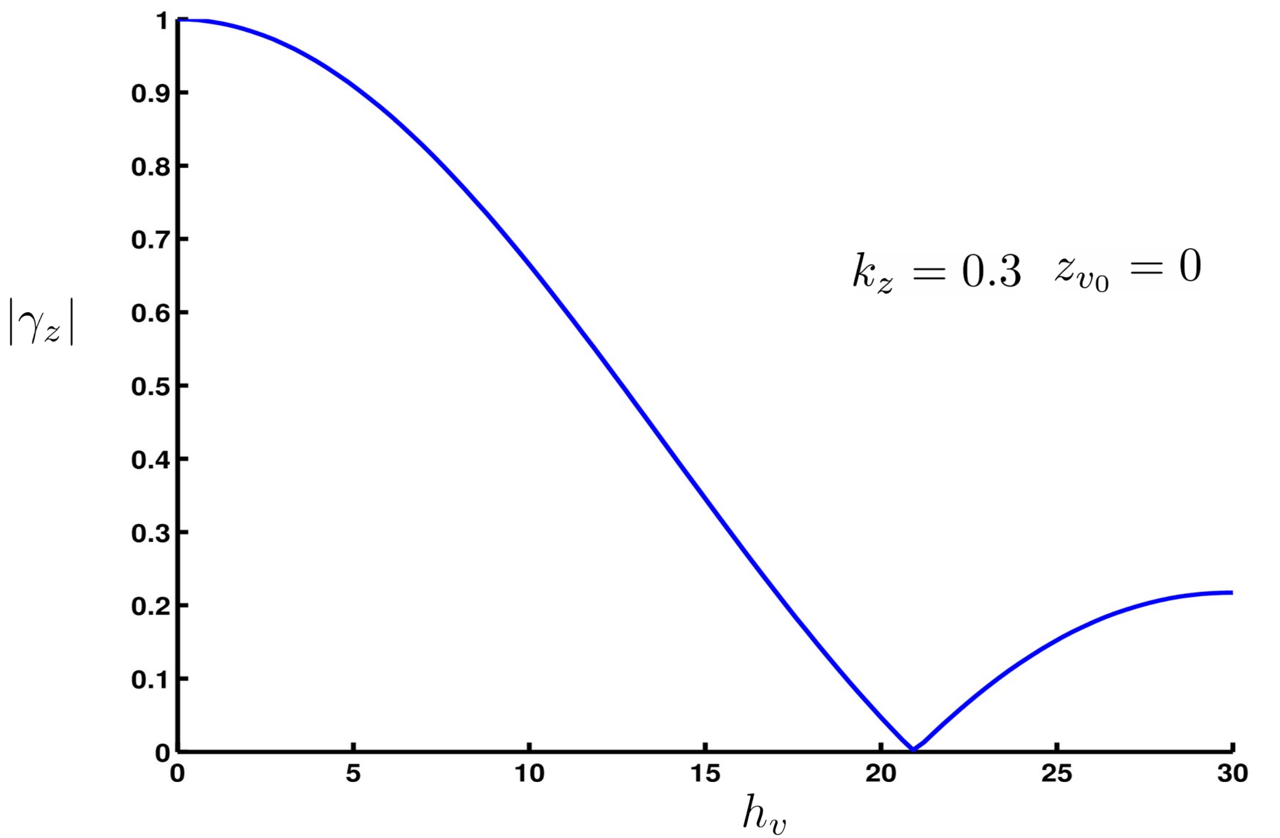

Volume center height

Volume width

$$\gamma_z = e^{jk_z \frac{h_v + z_{v0}}{2}} \operatorname{sinc}\left(\frac{k_z d}{2}\right)$$

InSAR well adapted to volume analysis under specific conditions

Attenuating random volume only

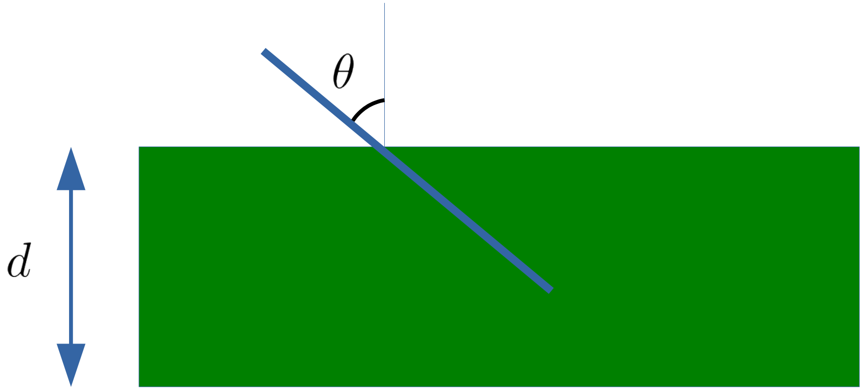

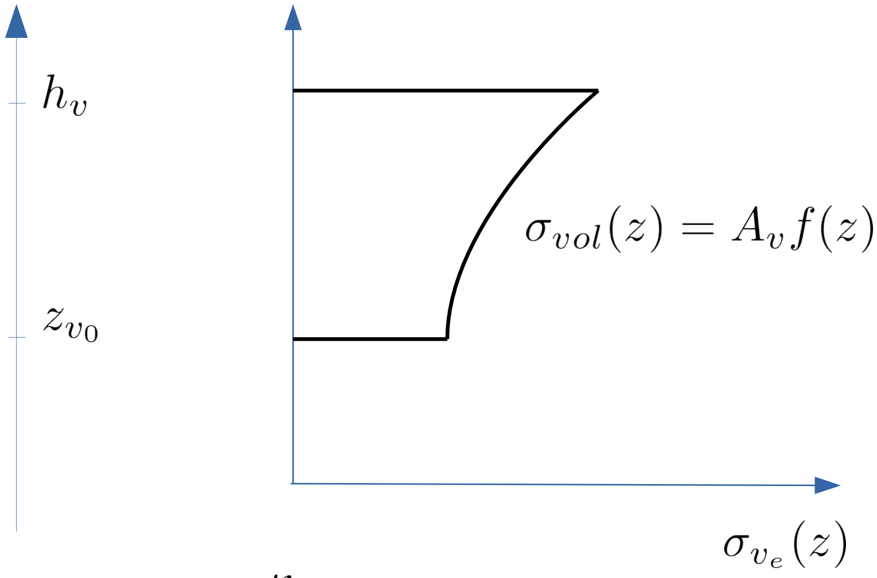

Linear differential extinction $$\mathrm{d}I = -\kappa_e I \mathrm{d}s = -\frac{\kappa_e}{\cos\theta} I \mathrm{d}z$$

Effective reflectivity density
constant extinction $$\sigma_{vol}(z) = A_v\, \mathrm{e}^{-2\frac{\kappa_e}{\cos\theta}(h_v - z)} = A_v f(z)$$

Backscattered volume intensity $$I_v = \int_{z_{v0}}^{h_v} \sigma_{vol}(z)\mathrm{d}z = \int_{z_{v0}}^{h_v} A_v f(z)\mathrm{d}z$$

InSAR RVOG analysis

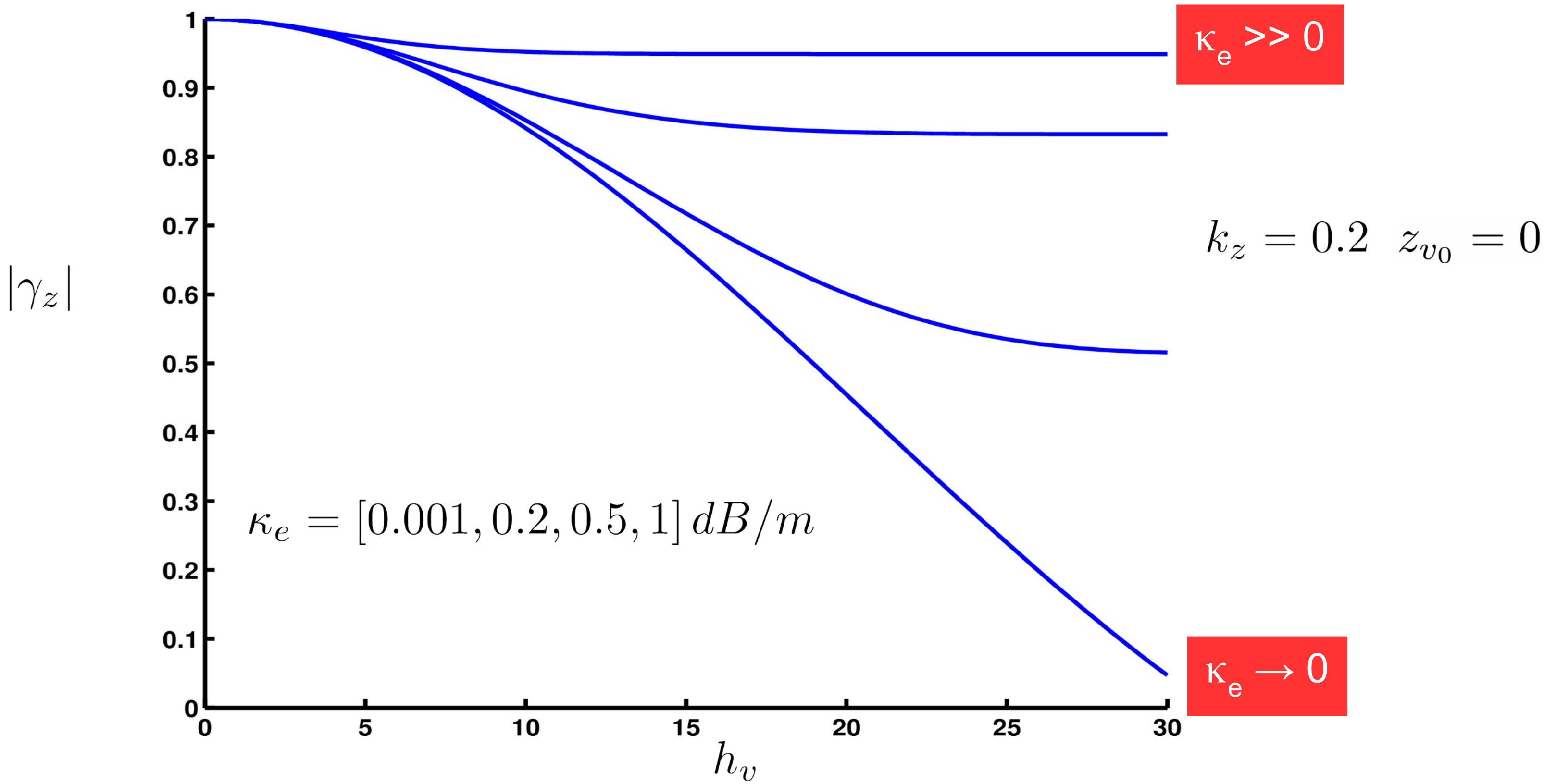

$$\gamma_{vol} = \gamma_z = e^{jk_z z_{v0}} \frac{p}{p_1} \left(\frac{e^{p_1 d} - 1}{e^{pd} - 1} \right) \qquad p = \frac{2\kappa_e}{\cos\theta} \qquad p_1 = \frac{2\kappa_e}{\cos\theta} + jk_z$$

InSAR $|\gamma_z| \rightarrow \hat{h}_v$ ambiguous estimation

InSAR RVOG analysis

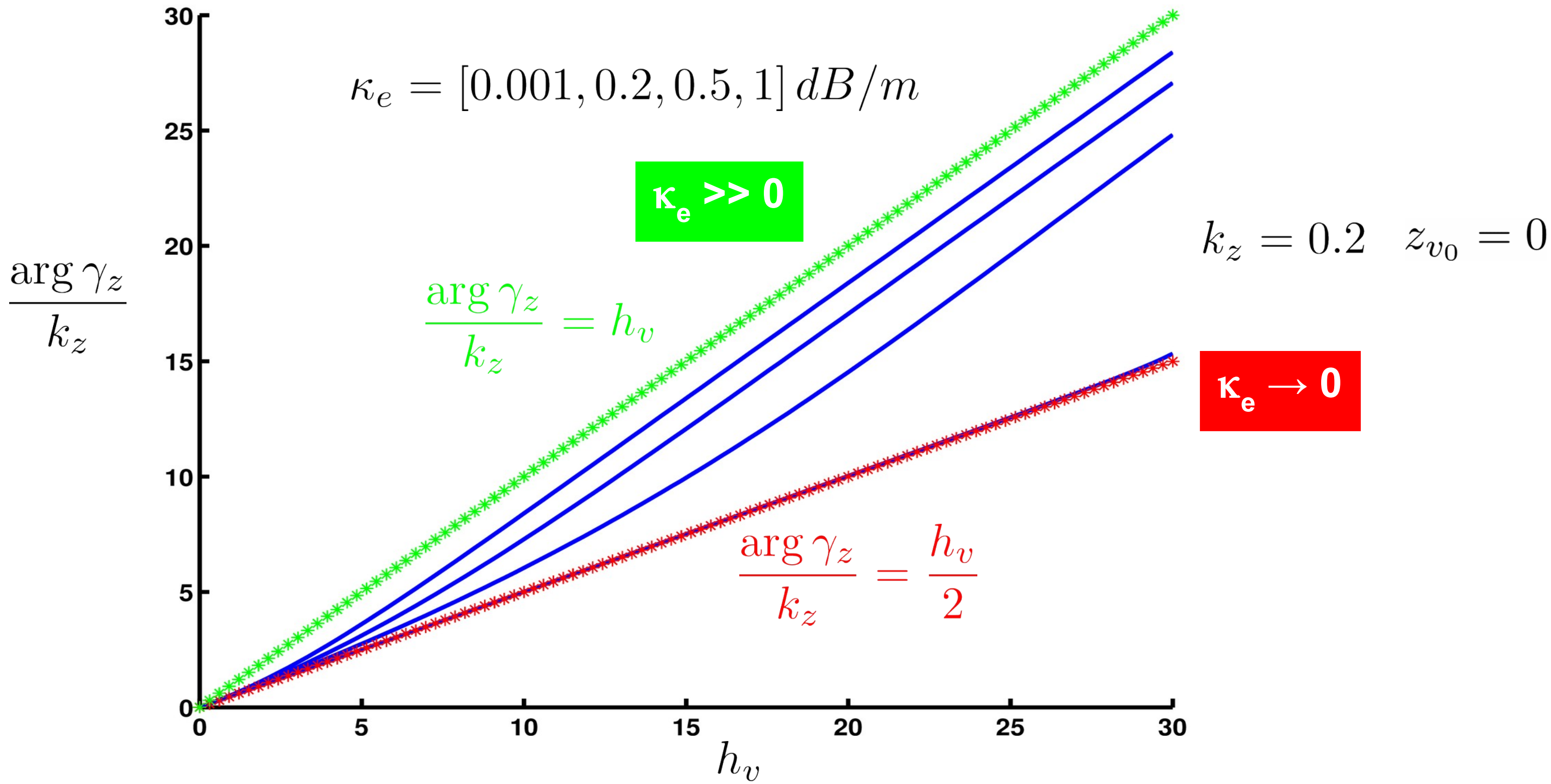

InSAR $\arg(\gamma_z) \rightarrow \hat{h}_v$ **ambiguous estimation**

Unambiguous solution for known $\sigma_{vol}(z)$ **shape :** $|\gamma_z|, \arg(\gamma_z) \rightarrow \hat{h}_v$

Attenuating random volume and ground

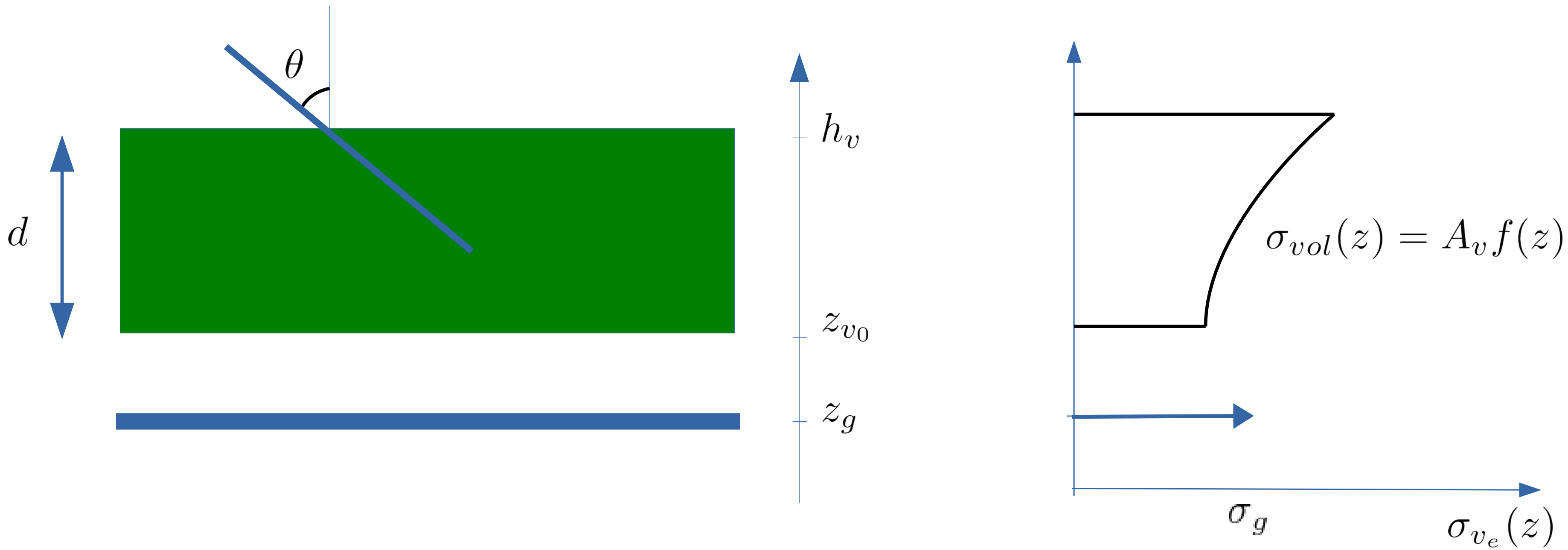

Backscattered volume intensity $I_v = \int_{z_{v0}}^{h_v} \sigma_{vol}(z)\mathrm{d}z = \int_{z_{v0}}^{h_v} A_v f(z)\mathrm{d}z$

Backscattered ground intensity $I_g = f(z_{v0})\sigma_g = \mathrm{e}^{-2\frac{\kappa_e}{\cos\theta}d}\,\sigma_g$

InSAR RVOG analysis

- Coherence formulation $\sigma_{v_e}(z) = \sigma_{vol}(z) + \delta(z - z_g) I_g$

$$\gamma_z = \frac{\int \sigma_{v_e}(z)\, \mathrm{e}^{jk_z z}\, \mathrm{d}z}{\int \sigma_{v_e}(z) \mathrm{d}z} = \frac{\int \sigma_{vol}(z)\, \mathrm{e}^{jk_z z}\, \mathrm{d}z + I_g\, \mathrm{e}^{jk_z z_g}}{\int \sigma_{vol}(z) \mathrm{d}z + I_g}$$

$$\boxed{\gamma_z = \frac{\gamma_{vol} + m\, \mathrm{e}^{jk_z z_g}}{1 + m}}$$

- Ground to volume intensity ratio $m = \dfrac{I_g}{I_v} \in \mathbb{R}^+$

- Coherence interpretation

$$m \to 0 \Rightarrow \begin{cases} \arg \gamma_z & \approx \arg \gamma_{vol} \\ |\gamma_z| & \leq 1 \end{cases} \qquad m \to +\infty \Rightarrow \begin{cases} \arg \gamma_z & \approx \phi_g \\ |\gamma_z| & = 1 \end{cases}$$

$$0 < m < +\infty \Rightarrow ?$$

InSAR based RVOG analysis: under-determined problem

→ another source of diversity is needed : polarization ?

TomoSAR (MB-InSAR) RVOG analysis

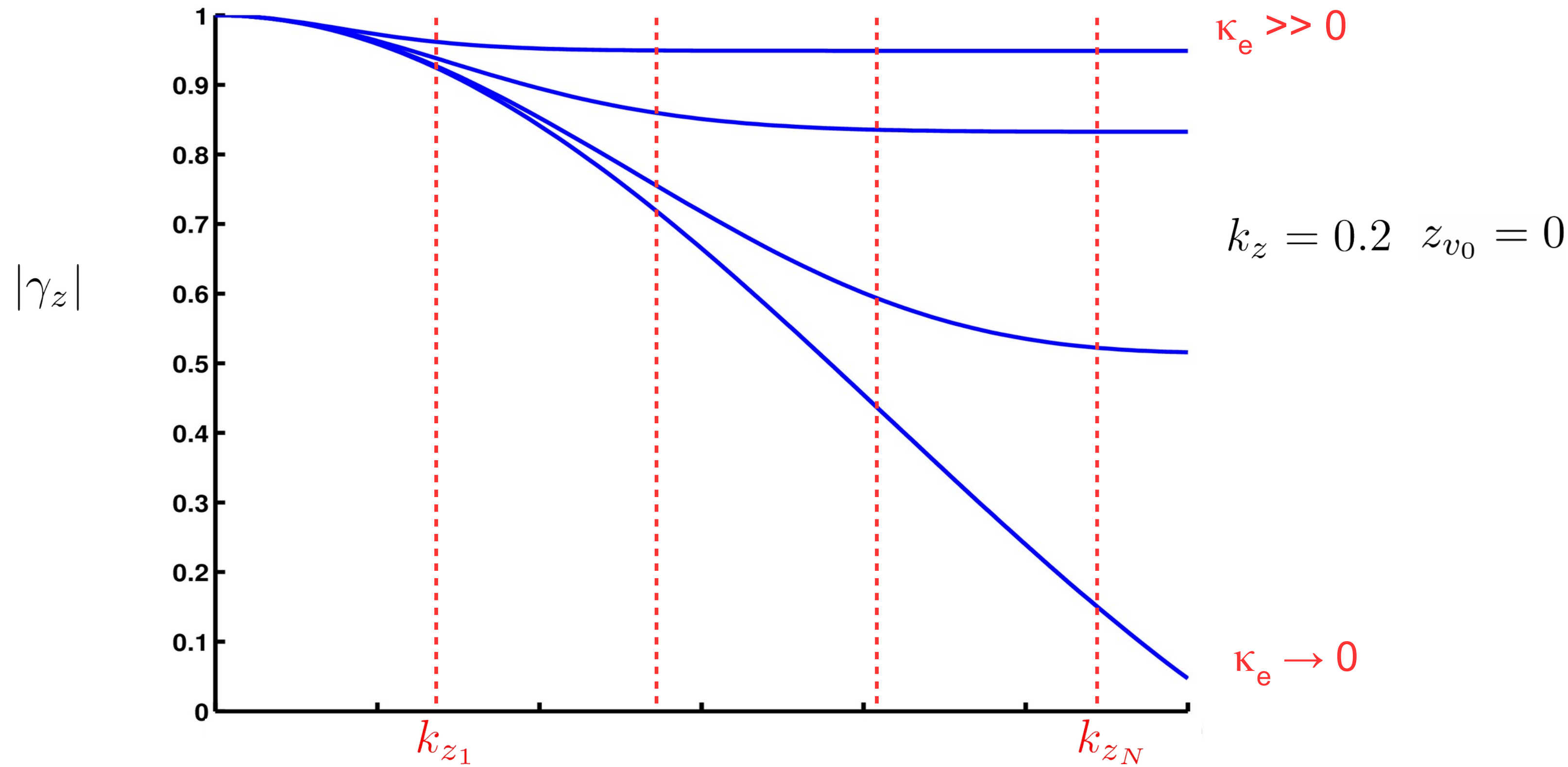

Additional spatial diversity

$\{\gamma_z(k_{z_n})\}_{n=1}^{N} \longrightarrow$

- Unambiguous height estimation for known f(z) shape
- Estimation of f(z) or **non-parametric analysis**
- PolTomoSAR (MB-Pol-InSAR) : $\{\gamma_z(k_{z_n}), \mathbf{w}\}_{n=1}^{N}$

InSAR phases, polarization & TomoSAR

L-band BIOSAR2, Capon tomograms

HH

HV

VV

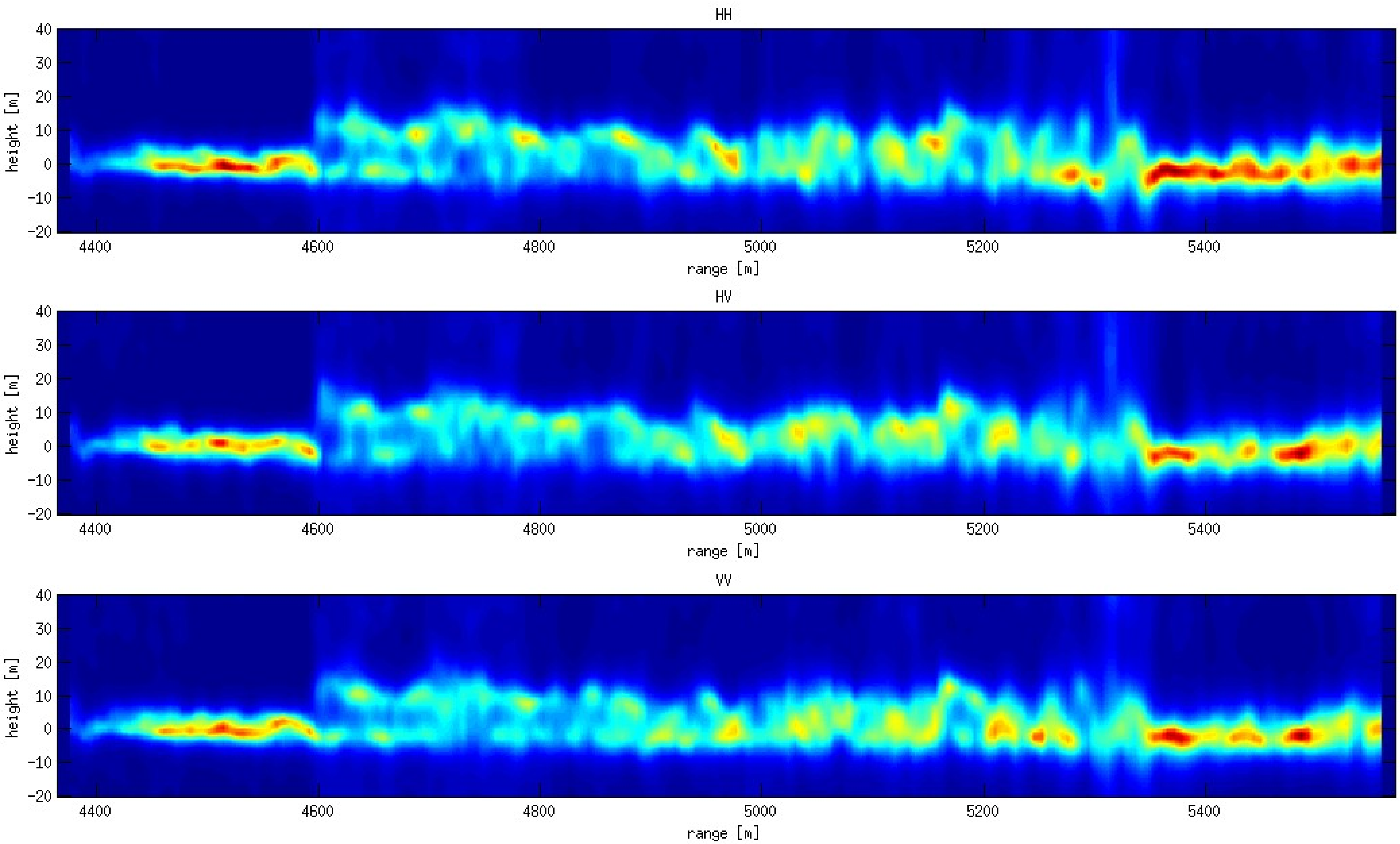

InSAR phases, polarization & TomoSAR

InSAR phase center heights

$h(\phi_{12})$

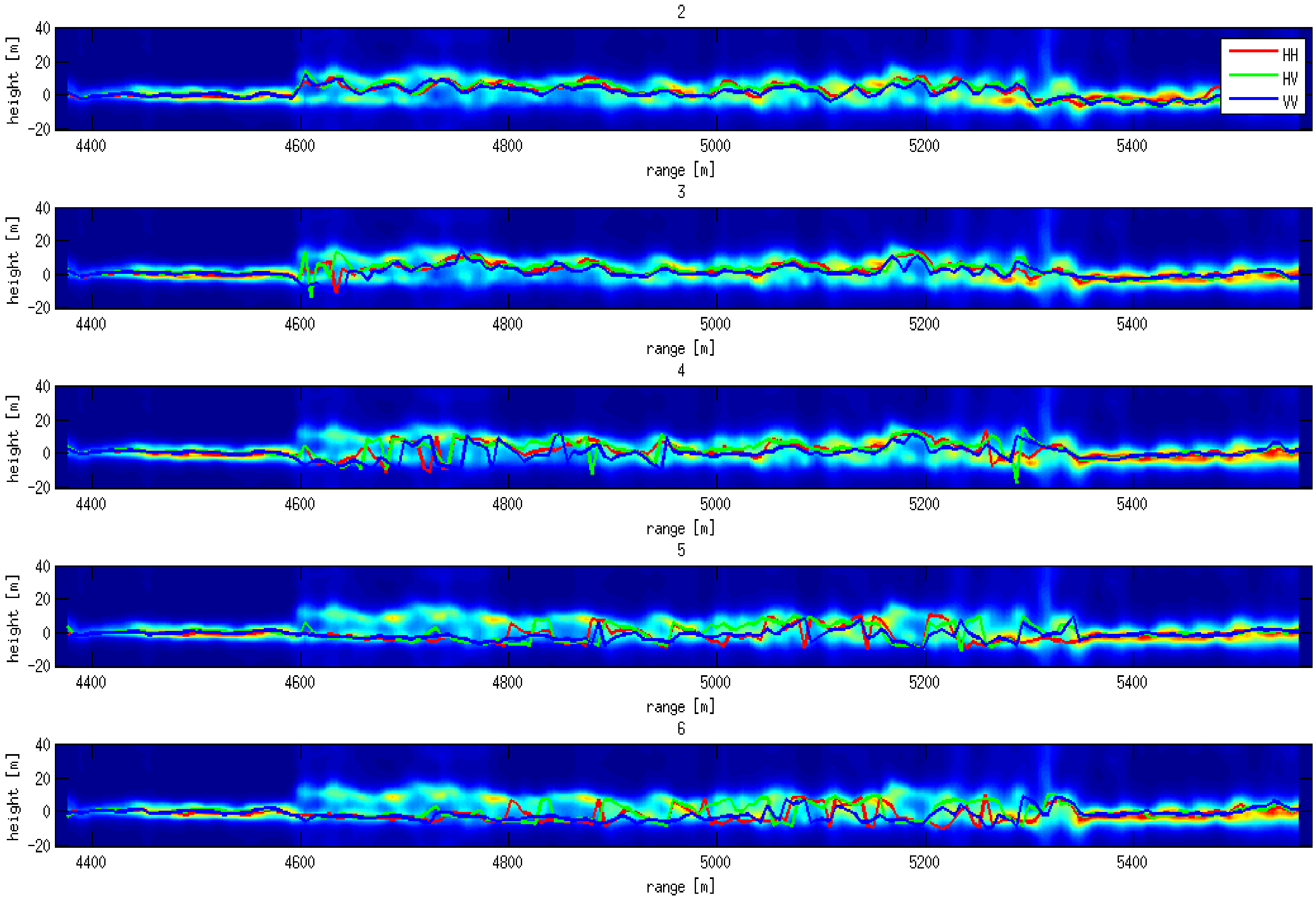

$h(\phi_{16})$

Near Range

Far Range

$$B_{i+1} \geq B_i$$

Polarimetric diversity

POL-InSAR phase center heights

$h(\phi_{12})$

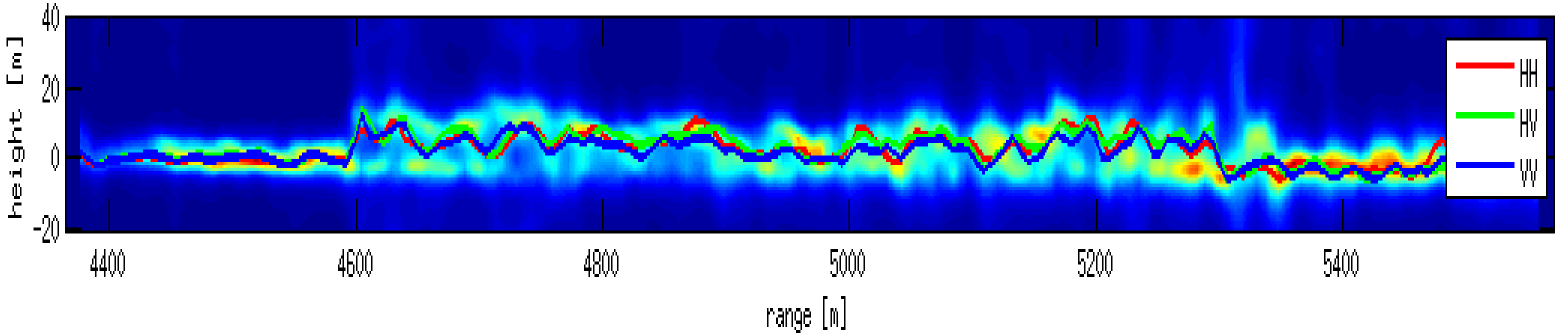

$h(\phi_{16})$

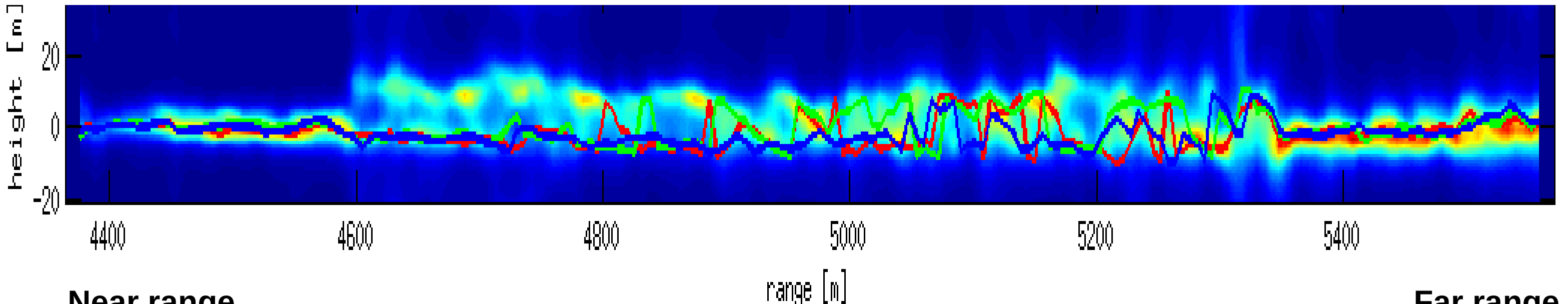

Near range **Far range**

Single-baseline PolinSAR:

- Phase Center height diversity not always guaranteed
- Requires **specific k_z** (baseline) values: **adequate volume decorrelation**

Illustration of coherence features

Campaign	BioSAR 2008 - ESA
System	E-SAR - DLR
Site	Krycklan river catchment, Northern Sweden
Scene	Boreal forest Pine, Spruce, Birch, Mixed stand
Topography	Hilly
Tomographic Tracks	6 + 6 – Fully Polarimetric (South-West and North-East)
Carrier Frequency	P-Band and L-Band
Slant range resolution	1.5 m
Azimuth resolution	1.6 m
Vertical resolution (P-Band)	20 m (near range) to >80 m (far range)
Vertical	6 m (near range) to 25 m (far

Illustration of coherence features

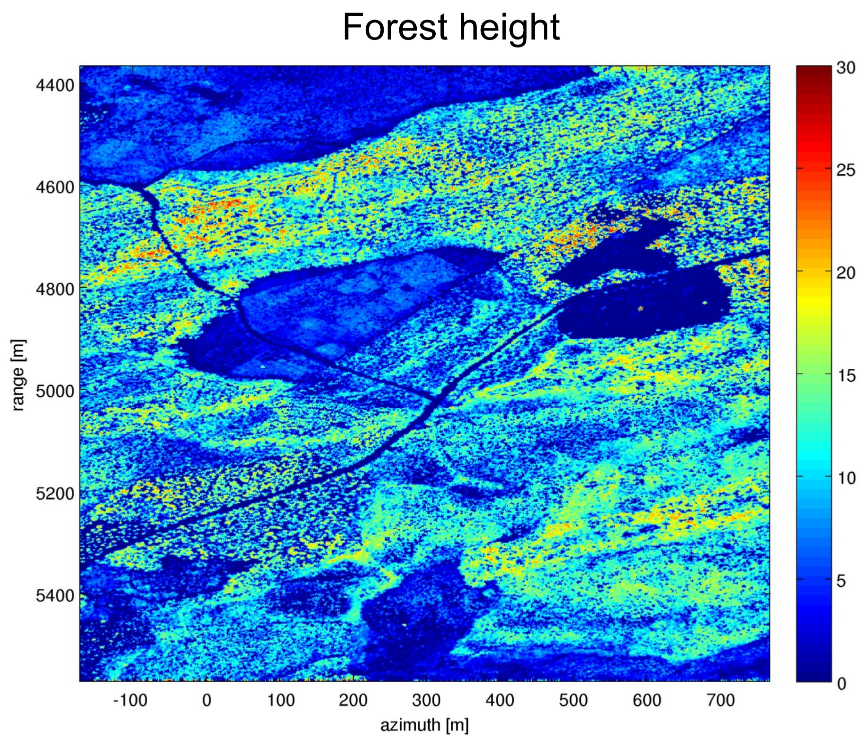

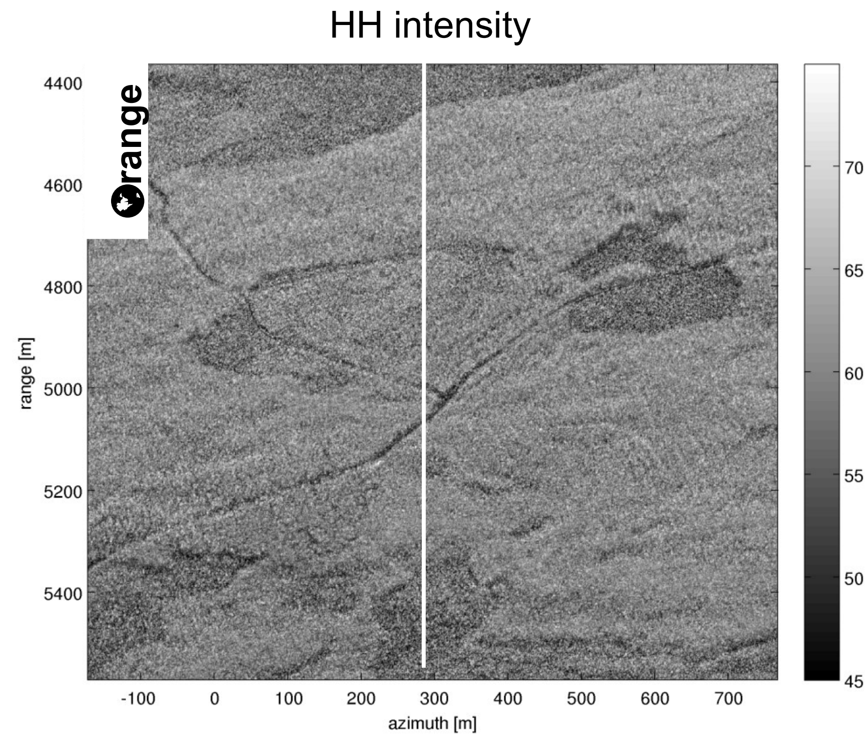

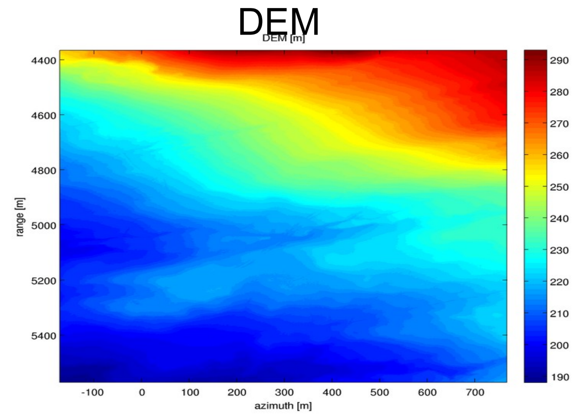

Illustration of coherence features

Forest height

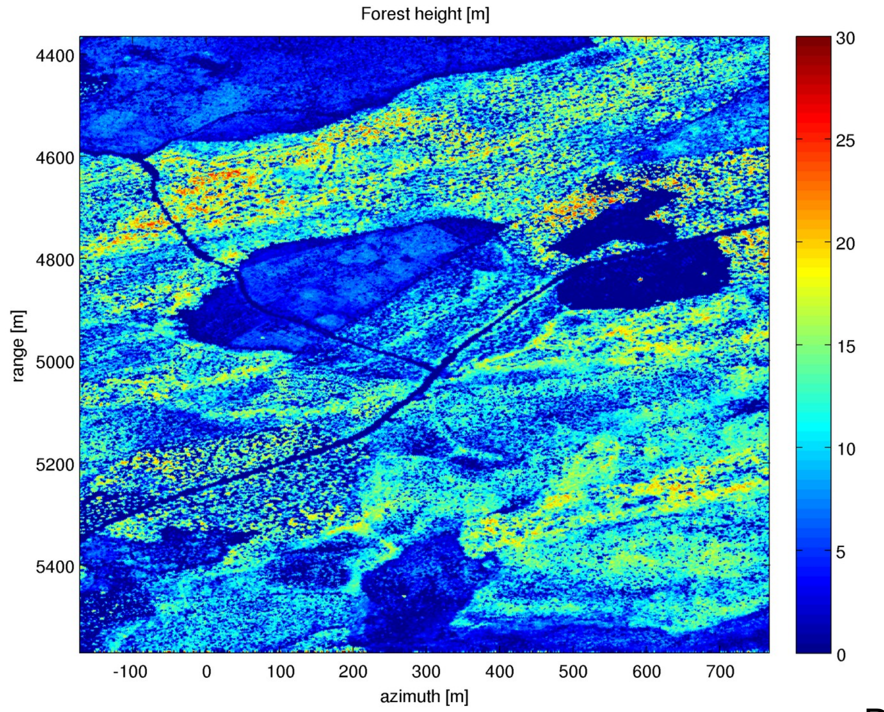

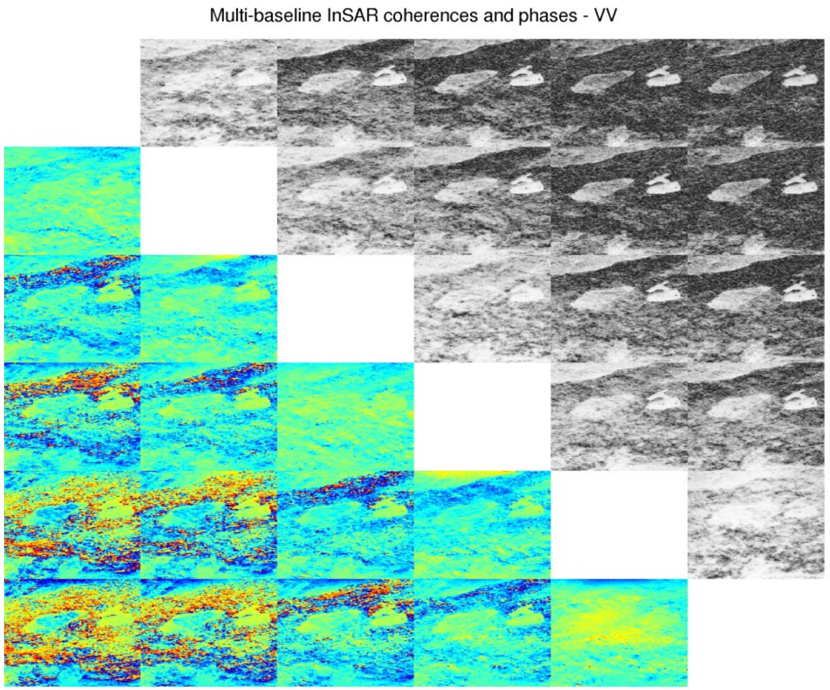

DEM